On the use of a weather radar for flood forecasting in the Centre of Portugal

Ana Sofia António Pereira

Thesis to obtain the Master of Science Degree in

Environmental Engineering

Supervisors: Professor Rodrigo de Almada Cardoso Proença de Oliveira

Professor Rui Miguel Lage Ferreira

Examination Committee

Chairperson: Ramiro Joaquim de Jesus Neves

Supervisor: Professor Rui Miguel Lage Ferreira

Members of the Committee: Professor Maria Manuela Portela Correia dos Santos Ramos da Silva

Master Tânia Helena Lopes da Silveira Viegas Seita Costa

December of 2020

Acknowledgements

I would like to thank all the people that contributed to the elaboration of this work.
Firstly, to my supervisors Rodrigo Proença de Oliveira and Rui Ferreira, thank you for allowing me to participate on the project Rivercure that led to the existence of this thesis. I would also like to express my gratitude for their never-ending patience and guidance throughout this thesis.
This dissertation would be non-existent without the data kindly provided by Agência Portuguesa do Ambiente and Instituto Português do Mar e da Atmosfera. Therefore, I owe my thanks to Maria Manuela Saramago for her availability to clarify any doubt I had; to Paulo Pinto and Sérgio Barbosa, I appreciate the readiness to share their data and knowledge regarding this subject.
Lastly, I would like to express my appreciation towards my family and friends, for their unconditional support and for being the raft that kept me from drowning in the flood that was this work.
This thesis is dedicated to my parents.

Resumo

Tem-se verificado um aumento da frequência e perigosidade das cheias. A implementação de sistemas de aviso antecipado e ferramentas de previsão de cheias são uma das medidas que permite a tomada de ações que reduzem a vulnerabilidade e potencialmente salvem vidas. Uma combinação judiciosa entre análise em tempo real de dados de udómetros e modelação hidrológica e hidráulica são imprescindíveis para a execução de um sistema de aviso de cheias. Estimativas de precipitação captadas pelo radar meteorológico têm sido cada vez mais usadas para fornecer informação complementar sobre a precipitação. O objetivo desta tese é avaliar a contribuição que o radar tem para sistemas de previsão de cheias em bacias propensas à ocorrência de cheias, como Águeda. Estudaram-se dois eventos de cheia, com diferentes regimes de precipitação (estratificados e convectivos), que ocorreram nesta localidade, em 2016 e 2019. Para compreender se as estimativas de radar fornecem informação relevante para a modelação e previsão de cheias, os dois eventos foram simulados com o programa HEC-HMS, utilizando como *input*, as estimativas de radar originais e corrigidas, assim como os dados udométricos. As estimativas corrigidas resultaram de uma análise de correlação entre as medições de precipitação obtidas pelas estações udométricas e pelas estimativas de radar nas imediações das estações. Os valores de radar corrigidos, assim como os originais e os udométricos, foram seguidamente utilizados como *input* no HEC-HMS. Os caudais resultantes foram comparados com os caudais observados nas estações hidrométricas. Esta comparação permitiu compreender os impactos que o uso do radar tem na computação dos caudais. Os dois eventos apresentaram resultados divergentes. A simulação do evento de 2016 sugere que o radar meteorológico é suscetível a erros que tornam a sua utilização em contexto operacional problemática. Enquanto o evento de 2019, evidencia a utilidade operacional, numa ótica de redundância, em sistemas de previsão. Concluindo, a contribuição do radar para a modelação e subsequente previsão de eventos de cheia é importante, mas apenas em sistemas com redundância. Para bacias sem sistemas de medição, como os udómetros, a utilidade deste instrumento ainda não se encontra provada.

Palavras chave: Radar Meteorológico, Udómetro, Precipitação, Caudal, Cheia.

Abstract

There has been an increase in the frequency and severity of floods. Accurate forecasting tools and early warning systems are needed to increase preparedness, to reduce vulnerability, and to potentially save lives. A judicious combination of real-time analysis of udometer data and hydrological and hydraulic modelling lies at the heart of most flood warning systems. Estimations of precipitation obtained with meteorological radar have been increasingly used to provide complementary precipitation data. The aim of this master thesis is to evaluate the contribution of the weather radar to flood forecasting systems in flood-prone watersheds, like the catchment of Águeda. Two flood events, with different precipitation regimes (stratified and convective), that took place in 2016 and 2019, in Águeda, were studied. To understand if the weather radar offers relevant data for flood modelling and forecasting, the two events were simulated with the hydrological model HEC-HMS, using as input, modified radar and udometer precipitation data. The modified radar estimates were the result of a correlation analysis between precipitation measurements obtained at udometric stations and radar estimates in the near vicinity of those stations. The adjusted radar, along with raw data and udometer data, were then used as input of HEC-HMS. The resulting computed discharges were compared with observed ones, at river gauge stations. This comparison allows to understand how radar data impacts the computed discharges. The two events presented very dissimilar results. The simulation of the event of 2016 suggests that the weather radar may suffer from errors that render problematic its use in operational context. The event of 2019, however, is an interesting example of the usefulness of the weather radar to provide redundancy to operational forecasting systems. In conclusion, the contribution of the meteorological radar for modelling and subsequent forecast of floods is valuable but only within systems with redundancy. For ungauged basins, the relevance of the weather radar is not firmly proved.

Key words: Weather Radar, Udometric Station, Precipitation, Discharge, Flood.

Contents

The remaining annexes are available on Digital Support, accessible on https://drive.tecnico.ulisboa.pt/download/1414452990160081.

Annex E, F, G, H, I, J, K (Digital Suport)

Annex C – Images of precipitation measurements executed by radar Arouca on 12th of February 2016, at 13h, without the application of the median and with the application of the median filter.

Annex E – Water levels measured by the river gauge stations of Ponte Redonda, Ribeiro and Ponte Águeda on the event of 2016.

Annex F – Water levels measured by the river gauge stations of Ponte Redonda, Ribeiro and Ponte Águeda on the event of 2019.

Annex G – Hourly precipitation values for the event of 2019 on the subcatchment of Águeda, for the different methods.

Annex H – Simulated discharges (m^3/s) resulting from the application of the corrective and spatial interpolation and observed discharge values for the river gauge stations of Ponte Redonda and Ribeiro, as well as the normalized discharges for Ponte Águeda, event of 2016.

Annex I – Hourly precipitation values for the event of 2019 on the subcatchment of Águeda, for the different methods.

Annex J– Simulated discharges resulting from the application of the corrective and spatial interpolation and observed discharge values for the river gauge stations of Ponte Redonda and Ribeiro, as well as the normalized discharges for Ponte Águeda, on the event of 2019.

Annex K – Individual equations for each udometer, only considering the data of the correspondent event.

Annex L – Parameters used in HEC-HMS.

List of Tables

List of Figures

List of Abbreviations

APA - Agência Portuguesa do Ambiente

CAPPI – Constant Altitude Plan Position

CHMI – Czech Hydrometeorological Institute

COST – European Cooperation in Science and Technology

EUMETNET – Network of European Meteorological Services

G2G – Grid to Grid

HEC – HMS – Hydrologic Modelling System – Hydrologic Engineering Center

HYRAD – Hydrological Radar

IDW - Inverse Distance Weighting

IM – Meteorological Institute

IPMA - Instituto Português do Mar e da Atmosfera

KNMI – Royal Netherlands Meteorological Institute

NEXRAD - Next Generation Radar

NFFS – National Flood Forecasting System

OPERA – Operational Program for Exchange of Weather Radar Information

PCAPPI – Pseudo Constant Altitude Plan Position

PPI – Plan Position Indicator

QPE – Quantitative Precipitation Estimation

RAIN – Estimations of Precipitation Intensity of weather radar

SVARH – Sistema de Vigilância e Alerta de Recursos Hídricos

TRMM – Tropical Rain Measuring Mission

WMO – World Meteorological Organization

UNESCO – Organização das Nações Unidas para a Educação, a Ciência e a Cultura

1. Introduction

1.1 Overview

Precipitation is defined as any form of water that originates in the clouds and falls under gravity towards the planet surface, (Chow et al., 1988). By definition, it includes rain, snow, sleet, hail and virga. It is one of the main processes that constitute the hydrologic cycle, allowing the continual exchange of water between the atmosphere and the surface, therefore ensuring the deposition of most of the freshwater on the planet's surface, (Chow et al., 1988).

Precipitation, in particular its liquid form, rainfall has an obvious social, environmental and economic value since it replenishes water supplies for plants, animals, agriculture and human uses, ensuring the development and functioning of all the economic activities, even when not directly connected or dependent on the weather. Below average values can lead to drought and an above average event can lead to flooding or inundations, meaning that although essential, rainfall can also be a cause of hazards.

Floods are defined as temporary natural event caused by moderate and lengthy precipitation or sudden and high intensity precipitation (Cheias |Prociv ,2020). This excess of precipitation may lead to a river discharge that exceeds its channel's volume causing the river to overflow onto the area surrounding the channel known as the floodplain, (Jackson, 2014). When this overflow permanently submerges a dry area, it becomes an inundation, (Flick et al., 2012).

Due to climate change, there has been an increase of flood events in Portugal, (Jacinto et al., 2015; Cunha et al., 2017) arising from the increase of intense precipitation events, (Soares et al., 2014). Floods usually have major impacts in the communities that are affected by it, since they can cause massive asset damage and human losses. Taking as an example the flood that occurred in Lisbon, in November of 1967, heavy precipitation originated a flash flood, causing major socio-economic impacts. The occurrence of the flood and the lack of a proper warning system contributed to the death of almost 700 people and nearly 900 became homeless, (Trigo et al., 2016). A less dramatic example occurred recently in Águeda when the storm "Elsa" caused heavy precipitations and a flood. This event affected dozens of retailers, and the total amount of compensation and provisions is expected to reach up to one and half million euros, (Carvalho,2020).

To prevent a flood, actions regarding territory management, basin drainage and discharge conditions should be taken. In circumstances where the preventive actions are already applied or unapplicable, and the risk of flood events occurring is a reality, mitigation actions should be taken. The implementation of flood warning systems can reduce the damage caused to people and property, ensuring that emergency actions, such as evacuation of people, can be taken, (Kundzewicz, 2013. This system relies on scientific forecasts that account for meteorological (precipitation and wind) and hydrological monitoring systems, (Kundzewicz, 2013).

Although the measurement of precipitation seems like an elementary task, accurate precipitation measurement is a complex process because of its significant spatial and temporal variability and because of its different forms (liquid, solid, mixture), (Hillel and Hatfield, 2005; Chow et al., 1988).The most used instruments to measure rainfall is the udometer, also known as, rain gauge. This device measures the amount of precipitation that reaches the ground, in the form of rain or snow, unobstructed by surface effects. It consists on a container placed in an open area that measures the water in terms of height accumulated per a given time, (Ingraham, 1998). As each udometer only provides data for a specific location, a dense network of udometers is needed to estimate the spatial variability of precipitation. Henceforth, udometric networks are generally unable to accurately describe the spatial variability of precipitation. The use of a complementary device may reduce this effect.

The radar is an instrument that can also measure precipitation and has the benefit of providing the measure of water volume per area considered, which is crucial for the study and understanding the precipitation conditions that cause a flood. The operation of radars introduce some difficulties and disadvantages, such as ground clutter, beam blockage, anomalous propagation and reflectivity-rainfall equations, that originate less exact quantitative estimates. Which raises the key question that motivates this thesis: is the use of radar in hydrology, in particular for flood forecasting, an unfulfilled promise or an unknown potential, (Berne & Krajewski, 2013)?

1.2 Objectives and Methodology

In Portugal, both rain gauges and the radars are used to measure precipitation. However, when it comes to the analysis of hydrological events and flood forecasting, the data generally used as input is the one measured by the rain gauges. The key objective of this thesis is to contribute to a better understanding of the potential of the weather radar for flood forecasting. This includes assessing the feasibility of current techniques to estimate precipitation in specific contexts and evaluating the added value of radar data for flood forecasting. This is mainly achieved by comparing the discharge estimates obtained by hydrological models with and without radar input data, and their evaluation vis-à-vis field river gauge data. By radar input, it is meant precipitation estimated by the weather radar and adjusted by the rain gauges, to account for spatial variability of rainfall.

Several methodological steps are needed, whose specific objectives are:

1. Assess the compatibility and consistency of radar and udometer data. This step relies on the analysis and comparison of precipitation patterns measured by the two instruments.
2. Devise a method to use the rain gauge data, considered the ground truth, to correct the spatial pattern of the radar data. Using the gauge adjustment technique, the radar precipitation estimates were approximated to the ground truth values. This technique leads to the consideration of two methods that correct the pattern of the radar data.
3. Employ both spatialized udometer data and corrected pattern of radar data as input to generate flood through standard hydrological modelling, that simulates complete hydrologic processes, such

as the transformation of the precipitation into discharge, and accounting for the general losses that occur on the watershed considered.

4. Assess the value added by the radar data through the comparison of the resulting simulated discharges with the discharges calculated using the rating equations and the river gauge measured levels.

The flood events considered in this study took place in Águeda, in the years of 2016 and 2019. The periods of simulation considered were from 9th to 16th of February 2016 and 16th to 23rd of December 2019.

1.3 Outline

This thesis has been divided in four key chapters: state of the art, methods and data analysis, results and discussion and conclusion and recommendations.

The state of the art chapter summarizes, in a clear and objective way, the most relevant concepts that serve as the basis for this dissertation. The term precipitation is defined, the most common precipitation measurement instruments are introduced, with a focus on the radar system. The error sources of this device are presented, and the term gauge adjustment is discussed. An overview of the international and national operational use of the weather radar is offered. Finally, a brief description of the hydrological model is executed.

The methods chapter is divided in three sections: introduction, case studies and data analysis. In the first section, a small summary of the actions taken is introduced. In the case studies, the study area is described, and the events presented. The last section presents the base data used in this work, udometric, radiometric, and river gauge, as well as the precipitation correction procedure.

The results chapter is divided into two sections: comparison between the corrected radar estimates to udometer measurements (at the udometer location) and comparison between observed/real discharge and generated discharge (discharge that uses the new radar precipitation values as input).The first section highlights the direct effects that the application of the corrective equation has on the precipitation data, in comparison with the rainfall measurements executed by the udometric stations, while the last section results consists on the outcome of the use of the corrected radar precipitation values as input variables on the hydrological modelling program HEC-HMS, in order to generate the discharge per hour of the flood events that will then be compared with the discharge, considered the real discharge. The observed discharge was calculated using the rating equation and the water height measured by the river gauge stations located within the watershed limits. This section will allow the drawing of major conclusions regarding the use of the corrected radar data, and the usage of the weather radar on the simulation of the flooding events of February 2016 and December 2019, in Águeda. The discussion part discusses the results obtained in this research and examines the success of using adjusted weather radar information as input on a hydrological model, and the performance of the resulting discharge.

Lastly, the conclusion highlights the relevant outcomes of this work and offers recommendations on how to validate and improve the methodology.

2. State Of The Art

2.1 Precipitation Measurement – Udometers And Its Limitations

According to the World Meteorological Organization, precipitation is designated as *a hydrometeor made up of an aggregate of aqueous particles, liquid or solid and crystallized or amorphous, which fall from a cloud or a group of clouds and reach the ground,* ("Glossary | International Cloud Atlas", 2020).

An episodic event can be characterized according to its phase, mechanism and defining properties (amount, frequency, and intensity, i.e. amount of precipitation collected per unit time interval), (Dai,2005).

In what concerns its phase, precipitation may be categorized as liquid precipitation, that includes drizzle and rain, freezing precipitation that includes freezing drizzle or rain and frozen precipitation like snow and hail, (World Meteorological Organization, 2018).

Considering the different physical and thermodynamic processes, three types of precipitation can be enunciated, (Gad, 2002): convective precipitation, stratiform precipitation and orographic precipitation. While convective precipitation presents a high level of intensity with high temporal variability and generally affects small areas. Stratiform precipitation, has a lower level of intensity, when compared to the previous mechanism, longer duration and a more uniform rainfall rate, acting on a larger area. Lastly, the orographic precipitation occurs in the presence of an elevated land formation, like a mountain; its rainfall has low intensity and high duration, far reaching a large area.

Precipitation is one of the most important climate variables since it has a powerful impact in many hydrological processes, such as runoff and acts as a primary driver of terrestrial hydrology. This phenomenon can also originate environmental hazards that have a high societal impact, like floods and landslides, (Berne & Krajewski,2013).

Considering the environmental and socio-economic repercussions caused by precipitation, it is important to understand the rainfall dynamics and pursuit systems that allow more reliable precipitation estimates and forecasts, since small changes in the rainfall gauged can lead to large change in a watershed response, (Bonta, 2005).

Precipitation measurement intends to quantify the volume of water that reaches the ground of the Earth's surface. The unit of precipitation mostly used is mm (volume/area), since this measurement entails the vertical depth of water on the ground, (World Meteorological Organization, 2018)

Currently, in Portugal, the main sensor used to quantify rainfall is the udometer (Figures 2.1 and 2.2). This instrument, also designated as rain gauge, performs at ground level, thus offering an approximate value of water that effectively reaches the surface, due to the wind effect, (Wilson & Brandes, 1979). Even though it provides direct measurement of precipitation, it covers a very limited area, hence only having representativeness on the place where it is located, (Barbosa, et all., 2017).

Figure 2.1-Udometer of São Julião do Tojal. Source: snirh.apambiente.pt

Figure 2.2- Udometric Station. Source: snirh.apambiente.pt

It can also be argued that even a dense network of rain gauges can miss significant rainfall data. For instance, if the maximum precipitation occurred between udometers, it would not be detected. Hence, there is a demand to acquire a more complete description of precipitation, its temporal and spatial variability, whilst maintaining the accuracy of the water volume assessed by the gauges.

2.2 Radar–Characteristics and Precipitation Measurement Process

2.2.1 Basic Description of the Radar System

Radar is an acronym that stands for Radio Detection and Ranging. This observational tool was initially developed with a military intention of remotely detecting aircrafts and ships. During World War II, it was noted that weather phenomena, like rain and snow, would cause undesirable echoes that could dampen the detection of military targets. Soon after this discovery radars started being used for weather related applications (Rauber & Nesbitt, 2018).

The radar is considered a remote detection equipment because it has the capacity to detect objects from a distance through the emission and reception of electromagnetic waves, (Figure 2.3). The objects detected include not only raindrops, but also hail, dust and insects, (https://www.ipma.pt/pt/educativa/, Berne & Krajewski, 2012).

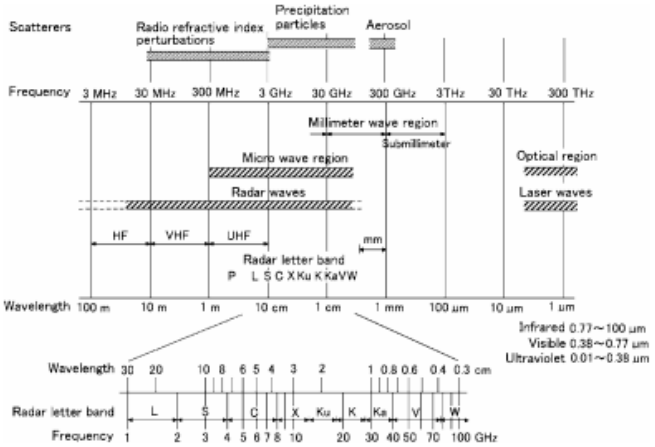

Figure 2.3 -Operational frequency band of various radars and their adjoining frequency bands. (Fukao & Hamazu,2014)

The modern meteorological radar transmits pulses of typically microwave signal, through an antenna in quasi-monostatic mode, (Figure 2.4). Upon encountering a hydrometeor, part of the energy emitted is scattered back towards the receiver antenna, where it is amplified, (Montopoli & Marzano, 2010). From the light speed and the interval of time between the pulse transmission and the reception of the same pulse it is possible to calculate the distance of the hydrometeor to the receiver antenna. The power of the signal backscattered by the hydrometeors is then used to compute a non-ambiguous measure of radar reflectivity, which is then converted into rain rate.

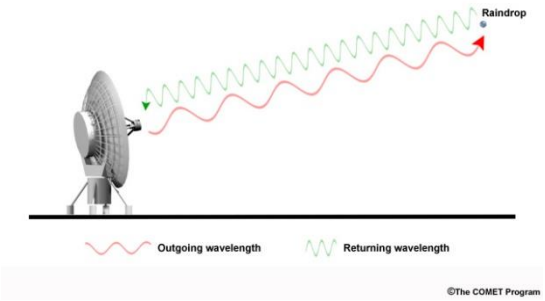

Figure 2.4-Representation of weather radar, ("How Do Radars Work? | Earth Observing Laboratory", n.d.)

The doppler capability that these radars possess permits not only to measure the intensity of the precipitation but also to detect its motion and location, in particular, it allows the receiver to measure the radial velocity of the backscatters, due to the frequency shift associated to the Doppler effect. Using the velocity and the interval of time between the original pulse transmission and the received one, it is possible to deduct the distance of the particle to the receiver antenna and get supplementary information, such as the wind vertical profile, (https://www.ipma.pt/pt/educativa/).

Another ability that increases the amount of information collected is the polarimetry, in this case, the dual polarization. Unlike the single polarization, (Figure 2.5), where the emitted radiation by the antenna

oscillates on a horizontal plane, simply measuring the horizontal dimension of the observed particles; the dual polarization, (Figure 2.6), emits alternately a horizontal and vertical pulse, measuring the vertical and horizontal dimensions of the hydrometeors,(https://www.ipma.pt/pt/educativa/, Krajewski & Smith, 2002). The polarimetric radar possesses extra variables, such as: differential reflectivity, that gives information about the shape of the reflector; differential phase shift, that depends on the shape and concentration of drops and the correlation coefficient, whose value depends on the homogeneity of the hydrometeor types, (Berne & Krajewski, 2012).

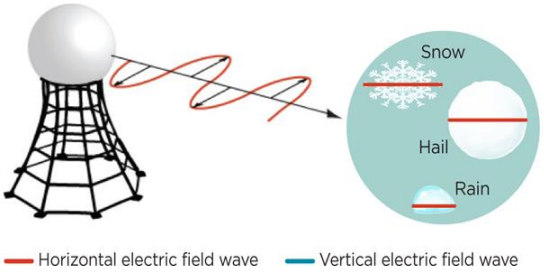

Figure 2.5-Horizontal Polarization System. Source: National Weather Service Weather Forecast Office

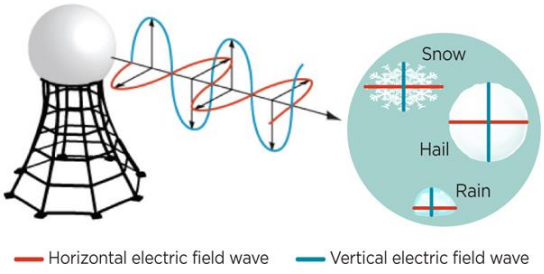

Figure 2.6-Dual Polarization System. Source: National Service Weather Forecast Office

This capability enables the improvement of the analysis of various hydrological events by offering additional information on echo classification, microphysical characteristics, and raindrop size distribution. The development of echo classification allows a better distinction between different precipitation forms and between meteorological and non-meteorological echoes, such as birds, insects or planes. Better microphysical interpretation enhances accuracy, namely including microphysical processes that occur in clouds and precipitation events and its kinematics. Considering that the concentration and size of the drops has a strong influence on the radar measurements, the ability to assume a functional form of raindrop size distribution is extremely valuable. All these new abilities contribute to an improvement on the radar rain-rate estimation, (Berne & Krajewski, 2012).

2.2.2 Radar Precipitation Estimation. Theoretical Aspects

The weather radar relies on the backscattered signal power to measure the precipitation, instead of measuring the rain-rate directly. Thus, this system provides indirect measures of rainfall. This characteristic implies that to achieve its goal, two steps must occur, the conversion of the returned power into a reflectivity factor and the conversion of this factor into the rainfall rate.

The first step is accomplished using the radar equation, that expresses the relationship between the transmitted power and the backscattered received power from the precipitation targets, namely water droplets and ice particles, accounting for the radar hardware characteristics and the distance between the antenna and the hydrometeors.

If we consider that the hydrometeor targeted does not absorb any power of the incident beam, and radiates the received energy isotropically, the power backscattered to the receiver, P_r, would be (Yuter, n.d.):

$$P_r = \frac{P_t . A_t}{4 . \pi {r_1}^2} . \frac{A_e}{4\pi {r_2}^2} \quad (2.1)$$

where, Pt is the transmitted power (W), At is the target cross sectional area (m^2), r_1 is the range from the isotropic transmitter (m), A_e is the effective cross-sectional area (m^2) and r_2 is the range of the power received (m).

However, the energy is not isotropically received in real life, since the scattered energy also depends on the characteristics of the precipitation drops, such as size, shape, composition, and angular beam between the target and the transmitter and the velocity, not only on the radar wavelength and incident power. Since the water drops are not isotropic, the cross section A_t does not equal the size of the scatterer. So, a new backscattering cross section is defined, σ, which is the apparent area that would return an equal receiver and received power if scattered isotropically. Since the transmitter is focused with an antenna, another constant must be considered, the antenna gain (G), that represents the ability of the antenna to radiate isotropically (Yuter, n.d.). Thus, an equation that represents the power received by the radar is presented:

$$Pr = \frac{PtG^2\lambda^2\sigma}{(4\pi)^3 r^2} \quad (2.2)$$

Since the antennas used in meteorology are circular, the antenna gain can be presented as an approximation of the inverse of horizontal $(\theta\mathrm{h})$and vertical $(\theta\mathrm{v})$ beam widths (rad) or the effective cross section area, A_e , over the radar wavelength, λ (cm):

$$G = \frac{\pi^2}{\theta\mathrm{h}\theta\mathrm{v}} = \frac{4\pi Ae}{\lambda^2} \quad (2.3)$$

The radar emits a large number of short pulses (typically of the order of magnitude of 1 ms) per second. The pulse repetition frequency (PRF) typically varies between 150 and 2500 Hz. To avoid ambiguity a pulse must be emitted and reflected before the next pulse is emitted. Since the returned power fluctuates from pulse to pulse, the actual power measurement is an average of typically 50 pulses (Yuter, n.d.) Taking this fact into consideration, there is a need to consider not only a solo target but a volume of randomly distributed scatterers, $\sum_{vol}\sigma i$, that substitutes the radar reflectivity, resulting in an average power equation given by :

$$Pr = \frac{Pt\ G^2\theta h\ \theta v\ \lambda^2 c\tau}{1024\ln(2)\,\pi^2 r^2} \sum\nolimits_{vol} \sigma i \quad (2.4)$$

Where, τ is the pulse length, (m).

In equation 2.5 (Yuter, n.d) it is assumed that the type of scattering that occurs is the Rayleigh regime. Even though this type of scattering is only valid when the diameter (D, cm) of the water droplet is lower than $\lambda/16$, it is the only that does not fluctuate its returned power and allows a monotonically increase of the cross section given by:

$$\sigma_d = \frac{\pi^6}{\lambda^4} K^2 D^6 \tag{2.5}$$

Where σ_d, is the backscattering cross section of a single drop and K is the complex index fraction.

Thus, the resulting radar equation is the following:

$$Pr = \frac{Pt\ G^2 \theta h\ \theta v\ c\tau\pi^3}{1024 \ln(2)\ \lambda^4} \frac{K^2}{r^2} \sum_{vol} Di^6 \tag{2.6}$$

The radar reflectivity factor (Z, cm6.cm^3) is proportional to the summation of the sixth power of the particle diameters divided by the volume of the contributing region, (Yuter, n.d.). It is defined by:

$$Z = \sum_i Ni\ Di^6 = \int_0^\infty N(D) D^6 dD \tag{2.7}$$

Where, Ni is the number of drops per unit volume of atmosphere, Di is the diameter of the hydrometers (cm) and $N(D)$ is the number of drops per unit volume with diameters between D and $D + dD$.

Since the weather radar measures the magnitude of the echo signal, this function depends solely on the size, composition, position, orientation, and number of hydrometeors per unit volume (Yuter, n.d.). Which means that the individual parameters of the radar (Pt, θ, and λ) are usually grouped in a constant C_r, obtaining the following simplified version of the radar equation:

$$Z = \frac{P_r\ r^2}{K^2 C_r} \tag{2.8}$$

The second step in the estimation of the rainfall rate, is to convert the reflectivity into rain rate. Assuming that the atmospheric vertical motions are absent, it is known that the reflectivity is expressed by the equation 2.7 while the rainfall rate equals, (Bringi & Chandrasekar, 2001):

$$R = 0.6\pi \times 10^{-3} \int_0^\infty v(D)\ D^3\ N(D) dD \tag{2.9}$$

Where, R is the rainfall rate (mm/h), $N(D)dD$ is the raindrop diameter distribution in number of drops per cubic meter of air per unit raindrop size interval at ground level and $v(D)$ is the drop terminal velocity (m/s), this velocity is usually approximated to 1,4 x 10 $^{-3}$ D$^{1/2}$ (Spilhaus, 1947).

The drop size distribution is a variable that cannot be estimated using only the reflectivity factor, since it varies in time and space and with physical processes, like evaporation and advection, that happen

between the cloud level and the surface. All of this affects the establishment of a process model that relates the reflectivity and the precipitation intensity that is widely accepted, (Gad,2002). However, on an operational context the empirical approximation of this relation is obtained using a power law equation:

$$Z = AR^b \tag{2.10}$$

Where Z is the reflectivity factor (mm^6/m^3), R is the rainfall rate (mm/h) and A and b are constants.

The parameters A and b are different according to the geographical location considered and the raindrop size distribution in space and time, which implies the inability to define a universal relationship that works for all precipitation fields. These parameters are generally computed by minimizing the normalized errors between radar estimations and udometer rainfall, (Mapiam & Sriwongsitanon, 2008). The Z-R relationship developed by Marshal and Palmer, in 1948, is still one of the most broadly used nowadays, even in Portugal and is defined as:

$$Z = 200R^{1.6} \tag{2.11}$$

Many other authors, all over the world, have developed new Z-R relationships, not only dependent on climatological and geographical aspects, but also on the characteristics of the instruments used to measure the data that leads to the simple power equation. Some choose to focus on minimizing the difference between precipitation estimates executed by the radars and precipitations measurements performed by udometers, such as, Alfieri, Claps & Laio, (2010); Wu, Zou, Shan & Wu, (2018); Tenório, Moraes & Kwon, (2010), etc. Ciach & Krajewski, (1999), used a Darwin Radar, in Australia, to create a statistical method that accesses this relationships estimation error variance, through the study of raw estimates and gauge measurements resulting in the following equation, $Z = AR^b$, where the b value was calculated, with the sole goal of minimizing the mean square differences between the single scan radar rates and the gauge rates, while the parameter A is dependent on the calibration of the radar.

Other authors trust algorithms developed to increase the measuring accuracy of the radar and develop accurate reflectivity-rainfall relationships. Smith, Seo, Baeck & Hudlow, (1996), used the anomalous propagation algorithm present in the American radar NEXRAD to detect and eliminate the data affected by the anomalous propagation, only processing the non-affected data. This situation leads to a big reduction of the bias associated with the loss of beam filling and loss of reflectivity with altitude, resulting in yet another equation, $R = 0.017Z^{0.714}$

Besides the characteristics of the radar, other important factors that affect the constants associated with the Z-R relationship equation are other hydrological processes, type of precipitation, height of measurement, the different instruments used to calculate it and the data considered. Comstock, Wood, Yuter & Bretherton, (2004), observed 23 separate drizzle events and collected data regarding the rain drop size distribution using 4 different instruments and measuring methods: EPIC filter-paper (surface measurements), aircraft (cloud level), millimetre cloud radar (cloud base) and a shipboard ceilometer. As a result, 4 different equations were developed: $Z = 57R^{1.1}$ (2.12), $Z = 32R^{1.4}$ (2.13), $Z =$

$22R^{1.1}$ (2.14) and $Z = 25R^{1.3}$ (2.15), respectively. It is possible to see that the reflectivity-rainfall equation is easily influenceable, even if it is possible to conclude that the b value is always smaller than the one considered by Marshal and Palmer and that the A coefficient is heavily affected by the evaporation, increasing with the distance to the cloud.

Approaches that consider dynamic reflectivity-rainfall relationships that are continuously updated in time are also being considered, (Alfieri, Claps & Laio, 2010; Wu, Zou, Shan & Wu, 2018).

In short, the development of a universal Z-R relation is still further from being a reality. This equation is dependent on several unpredictable variables that are also dependent on uncontrollable factors, leading to radar precipitation estimates that may not be precise especially if the equation is applied outside of the climatological and physiographic conditions for which they were deduced. This highlights the need to benchmark existing Z-R relations in different contexts.

2.2.3 Radar Data Visualization

This measuring instrument collects and analyses a big quantity of reflectivity data, requiring a software that has the capacity to extract precipitation intensity maps from the gathered information. This software can present two types of precipitation intensity maps, the PPI and the most used one, the CAPPI. The PPI, Plan Position Indicator, relies on the data collected from a single rotation of the antenna at a given elevation, projected on a horizontal plan, with a constant elevation angle, presenting the precipitation intensity data as viewed from the top-down. The Constant Altitude Plan Position Indicator, CAPPI, creates maps of precipitation that combine information from multiple PPIs to produce a 2D map of the measured data at a given altitude.

To better illustrate these concepts, the available images of PPI and CAPPI maps from the McGill S-band radar, from the McGill University were used.

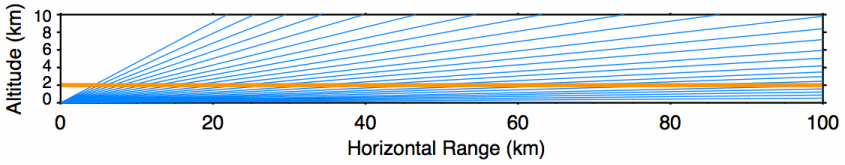

Figure 2.7 -Altitude of the radar McGill beam depending on the horizontal distance. Source: http://www.radar.mcgill.ca/

Considering the image 2.7, the blue lines represent the different angles that the McGill S-band radar collects information. When using a PPI map, the data presented are a result of the data measured along the blue lines, yet, when adopting the CAPPI maps, the exhibited image that will be produced by using the intersection of the blue lines (PPIs) with the orange line. As a result of its differences, the type of image presented by each of these intensity maps is very different, (Figure2.8).

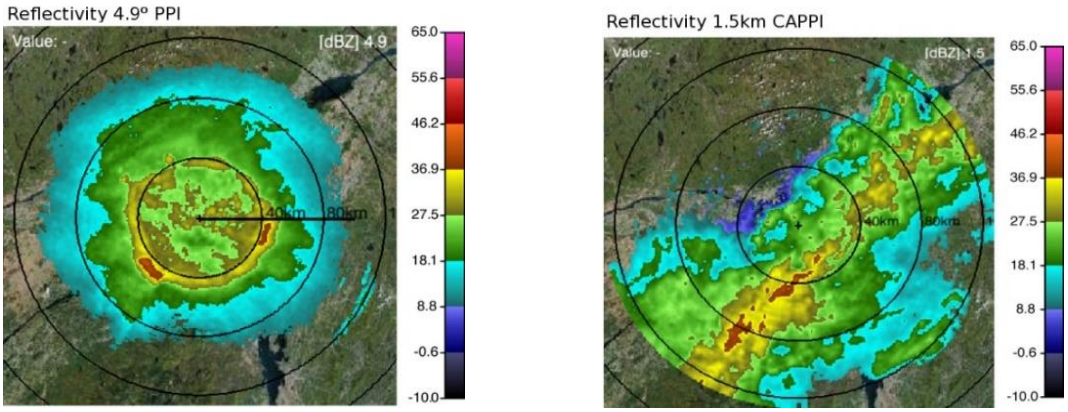

Figure 2.8 - Illustrative Figures of reflectivity data captured by the McGill radar, presented by two data visualization methods: PPI (right) and CAPPI (left). Source: http://www.radar.mcgill.ca/

In an attempt to visualize the areas within the radar range that are not directly measured, such as the area surrounding the radar and the volume border with the highest altitude, a modified version of CAPPI was created, the Pseudo CAPPI (PCAPPI). This algorithm results from the interpolation between reflective data at different elevations, like CAPPI, but measures additional information. At long ranges, the lowest beam can be found above the chosen altitude so the data is taken from the lowest elevation; when considering short ranges, the highest radar beam is lower than the constant altitude, so the data is collected from the highest elevation, (Šálek, et al., 2004).

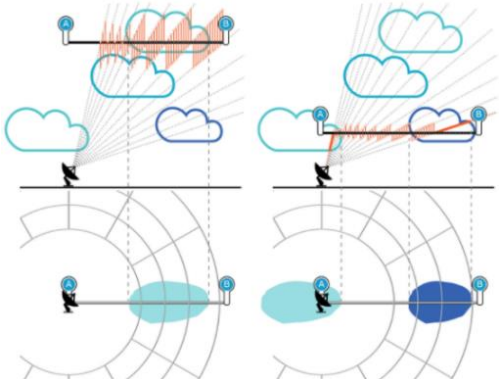

Figure 2.9 -CAPPI (left) and PCAPPI(right) product. Red lights represent interpolation from beam data,the black line represents the constant altitue and the heavy red line indicates how PCAPPI uses the closest beam to extend CAPPI product bellow and above altitude. Source:iris.vaisala.com

2.3 Sources of Error in Radar and Gauge Comparisons

2.3.1 Main Error Sources

Various factors can affect the radar precipitation measurements, leading to a big variability between rain gauges and radar measurements. These error sources may be clustered in three main groups: errors in the estimation of the reflectivity factor, variations in the Z-R relation and udometers and radar sampling differences, (Wilson & Brandes, 1979).

2.3.2 Radar reflectivity factor measurement

This type of error may or may not be related to the hardware calibration of the radar.

The lack of careful calibration of the hardware may lead to systematic errors in the rainfall measurement, it is important to assure that the emitting power is constant and that the signal processing optimizes the capacity of the system to collect information, reducing the variance on the reflectivity factor estimation.

The sources of error not associated with hardware, are the ground clutter, beam blockage, anomalous propagation of the beam, radome attenuation, attenuation by the precipitation and atmospheric gases, (Wilson & Brandes, 1979; Raghavan, 2003).

a. The ground clutter occurs when the weather radar picks echoes from ground features, such as hill, trees, buildings, birds and insect swarms, along with the meteorological echoes. This ground echoes can be falsely interpreted as precipitation, presenting an overestimation of the rainfall measurement.

b. The beam blockage leads to an underestimation of the precipitation value. It occurs when the signal intensity is affected by the intersection of the beam with the land surface, (Figure 2.10).

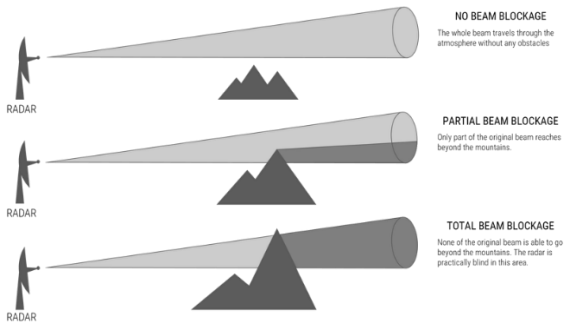

Figure 2.10-Illustration of an obstacle can affect the radar signal. Source: Philippine Radar Network

c. The anomalous propagation, (Figure 2.11), also known as super refraction, is caused by sharp inversions on the lower troposphere, this inversion bends the radar beam downwards as the signal travels away from the radar. Since the beam is bent in the soil direction, this type of error source can have the same issues as the ground clutter.

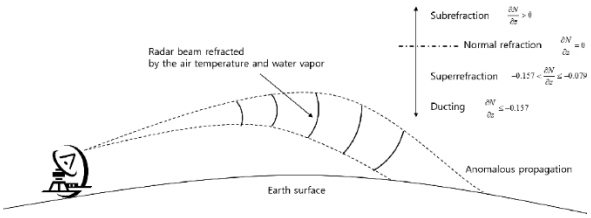

Figure 2.11-Illustration of the anomalous propagation (Lee & Kim, 2016)

d. The radome attenuation is caused by the radome that encloses the radar antenna, usually this attenuation is very small, however when there is rain, there can be the formation of a film of water on the surface that causes additional attenuation, Table 2.1.

Table 2.1-Two-way attenuation due to water film o radome (Raghavan, 2003)

R (mm h^{-1})	Attenuation dB two-way	
	$\lambda = 5.7$ cm; $r_r = 275$ cm	$\lambda = 10$ cm; $r_r = 450$ cm
1	0	0
10	1.4	1.4
20	2.0	2.0
40	3.0	2.4
100	4.6	3.0
200	6.0	4.0
400	8.0	5.6

e. The attenuation by precipitation and atmospheric gases is a result of the attenuation of the signal caused by the rain drops and the gases that compose the atmosphere. The impact of this source on reflectivity errors is dependent on the radar wavelength and on the distance to the hydrometeors. The smaller the wavelength, the bigger impact, contrarily a smaller distance to the water particles leads to a smaller attenuation effect.

2.3.3 Variability on Z-R relationship

The variation in the Z-R relationships is linked with the uncertainty concerning the drop size distribution of an event. It is assumed that precipitation events with the same reflectivity factor would present the same rainfall intensity, presuming that we can use the same A and b constants, but this first assumption is often incorrect, because different types of precipitation usually have different drop size distribution, therefore having dissimilar precipitation intensities. The difficulty of defining the most appropriate a and b values can also impact the Z-R relationship results. Lastly, if there is a small lack of accuracy in the conversion of the power into reflectivity, there will be an exacerbation of this error, because according to equation (2.7) the drop size increases exponentially with the reflectivity.

2.3.4 Sampling differences of radar and udometer

Radar and udometers are very different rainfall measuring devices. While radar samples precipitation on a volume aloft, relying on two conversion processes that result in the rainfall rate, the udometer makes a point measurement of the precipitation that reached the ground. This means that there is a disparity when comparing the measurements obtained by these two instruments, because it is assumed that the raindrops fall vertically into the ground, ignoring that factors such as wind drift and evaporation can alter the location at which the drop may fall and change the size of said drops. The weather radar procedure results in time and space sampling errors associated with the type of precipitation, its duration and intensity, additionally if the spatial features are too small, they can be undetected by the radar but accounted for by the udometer integration (Wilson & Brandes, 1979). Also, the bigger the range at which the radar measures, the bigger the differences of precipitation measured aloft and at ground level are, because there is an increase on the sampling volume and beam height the further away from the antenna. Besides differences between spatial sampling, there are also differences on the temporal sampling; while the radar rainfall is obtained by performing an integration of the data on the period of interest, the gauge measurements result from a mainly continuous time integration (Wilson & Brandes, 1979).

Therefore, considering the relevant difference between the two-systems sampling process, the variation between results cannot be simply assigned to the weather radar errors.

As a consequence of the errors previously mentioned, the weather radar does not present accurate measurements of the precipitation, which usually leads to an underestimation of the rainfall quantitative estimate, (van de Beek, et al., 2016; Pauthier et al., 2016; Eldardiry, Habib & Zhang, 2015),

2.4 Bias Reduction Techniques

2.4.1 Gauge Adjustment of the Radar Data

As mentioned in the section above, many factors can influence the values of precipitation measured by the weather radar. In an effort to reduce the bias suffered by the radar-rainfall estimates, an adjustment using the udometers precipitation measurements may be used, (Ochoa-Rodriguez et al., 2019).

Adjustment is defined as the modification of the radar quantity to “match” an external quantity, in this case the rain-gauges measurements, (Joe & Smith, 2001). This modification intends on reaching a quantitatively accurate and spatially continuous precipitation measurement, therefore combining the two rainfall measurement systems individual strengths.

Even though finding the most adequate adjustment technique is a complicated procedure, it can partially correct many errors, including incorrect Z-R relationships (by altering the multiplicative A factor), beam blockage, attenuation, and insufficient radar calibration (Gjertsen, Šálek & Michelson, 2004).

The gauge adjustment of radar precipitation measurements is many times mistaken by radar calibration, even though it has a different purpose. While radar calibration aims at defining a stable and reproducible

method for correction of radar measurements, the adjustment of radar precipitation is a statistical process with the goal of increasing the accuracy of radar precipitation estimates by comparing these estimates with the measurements made by udometers.

The application of this procedure is dependent of 4 main assumptions, (Gjertsen, Šálek & Michelson, 2004):

a. Udometer precipitation measurements are accurate at their location- the data collected by this tool will be used as reference information, making its quality a very important factor, since low quality gauge information will lead to a failure on the adjustment.

b. The precipitation spatial and temporal variability is displayed by the radar- this assumption is related to the existence of false echoes, such as insects, clutter, the sun, etc. The validity of this assumption depends on the application of algorithms that identify and remove the noise.

c. Both instruments offer valid measurements for the same location – this assumption is not valid, since udometers provide ground point values while radar express volumetric integrations at high altitudes but must be made.

d. Relationships based on the comparison between rain gauges and radar are valid for other locations and time- the variability with time and space associated with the reflectivity profile of a precipitation event, the veracity of this assumption is questioned, however it is crucial to admit that the relationships between radar and udometers measurements can be spatially interpolated and extrapolated in time.

In short, the type of gauge adjustment technique used depends on the accessibility and quality of the udometer data, the quality of the radar precipitation estimates, the total area for which the precipitation estimates were made, the temporal and spatial resolution of the radar rainfall measurements and the geographical aspects, such as orography and climate, of the area under analysis.

According to the COST-717 questionnaire, in 2003, IPMA was already experimenting with gauge adjustment, to reduce the experimental local bias. Considering this approach on a worldwide scale, almost half of the institutions used some type of gauge adjustment regularly, many of them, such as , CHMI in Czech Republic, Météo France, KNMI in the Netherlands , met.no in Norway, Einfalt and hydrotec in Germany, use the corrected information as input on hydrological models.

In conclusion, rain gauge adjustment is a generally recommended method, even if it cannot guarantee an acceptable result in the whole radar domain, (Gjertsen, Šálek & Michelson, 2004).

2.4.2 Low Pass Filtering

Radar estimates, and therefore the radar rainfall maps, are prone to the influence of external sources, such as surrounding environment, data acquisition devices and transmission devices, that generate

random errors/clutter incorrigible by rain gauge calibration, (Giuli, Baldini & Facheris, 1994). This is an issue can be mitigated by the application of the median filter to the radar rainfall maps.

This nonlinear low pass filter is very effective on the reduction and suppression of “salt and pepper” noise, while retaining the essential information of the image, Annex C. It works by replacing the grey level of each pixel by the median of the grey level in the neighbour pixels, known as window, of the pixel, (Tan & Jiang,2019).

The use of the median filter in radar rainfall maps in not a novelty. Authors such as, Giuli, Baldini & Facheris, (1994), Xumin & Xue,(2011) and Rinollo et al., (n.d)., refer the use of this filtering method to effectively reduce the noise of the image, while having a good protection effect. Giuli, Baldini & Facheris, (1994) have shown that the application of the median filter is effective in the reduction of the Normalized Standard Error of Error (NSED), i.e., the spatial fluctuation of errors in an area.

2.5 Weather Radar in Operational Forecast

2.5.1 Use of Radar Worldwide

The implementation of the weather radar in the understanding of precipitation events has transformed the meteorological field. This instrument used to locate precipitation, calculate its motion and intensity, allowed the understanding one of the most unstable phenomena of the hydrological cycle.

In 2016, the World Meteorological Organization (WMO), along with the Intergovernmental Oceanographic Commission, the UNESCO, The United Nations Environment Programme and International Council for Science, created an international team of radar experts and climate scientists for climate monitoring using this tool, the project was called Global Climate Observing System (GCOS) gcos.wmo.int. The main goal of this task team is to assess the importance of radar data for the monitorization of the climate , such as key parameters (horizontal reflectivity, radial velocity, spectrum width, differential reflectivity, correlation coefficient and differential phase), the metadata necessary, as well as offer guidance on the organization and standardization of the data stored, to allow the existence of homogeneous time series data of climate available for future generations.

Europe also has a regional entity that acts in studies regarding the weather observations and forecasting. This entity possesses a subsection responsible to coordinate the works related to the weather radar, the Operational Program for Exchange of Weather Radar Information (OPERA), www.eumetnet.eu/opera. This program offers recommendations about software and hardware issues, guidelines for effective radar measurements, shares and discusses advances made on the radar field and on its contribution for the operational radar work. In short, it intends to create a platform that shares expert knowledge about this tool within its members and the remaining radar community.

The existence of programs such as these, leads to an incentive on the search and development of radar functionalities, that allow better results in terms of precipitation measurement, extreme events warning

and application of this data in hydrological models. These advances are then applied at an operational level.

It is a known fact that the non-corrected radar data presents severe underestimation of the precipitation amount, as mentioned in section 2.3. This is a major concern, since quantitative precipitation estimation is an extremely important component on the modelling of hydrological events. Some operational systems are applying corrections using the ground truth values as indicators of the real precipitation volume that occurred in a single location, performing the so called gauge adjustment, (Gjertsen, Sálek & Michelson, 2004; Moore, Cole & Robson, 2012; Sinclair & Pegram, 2005), it has been shown that this technique provides, generally, good results, according to the type of adjustments performed and depending on the type of precipitation event under correction. Others create new quantitative precipitation estimation products (QPE) using only the radar data, like Météo- France. The French operational network implemented processing of QPE through the application of modules that correct specific errors associated with this instrument, like ground clutter, beam blockage and vertical profile of reflectivity. The results of this correction chain, show that the new QPE product outperforms the old one, and there is a reduction of positive and negative bias, offering great improvement not only on rainfall measurement but also on assimilation of this data in hydrological models, (Tabary et al., 2007).Other systems, like the NEXRAD, operational in the 50 states of the USA, have not noted an increase of accuracy on their operational systems since the improvement associated with the implementation of polametric radars depends on the characteristics of the events, mainly on the vertical structure of the storms, leading to the presence of relevant errors in the estimation of total rainfall, (Cunha, et al., 2013). In a more creative attempt to measure and comprehend the rainfall phenomena, the Tropical Rain Measuring Mission (TRMM) was created. First suggested in 1984, in the United States, this mission intended on using a radar to measure the precipitation from space. By 1988, the mission was a collaboration between the United States, that supplied the aircraft and Japan, that provided the precipitation radar. At an altitude of 350 km, this radar offered information on rain structure in great detail, that can be found in the work of many scientists, like Takayabu et al. (1999); Haddad et al. (1997); Viltard et al. (2000), providing critical precipitation measurements in the tropical and subtropical regions. TRMM ended officially in April 2015, since the fuel reserves of the satellite were over, (Kummerow et al., 2000).

Other important roles of this meteorological instrument is the capacity it has to detect and warn about extreme hazardous events, such hail, intense precipitation and tornadoes, as well as meteorological phenomena that may affect agriculture and offer warning for the possibility of a flood event to occur. The implementation of the NEXRAD system in the USA, has conducted to the improvement of short-range forecasts and warning of severe phenomena, such as tornadoes and flash floods, (Polger, et al., 1994; Serafin & Wilson, 2000). In Canada, the utilization of the Doppler radar has led to a considerable improvement on the forecast of severe weather. The direct measurement of wind elements enables the comprehension of the atmospheric state and evolution of precipitation systems, that contribute to an improvement of weather forecast and warnings of approximately 50%, (Joe et al., 1995).

The radar applications are expanding as hardware and data processing tools evolve, they are no longer limited to the hydrological processes that occur in the atmosphere but their data serves as input for processes that occur on the ground, such as flood forecasting. However, any perceived lack of accuracy of the quantitative measurements of the radar leads to a lack of confidence in the robustness of the data, requiring the adjustment of this value with rain gauges when possible. The following examples address these issues, by presenting two situations where the weather radar is used in flood forecasting, in Canada (Watfloof) and the UK (HYRAD).

Watfloof is a Canadian flood forecasting system that incorporates programs that enable real time use of radar data. It includes processes for a radar calibration model that adjusts the non-accurate radar measurements to the values measured by the ground truth tools, and a hydrologic simulation model that possesses an optimization algorithm to detect the best parameters considering the event occurring. This software provides the needed processing tools that allow the use of radar data along with the conventional used ones. This work, Kouwen, (1988), simulated two floods that occurred in Southern Ontario in 1977, using radar precipitation data. It was observed that when simulated, events characterized by uniform and widespread precipitation do not suffer relevant improvements, but on events with concentrated storms and located on watersheds with sparsely distributed rain gauges, great improvement on the detection of precipitation phenomena and on the calculated stream discharges was noted.

In the UK there is a plan to implement flood forecasting systems that use the radar information as input, (Moore, Cole & Robson, 2012). The operational use of the weather radar is achieved through the integrated system HYRAD (Hydrological Radar), that receives, stores and performs further processing of radar products from the Met Office, it also possesses a processing kernel that integrates a radar correction technique that consists of radar and udometer merging, since there is suspicion about the capacity of the radar to present quantitative measures. The results are used by the Environment Agency and the National Flood Forecasting System (NFFS) for England and Wales. The NFFS presents a set of regional flood forecasting systems at specific locations that is responsible for emitting the flood warning for each region. The use of radar for flood forecasting occurred by the application of a distributed model, Grid to Grid (G2G), that used the dynamic gridded rainfalls resultant from radar and rain gauge observations and weather models. This model was used as a complementary model to more detailed regional models by the Environmental Agency and the Met Office Forecasting Centre, due to the accuracy of the special variability displayed of the flooding and the temporal evolution of it, a situation that was not possible until this moment. However, when aiming for National calibration of the G2G model, it was noted that the estimators calculated using the radar data (raw or adjusted) were causing some difficulties in the model routine. It was observed that common errors associated with the radar, like beam blockage and discontinuity on the final mosaic that aggregated the data of different radars, were disturbing the G2G river simulations, and the removal of these errors was unsuccessful. In comparison, the udometers rainfall estimates provided the best outcome, without the mistakes

associated with the radar. In conclusion, this is a situation where the limitations of the rain gauges (only providing point estimation), were less pressing than the instrumental errors of the radar.

2.5.2 Use of Radar in Portugal

2.5.2.1 Portuguese Radar Network

In Portugal, the entity responsible for managing and operating the weather radar is IPMA. This public institute uses the radars to predict and monitor the different meteorological phenomena in national territory.

The Portuguese radar network is composed by five weather radars: Coruche / Cruz de Leão, Loulé / Cavalos de Caldeirão, Arouca, Madeira/Porto Santo and Açores/ Santa Bárbara, (Figure 2.12).

The continental weather radars are Cruz de Leão, that covers the centre of Portugal, Cavalos de Caldeirão, that monitors the south of Portugal and Arouca, that covers the north of the country. Two weather radars are installed in the Portuguese islands, the weather radar of Porto Santo which is responsible for the monitorization of the events occurring in Madeira, and the radar of Santa Bárbara that covers the Azores islands, this is the newest addition to the network and was implemented on the same location where the previously operational radar of the USA military was stationed,(https://www.ipma.pt/pt/educativa).

Figure 2.12 - Image of the Portuguese radar network. Source: https://www.ipma.pt/pt/educativa

The mentioned radars are band C systems, which means that they emit microwave radiation with a wavelength between 4 and 8 cm. This type of band is commonly used in Europe, due to the good relationship between cost and operational capability (capacity to detect and measure rainfall), even though its signal suffers slightly more attenuation than other bands. These are also Doppler radars, providing information regarding reflectivity and wind. The collected data are then transformed into precipitation maps of precipitation intensity or total rainfall and wind profile maps that contribute to the prediction and meteorological monitoring of atmospheric events, since they allow the identification of convective areas. The radar of Arouca is one of the most recently acquired instruments, possessing some functionalities that the other radars do not possess, like double polarization. Which permits the improvement on precipitation estimates, weather phenomena detection and capacity to distinguish

between different hydrometeors and other particles, like insects and dust, (Berne & Krajewski, 2012, Krajewski & Smith, 2002).

Since the meteorological phenomena does not respect political borders, IPMA also receives data from the Spanish radar network, which allows for an improvement of the prevision and monitoring ability of peripheral areas of Portugal Continental.

IPMA has a phased treatment of the data collected by the radar. First there is an initial raw data treatment in each radar station and a final processing that occurs in the IM headquarters. In order to assure that the data gathered by this system is as accurate as possible, IPMA executes radar preventing maintenance, calibration, and quality control. All the periodical procedures include the preventive maintenance (remote check) and the receiver calibration, but the while the daily checks are more focused on quality control procedures, the monthly, quarterly, semi-yearly and yearly procedures are more focused on the system monitoring, (Michelson et al., 2004).

2.5.2.2 Development of the Weather Radar in Portugal

The weather radar was first installed in Portugal, in 1969, in the city of Lisbon. The use of automated stations was only implemented in 1991.

Since then, the participation of Portugal in multiple projects of EUMETNET has encouraged the development of the methods and techniques that increase the accuracy of radar data in multiple hydrological processes, as well as the investment in advanced meteorological technology.

The first application of the weather radar in an operational weather was on the detection and following of the meteorological events, like heavy precipitation and strong wind and also on the monitoring and warning of the possibility of occurring a severe weather event, (Barbosa, 2006;Prior et al., 2008).

When aiming to model and forecast hydrologic events, a need to use accurate quantitative precipitation estimates arises, since it is precipitation that triggers events like floods. Alpuim & Barbosa, (1999), used two approaches to obtain accurate precipitation estimates, cokriging techniques and a model based on the Kalman filter algorithm. This last, suggests a three stepped radar adjustment model that aims to obtain accurate area precipitations estimates. This model starts by pre-calibrating the radar estimates using an exponential function, then applies the Kalman filter to calculate calibration factors and lastly, uses the factors to obtain the bias for all points of the radar grid. It resulted in the reduction in the error of radar estimates of rainfall and in most cases, an improvement on the areal rainfall estimations, which is a relevant issue in flood forecasting. Other works, like that Narciso, Silva, Moreira & Diogo, (2016) studied, uses a gauge adjustment technique to correct the estimations performed by the radar. This technique consists on calculating the difference between udometric and radar values and the corresponding pixel, these differences are then interpolated using normal kriging and the final product is added to the original product. It was observed that the application of the gauge adjustment method improved the precipitation estimates, since it allows for a better characterization of the spatial variability of the estimates.

The application of the weather radar in hydrological forecasting has been explored by Macedo & Hipólito,1997. In this work, forecast rainfall values, originated from the Lisboa/ Aeroporto radar, are used as the precursor of an alert system. When the precipitation predicted by the weather radar reaches a maximum defined value, a new level of warning is reached, where the data from the udometric stations is considered. If the discharges simulated using the forecast rainfall values and the udometric values exceed the defined flood threshold an alert is issued. This methodology was applied on the watershed of Alenquer and the discharge results imply this might be a good methodology to predict flooding events. Recently, Brandão, (2018) studied how the improvement of hydrological forecast modelling can reduce the vulnerability level of a society affected by a flood event. The goal was to increase the capacity of the system used by APA, to manage flood events at a selected location, by creating a method that would allow the anticipated emission of warning alerts and the increase of accuracy previsions. To achieve that, many hydrological models that simulated the response of the Lisbon watersheds under study, were calibrated. The rating equations were evaluated and recalculated, especially for higher discharges, different spatial distribution methods were tested, and the radar precipitation estimates were incorporated. Brandão,2018 defended that the increase of accuracy of prediction depended on the use of valid rating equations, for all stages of the event, the use of models calibrated with different combinations of rain gauges and consideration of spatial distribution using udometers, incorporation of the radar precipitation after calibrating the radar estimates, implementing precipitation forecast or the incorporation of distributed hydrological models, would increase the accuracy of the model and therefore emit a warning sooner. Additionally, the methodology used by Brandão can be applied to the rest of the Portuguese meteorological radars, allowing an improvement of the hydrological modelling and vulnerability reduction, all over the country.

In short, while the radar is already actively used for meteorological events prediction and warning, the use of it has a quantitative measurement tool and consequent use in hydrological measurement and forecast (at a quantitative level) is still not standard.

2.6 Hydrological Models

2.6.1 Hydrological Models. Theoretical Concepts

Models articulate apparent causal relations of an underlying unknown reality. Should its empirical core be proved as robust, it can be used as a predicting tool.

A hydrological model is an approximation to a real world hydrological system. Its inputs and outputs are hydrological variables and its structure are a set of equations that represent the hydrological processes that occur and connect the inputs and outputs, (Chow, 1988).The model receives input data in this particular case precipitation and other meteorological variables, operates the processes that depend on the input and generates an output, the discharge, all within a defined boundary , Figue 2.13. In addition to meteorological data, the model requires information regarding the drainage area, such as soil characteristics, land use, topography and type of vegetation (Chow,1988). The processes simulated in

this type of modelling includes precipitation loss and runoff generation. For the first action, the processes considered are infiltration, interception, soil storage capacity, groundwater recharge and evaporation. While the processes that contribute to the increase of runoff are the precipitation, return discharge and the overland discharge (surface runoff), (Beven,2012). Lastly, the output of this system is the final discharge.

In hydrological models, the precipitation – flood relation is mediated by the surface and underground water since these are the most difficult discharge values to account for.

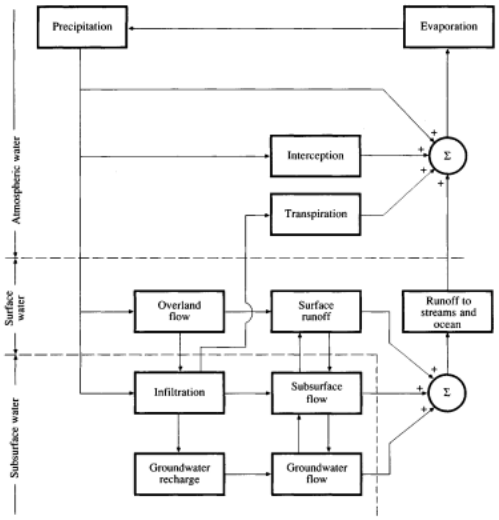

Figure 2.13-Hydrological System, (Chow, 1988)

Even if the structure (input, operator/process, boundary and output) is the same, the models can have different classifications, (Figure 2.14), depending on three factors: variables randomness, variables variation in space and variables variation in time.

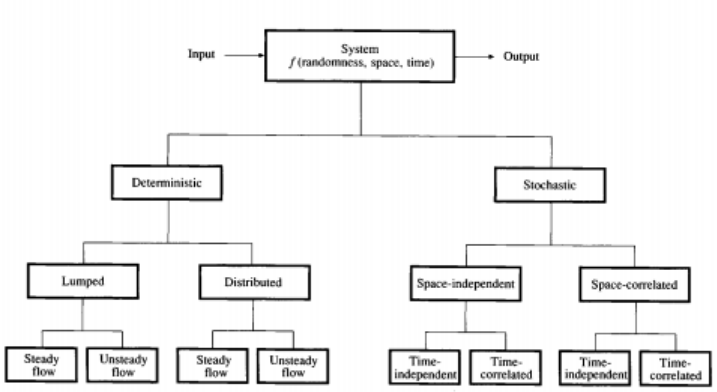

Figure 2.14-Classification of hydrological models, (Chow,1988)

According to the variable randomness, the models can be classified as deterministic or stochastic. Deterministic models do not consider variable randomness, making it a very good tool for forecast. The stochastic models are used in predictions, due to the ability to display output variability.

At a spatial variation level, deterministic models can be lumped or distributed. Lumped systems consider that the system is spatially averaged, while distributed models account for the spatial variability that the parameter may suffer. Stochastic models are classified as independent or correlated depending on the fact that the random variables can spatially influence each other, (Chow,1988).

When considering time variability, the deterministic systems may be classified as steady discharge or unsteady discharge. Steady discharge implies that the discharge rate is constant along the event simulated, while the unsteady discharge suggests that there are variations with time. Due to the randomness of variables attributed to the stochastic terms, these systems are always variable with time, and can be classified as independent or correlated. Equally to the spatial variability, the time-independent system represents non influenceable events, while the time-correlated represents models where the next hydrologic event is influenced by others, (Chow, 1988).

2.6.2 HEC-HMS

An example of a hydrological modelling program is HEC-HMS, which stands for Hydrologic Modelling System – Hydrologic Engineering Center. This software created by the United States Army Corps of Engineering, available at https://www.hec.usace.army.mil/software/hec-hms/, was created with the purpose of simulating the various hydrologic processes that occur in dendritic watershed systems, including infiltration, unit hydrographs and routing. Additionally, its latest versions can account for phenomena like evapo-transpiration and soil moisture, which are required for a continuous simulation.

This modelling system is classified as semi- distributed, because it presents spatial variability of the physical features throughout the watershed; semi-conceptual, considering the relation between the physical characteristics of the processes with the definition of parameters; discreet, due to the fact that it examines specific time intervals.

While this software allows for efficient computational processes, there are some limitations associated with the simplification of the model formulation and the discharge representation. In the model formulation, stationary parameters are assumed, and water losses and gains are calculated individually, i.e., some processes that may occur simultaneously are calculated separately. On the discharge representation, there is an inability to model ramifications of a river stream, since one element may only be connected to a single downstream element, and the discharge direction is considered unidirectional, not allowing the representation of backwater effects.

The software can be divided in three main components: watershed models, meteorologic models and time-series data. The watershed model is responsible for the physical characterization of the subcatchments. It is in this component that the canopy, surface, loss, transform and baseflow methods are defined. The canopy method represents the presence of plants in the landscape since they intercept

and extract water from soil. The surface method intends on representing the ground surface where water may accumulate in a depression storage. The loss method defines the equations that separate precipitation volumes from runoff excess, depending on the method chosen, different parameters will be required. The transform method is the method that converts rainfall (after subtracting the losses) into a streamflow. Finally, the baseflow method represents the shallow groundwater that can contribute to the stream discharge. The meteorological model determines the meteorological input for each subcatchment. Here, the weight that each gauge has on the watershed is defined. Lastly, the time-series data is responsible for storing the input data. In this component the precipitation values for each gauge are inserted, as well as the hourly temperature for the time interval under consideration, and the observed discharges, that will then be used to compare with the simulated ones and sometimes to execute optimization trials that maximize the watershed and routing parameters.

3. Methods and Data Analysis

3.1 Introduction

The focus of this work is the understanding of the contributions that the weather radar can provide to the field of hydrological modelling and flood forecasting.

The methodological approach used comprises the application of corrective equations to the original radar precipitation estimates, in order to increase the accuracy of the values estimated by the radar and assure they can be used as a reliable source of precipitation data. The gauge adjusted radar values and the udometric measurements are used as input on the program HEC-HMS. This program will then transform the precipitation data into discharge.

A consistency analysis is performed to the initial data provided by comparing the radar precipitation estimates and the rain gauge measurements at the gauge location, in a qualitative manner.

To understand the impact of the radar, two precipitation events that lead to floods were analysed. The first event occurred in February of 2016, while the second took place in December 2019, both in Águeda.

The radar data some rain gauge records were provided by the Instituto Português do Mar e da Atmosfera, while the river gauge data and remaining udometric records were supplied by the Agência Portuguesa do Ambiente.

3.2 Case Studies

3.2.1 Characterization of the Watershed

The events under study occurred in the city of Águeda, located in the centre of Portugal, more specifically in the sub-region of Aveiro. The city is located by the Águeda river that originates at Serra do Caramulo, in the parish of Varzielas (Oliveira de Frades), and converges into the Vouga river, downstream of the Águeda. The watershed under study is therefore a sub catchment of the Vouga river basin and belongs to the Hydrographical Region 4, managed by the Centre River Basin Authority, from APA.

The watershed boundaries and the drainage paths were determined using the tools available at ArcGIS, namely the ArcHydro and the HEC-GeoHMS extensions, using the digital terrain model (DTM), from nasa.gov, with a resolution of 30m, as an input, (Figure 3.1).

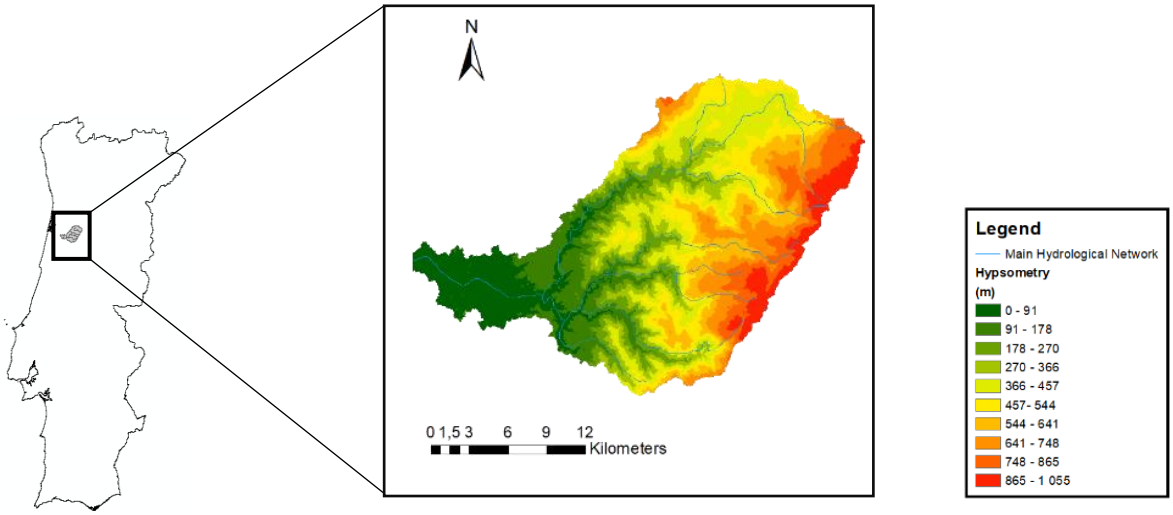

Figure 3.1- Location of the Águeda catchment in Portugal and hypsometry map of the area.

The watershed is divided in three main sections, defined by three main river cross-sections: Ponte Águeda, Ponte Redonda e Ribeiro, corresponding to existing river gauge stations. The sections of Ponte Redonda and Ribeiro are then divided in three subcatchments, (Figure 3.2).

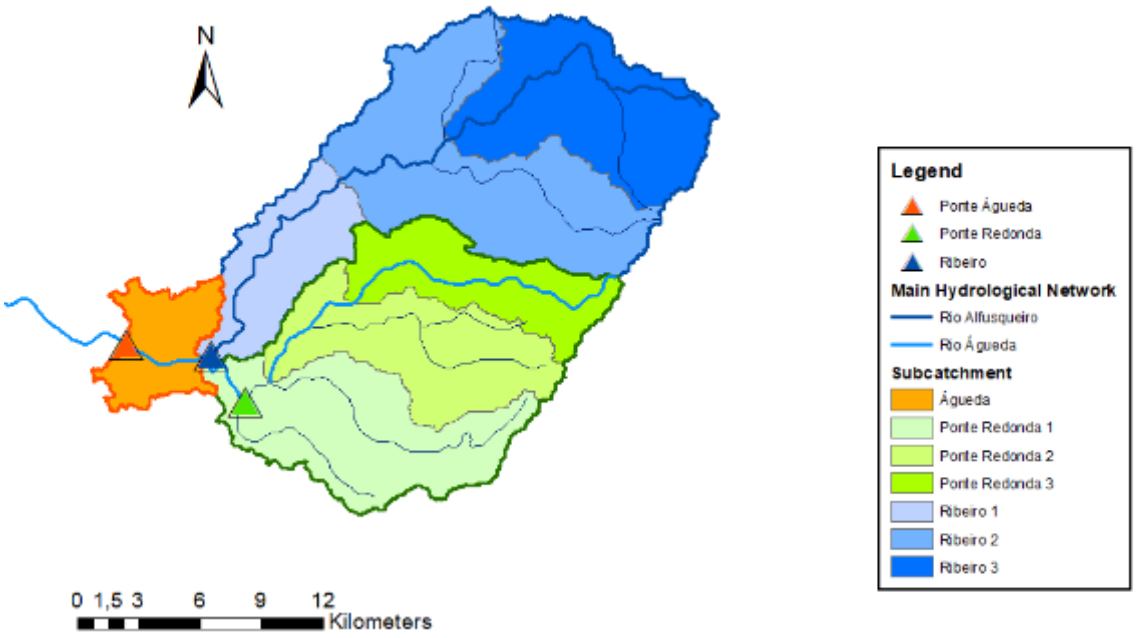

Figure 3.2-Delimitation of the hydrographical watershed and signalling of the river gauge stations.

Table 3.1 presents the main physiographical features of the subcatchments under study.

Table 3.1-Fundamental physiological characteristics of the subcatchments.

Watershed	Watershed Area (km^2)	Slope	River	River Length (km)	Elevation (m)
Águeda	25,24	0,0024	Águeda	4,45	10
Ponte Redonda 1	63,47	0,0058	Águeda	5,47	75
Ponte Redonda 2	51,79	0,011	Águeda	6,28	115
Ponte Redonda 3	36,31	0,0138	Águeda	15,82	166
Ribeiro 1	38,56	0,0052	Alfusqueiro	13,35	21
Ribeiro 2	96,38	0,016	Alfusqueiro	7,27	125
Ribeiro 3	70,93	0,023	Alfusqueiro	16,92	260

The soil texture of this region is highly homogenous and is classified as sandy-loam. The soil texture conditions the parameters of the soil loss component of HEC-HMS.

3.2.2 Selection of the hydrological event

3.2.2.1 Event of February 2016

The flood event of February 2016 caused great disturbance in the community of Águeda, affecting public services, road networks and the residents closer to the river, (Figure 3.3 and 3.4).

Figure 3.3-Image of flood event in Águeda. Published on Facebook at 12th Feb 2016, at 22:34h.

Figure 3.4-Image of flood in Águeda. Published by JN, on 12th Feb 2016, at 21:06h.

The origin of this disaster was attributed to the passage of a frontal perturbation, that possessed a stratified regime, that lead to heavy precipitation, between the 9th of February and the 16th of February. The total amount of precipitation that fell on the watershed was 353 mm, with 12th of February being the

day when the highest values of rainfall were measured. The subcatchment most affected by the precipitation was Ponte Redonda 3, where the precipitation was higher than in other sub catchments.

During the month before this event there has been an extended period of raining, which probably led to wet soil conditions or even soil saturation and exacerbated the watershed hydrological response.

The peak discharge in Águeda was reached on 12th of February, at 17h, when the station of Ponte Águeda measured a river gauge level of 5,87m.

3.2.2.2 Event of December 2019

In December 2019 the strong precipitation caused by the Elsa depression led to floods that once again affected the Águeda area, (Figures 3.5 and 3.6), causing the malfunctioning of several rainfall measuring instruments and even on some river gauge stations.

Figure 3.5-Image of flooding event in Águeda. Published by Jornal Soberania do Povo, on 20th Dec 2019, at 01:10h.

Figure 3.6-Image of flood in Águeda. Published by Publico, on 20th Dec 2019, at 10:56h

This event was also characterized by the passage of a frontal perturbation, but this time the precipitation regime identified was convective. From 16th of December to 23rd of December of 2019, the average total amount of precipitation that fell on the watershed was 194,1mm, with 19th of December being the day when the highest values of rainfall were measured. The subcatchment most affected by the precipitation was Ribeiro 3, which registered a total amount of precipitation higher than the other subcatchments.

According to the stations of Varzielas and Campia, persistent precipitation occurred in the period before this event, probably leading to soil wetness and even soil saturation, and exacerbating the watershed response and a more severe flood.

The peak discharge in Águeda was, on the 19th of December at 23h, when the river gauge station of Ponte Águeda measured a water height of 6,01m.

3.3 Data Analysis

3.3.1 Udometric Data

Records of precipitation at ground level were obtained from APA and IPMA (Figure 3.7).

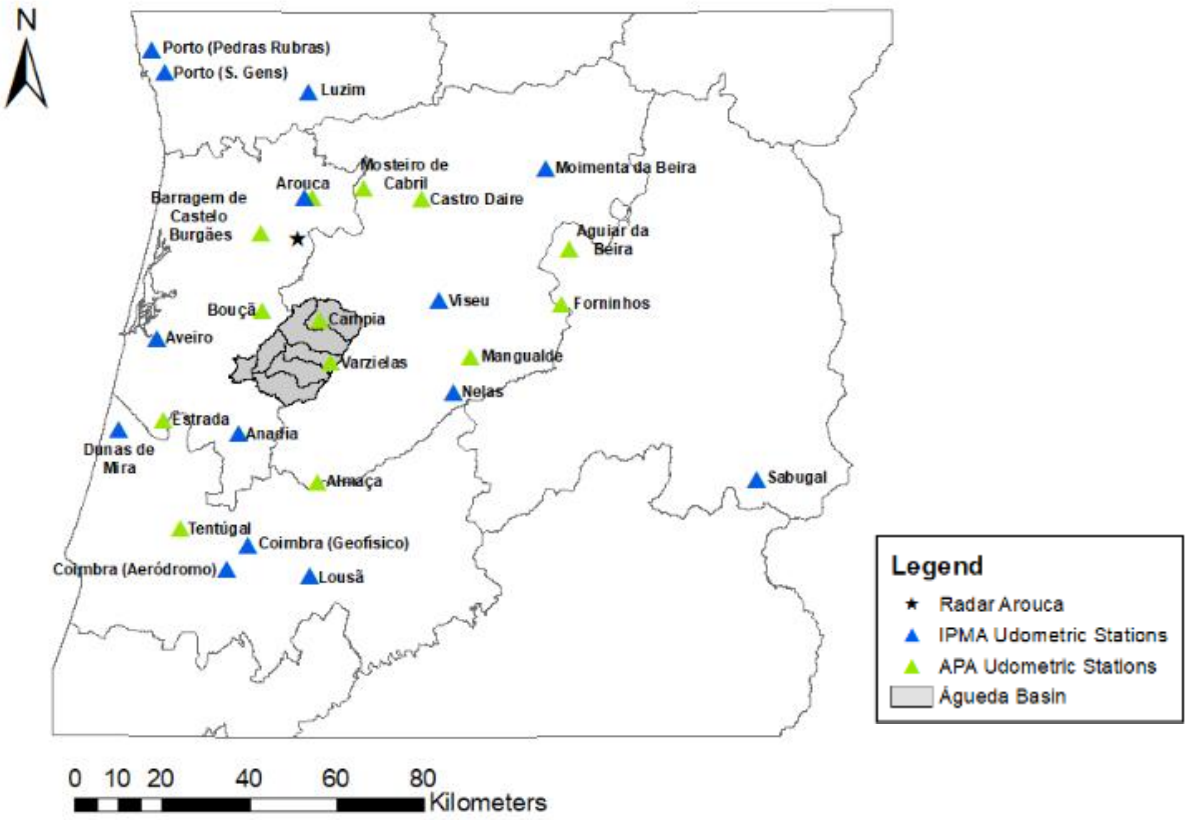

Figure 3.7-Location of the meteorological stations used in the event of 2016 and 2019

Both institutions possess instruments that record the rainfall measurements at a sub hourly scale, but in this work the data was aggregated to an hourly interval.

Table 3.2 presents the udometric records that were considered in this study. Due to gauge malfunction or data recording issues, not all rain records are available for both events.

Table 3.2-Identification and characteristics of the udometers considered in this study.

Designation of the stations	Code	Entity	Height (m)	Latitude (ºN)*	Longitude (ºW)*	APA Hydrographical Watershed	District	Event of 2016	Event of 2019
Aguiar da Beira	09L/01UG	APA	776	40,82	-7,54	Mondego	Guarda	√	√
Almaça	11H/01UG	APA	116	40,34	-8,23	Mondego	Viseu	√	×
Anadia	705	IPMA	45	40,44	-8,44	Vouga/Ribeiras Costeira	Aveiro	√	√

Table 3.2-Identification and characteristics of the udometers considered in this study.

Arouca	08H/01 UG	APA	355	40,93	-8,24	Douro	Aveiro	√	√
Arouca	669	IPMA	270	40,93	-8,26	Douro	Aveiro	√	√
Aveiro / Universidade	702	IPMA	5	40,64	-8,66	Vouga/Ribeiras Costeira	Aveiro	√	×
Barragem de Castelo Burgães	08G/01 C	APA	306	40,85	-8,38	Vouga/Ribeiras Costeira	Aveiro	√	√
Bouçã (Pessegueiro do Vouga)	09G/03 UG	APA	152	40,69	-8,37	Vouga/Ribeiras Costeira	Aveiro	√	√
Campia	09H/01 UG	APA	448	40,78	-7,92	Vouga/Ribeiras Costeiras	Viseu	×	√
Castro Daire (Lamelas)	08J/06 G	APA	697	40,92	-7,94	Douro	Viseu	√	√
Coimbra / Aeródromo	548	IPMA	171	40,16	-8,47	Mondego	Coimbra	√	√
Coimbra / Geofísico	549	IPMA	141	40,21	-8,41	Mondego	Coimbra	√	×
Dunas de Mira	704	IPMA	14	40,45	-8,76	Vouga/Ribeiras Costeira	Coimbra	√	×
Estrada	11F/02 UG	APA	45	40,46	-8,64	Vouga/Ribeiras Costeira	Aveiro	√	×
Forninhos	09L/02 UG	APA	498	40,70	-7,56	Mondego	Guarda	√	√
Lousã / Aeródromo	697	IPMA	193,769	40,14	-8,24	Mondego	Coimbra	√	√
Luzim	657	IPMA	287,174	41,15	-8,25	Douro	Porto	√	×
Mangualde	10K/01 UG	APA	512	40,60	-7,81	Mondego	Viseu	√	√
Moimenta da Beira	663	IPMA	715	40,99	-7,60	Douro	Viseu	√	√
Mosteiro de Cabril	08I/01 UG	APA	389	40,95	-8,10	Douro	Viseu	√	×

Table 3.2 -Identification and characteristics of the udometers considered in this study.

Nelas	685	IPMA	425	40,52	-7,86	Mondego	Viseu	√	√
Porto /Pedras Rubras	545	IPMA	69	41,23	-8,68	Leça e Ribeiras Costeiras	Porto	√	√
Porto / São Gens	649	IPMA	89,191	41,18	-8,64	Douro	Porto	√	×
Sabugal	800	IPMA	858	40,34	-7,04	Douro	Guarda	√	√
Tentúgal	12F/01 UG	APA	72	40,24	-8,59	Mondego	Coimbra	√	√
Varzielas	10H/02 G	APA	735	40,59	-8,19	Vouga/Ribeiras Costeira	Viseu	√	√
Viseu / Aeródromo	560	IPMA	636	40,71	-7,90	Vouga/Ribeiras Costeira	Viseu	√	√

*Geographical system: EPSG:3763 - ETRS89 / Portugal TM06 - Projetado

3.3.1.1 Spatial Interpolation of Udometric Rainfall Measurements

When using instruments like the rain gauges, that collect data at only one point, the application of spatial interpolation methods becomes essential to compute the mean areal precipitation for a catchment. For this work, two interpolation methods were used: Thiessen and IDW.

The Thiessen method relies on the creation of the so-called Thiessen polygons, using the udometers as connecting points. These polygons are then intersected with the watershed in study and the weight of each station is attributed according to the ration ($\frac{A_{polygon}}{A_{subbasin}}$). This ration is then multiplied with the precipitation measured by each udometer and the sum of these values declare what is the rainfall per subcatchment.

The IDW method, using a power parameter of two, assumes that values closer to the unknown point have greater weight than those that are further, i.e, the influence of the known points towards the unknown ones, declines with distance. The execution of this method consists on the attribution of the precipitation value on each of the udometer, the resulting raster that is generated by the ArcGIS is intersected with the studied watershed. Afterwards, the average of precipitation values per subcatchment is calculated.

The existence of two spatialization methods of the udometric data allows to comprehend how the precipitation calculated for each subcatchment varies and if the data collected by the radar presents results that are more similar to one process or the other.

3.3.2 Weather Radar Data

3.3.2.1 Weather Radar Options

The watershed under analysis, lies within the range area of two weather radar, Coruche and Arouca, (Figure 3.8).

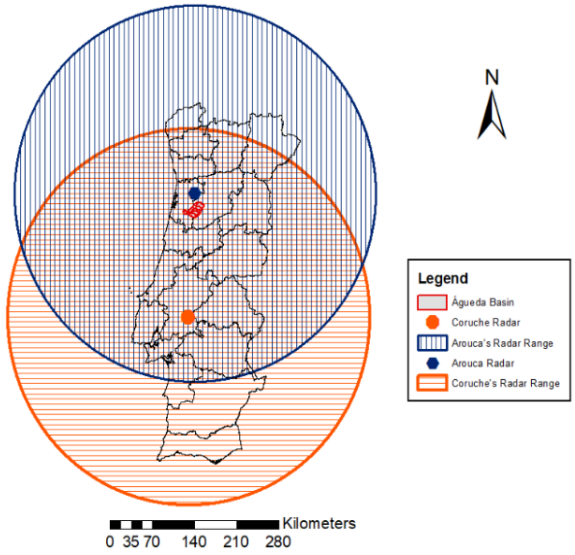

Figure 3.8-Representation of the area covered by each radar.

The weather radar of Coruche has been operating since 2000, in Cruz de Leão, (Geographical coordinates WGS 1984, 39,0724996 °N, -8,398889937 °W). It is a VR100 pulse radar and a Doppler magnetron band C system, that provides information about wind and reflectivity.
The weather radar of Arouca is located in Albergaria da Serra (Arouca), (Geographical coordinates WGS 1984, 40,844923 °N, -8,279637°W). This device is a WRM 200 doppler weather radar, with a dual polarization C-band magnetron, that provides data about wind and reflectivity. The dual polarization system, increases the precipitation measurement precision, making this device one of the most advanced weather radar in Portugal.

IPMA made available the radar records from both events as RAIN 1 products, which offer hourly precipitation estimates with a resolution of 1000x1000 m^2. These precipitation estimates are obtained using P-CAPPIs maps.

For the event of February 2016, the accumulated values were acquired with a periodicity of 5 minutes for the radar of Coruche, which implies the capture of 12 values per hour, while due to an anomaly on the information archive of radar Arouca, the precipitation values per hour were obtained with a periodicity of 10 minutes, 6 values per hour. For the event of December 2019, no anomalies on the archive were registered, and the accumulated precipitation data was acquired with a periodicity of 5 minutes for both radars. However, on the 21st of December, it was detected a failure on the data collection between 13h10 and 14h55. Before the comparison of the data collected by both weather

radars, the map precipitation files were filtered using a low pass filtering, median with a window of 3x3, An example of the effect of this filter is presented in Annex C.

3.3.2.2 Selection of Weather Radar

The selection of the weather radar was made taking into consideration theoretical and practical factors regarding the data accuracy of the weather radars. Jurczyk, et al., (2020); Friedrich, Hagen & Einfalt, (2006); Holleman and Michelson, et al., (2006), state that there is a loss of measurement accuracy with the increase of distance between object and the radar. The practical aspect analysed was the assessment of the relationships between the precipitation measurement data collected by the rain gauges and the rainfall measurement data determined by the radar of Arouca and Coruche.

The range reached by the radar, presented in Figures 3.9 and 3.10, is dependent on the vertical distance between the ground and the altitude of the radar beam, which increases with the horizontal distance. A large difference between altitudes increases the probability of occurrence of various phenomena, such as bright band effect, ground clutter contamination or overshooting of precipitation, which reduce the accuracy of precipitation measurement. The ideal pseudo-CAPPI height level to gather good estimates of precipitation intensity, stands between 800m and 1000m. At this altitude, the observation of precipitation is made as close as possible to the ground level, while assuring that these measurements are not crucially damaged by the presence of ground clutter.

On the radar of Coruche, the pseudo-CAPPI level used usually varies between 600 and 800m, because the altitude of the surrounding area is approximately 200m. Considering the use of the lowest elevation on the measurement of reflectivity, with a 0.1º angle, at a 100km range, the measuring altitude would be 1000m, therefore, the maximum range that allows the capture of good estimates is roughly 120km. Taking into account that the radar of Coruche is located at approximately 170km of the central point of the watershed, the measurements take place at a height of 2200m above ground, implying that at this range the estimates are no longer illustrative of the event.

The radar of Arouca is located at a higher altitude than Coruche. At an altitude of 1100m, this radar is surrounded by a complex orography that is also more elevated that the one found in Coruche. Although this is the configuration of the general region, the study area is located on a territory that is the exception. At an altitude level of 28m (in the city) and 9m (on the river level), this area is so low that the minimum beam altitude is of 1100m, because of the height difference of the radar and the study area. This radar is also located at only 26,11 km of distance of the centre of the watershed.

Thus, according to the theoretical criteria the radar of Coruche is less reliable.

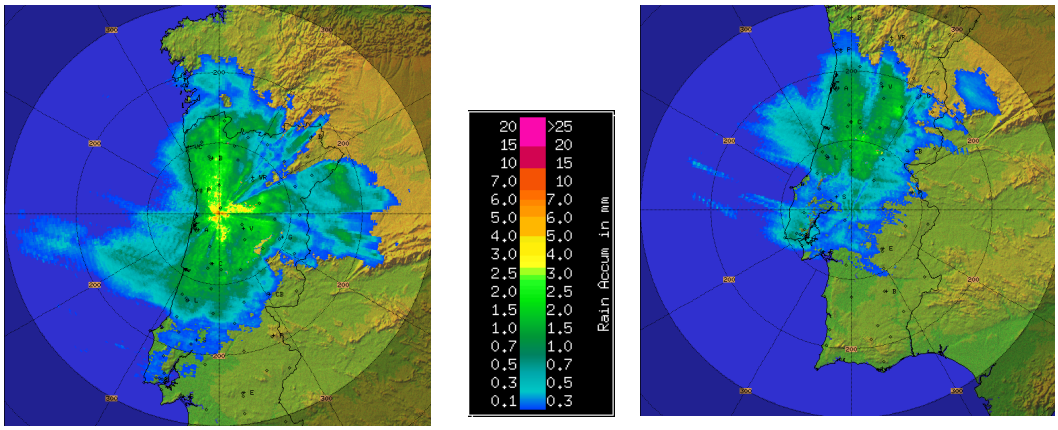

Figure 3.9-Precipitation map of 12/02/2016, at 13h, presenting the measurements of radar Arouca.

Figure 3.10-Precipitation map of 12/02/2016, at 13h, presenting the measurements of radar Coruche.

Graphs showing the relationship between weather radar and udometer measurements are presented in the annexes. Annex A includes the measurements of the 2016 event, and annex B of 2019. The radar measurements usually underestimate the udometer record, with Coruche radar presenting a larger underestimation error.

Figure 3.11 to 3.14 display the total dispersion cloud for the event of 2016. The underestimation of the radar measurement is again clearly visible in these graphs, specially of the Coruche radar. In addition, the data collected by the weather radar of Coruche is more disperse than the precipitation estimates executed by the Arouca radar, indicating that the correlation is weaker and the variation between the data collected by the udometers and the radar is more evident.

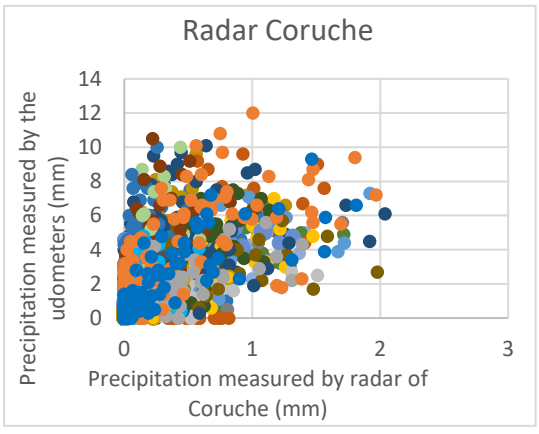

Figure 3.11-Dispersion graph that compares the udometric precipitation measurements with the Coruche radar estimates for the event of 2016.

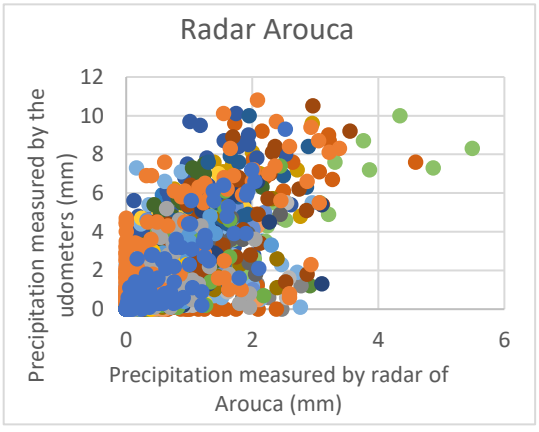

Figure 3.12-Dispersion graph that compares the udometric precipitation measurements with the Arouca radar estimates for the event of 2016.

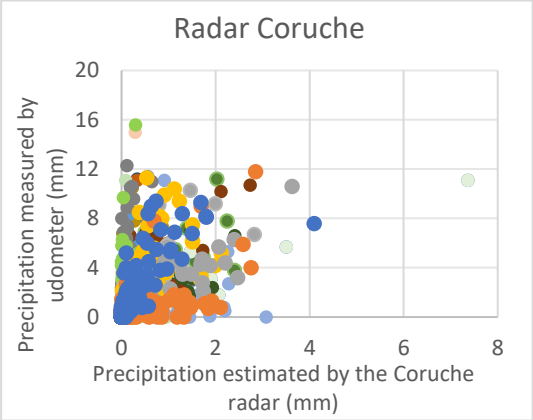

Figure 3.13-Dispersion graph that compares the udometric precipitation measurements with the weather radar of Coruche estimates for the event of 2019.

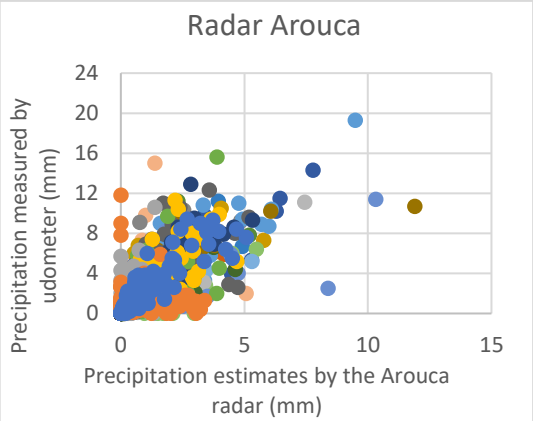

Figure 3.14-Dispersion graph that compares the udometric precipitation measurements with the weather radar of Arouca estimates for the event of 2019

Thus, the weather radar of Arouca was selected since it presented better results when considering both the theoretical and practical aspects.

3.3.2.3 Characteristics of Radar Arouca

Operating since 2015, the radar Arouca, (Figure 3.15), was installed with the goal of enriching the coverage of the northern region of Portugal, previously dependent on the Spanish installations, thus assuring a total coverage of continental Portugal by complementing the already existing radar network. This radar was also put in place to solve the under-detection problems found in the northern area. The technical characteristics of this device are presented in Table 3.3.

Table 3.3-Main Characteristics of the weather radar of Arouca.

Technical description	Characteristics of the radar
Transmitter	
Type	Coaxial magnetron
Operating Frequency Range	5,5 - 5,7 GHz
Peak Power	250 kW
Transmitter pulse widths	0.5, 0.8, 1.0, 2.0 µs
Transmitters pulse repetition frequency	200 - 2400Hz
Antenna	
Antenna type	Center-fed parabolic reflector
Antennas Diameter	4,5 m

Table 3.3 -Main Characteristics of the weather radar of Arouca.

Antennas Beam Width	< 1 degree
Pedestal	
Pedestal Elevation Range	-2 - 108 degrees
Pedestal Maximum Scan Rate	40deg/sec
Pedestal Position Accuracy	> 0,1 deg
RF to IF Receiver	
Radio Frequency to Intermediate Frequency Receiver Dynamic Range	> 115 dB option
Digital Receiver and Signal Processor RVP 900	
Radar Signal Processor Type	VAISALA SIGMET RVP900
IF digitizing	16bits, 100 MHz in 5 channels
Range Resolution	N*15m
Number of range bins	Up to 4200
Radar Controller	
Scans modes	PPI, RHI, Volume, Sector, Manual

Figure 3.15-Weather radar of Arouca. Photo taken by: Sérgio Barbosa.

3.3.3 Precipitation Correction

3.3.3.1 General Principles

This step intends on approximating the rainfall data to ground truth. To reach this goal, two different approaches were considered. The first method, named single equation, uses simultaneously the information collected by the udometers and the radar to deduce a relationship between the two measured values, in the form of a linear equation. The second method, named multiple equations, attends to the individual relationships also in the form of linear equation, between the radar and the chosen udometers measurements and relies on a spatial interpolation method, IDW.

The relationship between the weather radar and the rain gauge precipitation methods is dependent on the typology the precipitation event and amount of rainfall data considered, since different events may present different correction factors. Due to limited data and taking into consideration that on an operational context, only a general corrective factor is usually used, a common linear corrective equation was chosen per event.

To assess the performance of the gauge adjustment methods, the corrected radar values will be compared with the udometric measurements performed by the stations that surround the watershed, this comparison will account for the average accumulated precipitation per subbasin. To obtain rain gauge values per subbasin, the spatial interpolation methods IDW and Thiessen were used.

3.3.3.2 Single Equation

The single equation method takes into consideration all the values of precipitation measured during the events under study. For these values to be comparable and a relationship established, the weather radar values considered were measured on the exact location of the udometers used in this study. This step is achieved using the geographical program QGIS and the hourly precipitation maps provided by IPMA.

From the hourly precipitation data measured by both devices, a scatter plot is created, (Figure 3.16), with the radar data on the x-axis and the udometric data on the y- axis. To the resulting graph, a trendline is applied, its resulting equation is used as the corrective equation on the radar data. An empirical relation on the form of a linear equation was pondered:

$$P_{SE} = A\, P_r \tag{3.1}$$

where P_{SE} is the corrected precipitation value, A is a constant and Pr is the original radar precipitation value.

Thus, the corrective equation for this method is given by:

$$P_{sE} = 2.0431 * P_r \tag{3.2}$$

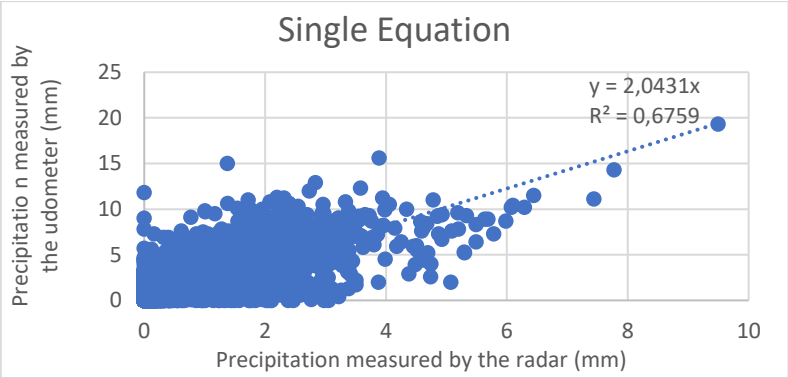

Figure 3.16-Single Equation scatter plot

The resulting equation is then used as a transformation to correct the raster files that represent the precipitation measurements of the radar, changing the value of each pixel according to this equation. The corrected raster files are then intersected with the watershed understudy and the new average values of precipitation per subcatchment are calculated. These corrected values per subcatchment will then be used as an input on the modelling program HEC-HMS.

A benefit of this method is that it does not require spatial interpolation, possibly reducing errors usually committed when interpolating precipitation fields with high spatial gradients. The disadvantage of this method is that it is less efficient in incorporating the spatial variability of rainfall.

On a statistical level, and in accordance with the r-squared coefficient, the statistical measurement chosen to evaluate the performance of the method based on how close the corrected data is to fit the regression line, 67,6% of the method variability can be explained by the regression model. This implies that this method is adequate to approximate the weather radar estimates to the udometers measured precipitation value, for the total data measured during both events.

3.3.3.3 Multiple Equations using IDW

This corrective method is slightly different from the previously explained one. Even though it still upholds the need to correct the radar precipitation values by approximating them to the ground truth values, analysing the relationship between these and extracting a corrective equation. This method relies on the use of distinct corrective equations that individually correct the radar files. Each equation displays the relationship between the selected udometer and the radar on the correspondent pixel, retrieved using the QGIS software. Thus, considering the hourly precipitation data measured by both devices, a scatter plot is created, (Figures 3.17 to 3.21), with the radar data on the x-axis and the udometric data on the y- axis. Considering the resulting graph, an empirical relation on the form of a linear equation was pondered for each rain gauge, Table 3.4. This equation is given by:

$$P_{ME} = A\,P_r \tag{3.3}$$

Where P_{ME} is the corrected precipitation value, A is a constant and Pr is the original radar precipitation value.

For this method, only the closest udometers were considered Anadia, Aveiro, Bouçã, Campia and

Varzielas, since these are the ones whose correction has a higher impact on the area studied.

Table 3.4 - Corrective equations applied to each pixel that possesses a udometer.

	Equations
Anadia	$P_{ME} = 2.3093\ P_r$
Aveiro	$P_{ME} = 1.9103\ P_r$
Bouçã (Pessegueiro do Vouga)	$P_{ME} = 2.2874 P_r$
Campia	$P_{ME} = 1.9406\ P_r$
Varzielas	$P_{ME} = 0.8358\ P_r$

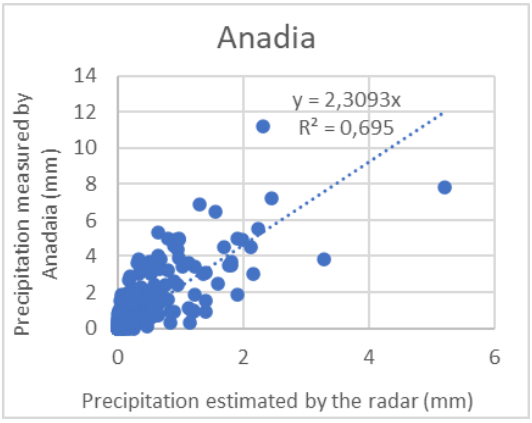

Figure 3.17- Scatter Plot of Anadia.

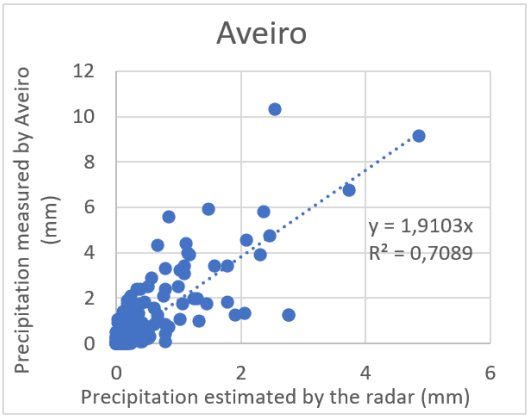

Figure 3.18- Scatter Plot of Aveiro.

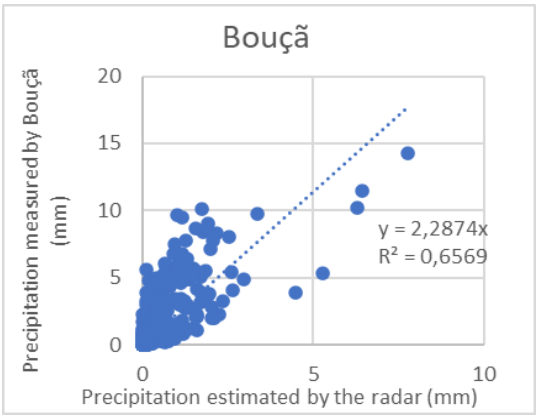

Figure 3.19 - Scatter Plot of Bouçã.

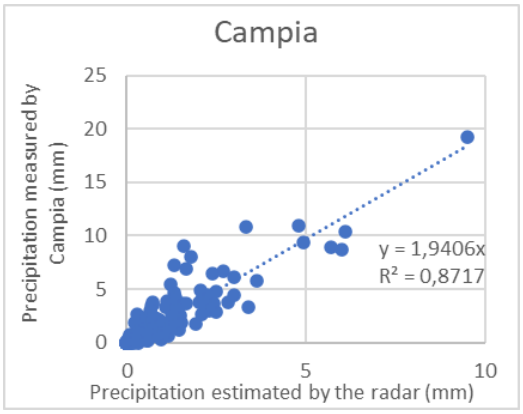

Figure 3.20- Scatter Plot of Campia

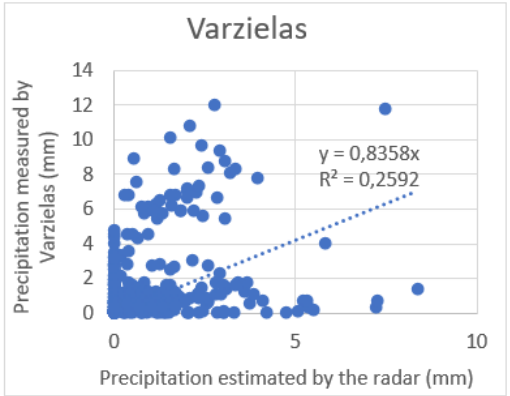

Figure 3.21 -Scatter Plot of Varzielas.

Each equation is then applied to the original precipitation map. As the goal of this method is to be applied equally in all the flood events, even though the station of Campia only collected data in 2019, the corrective equation of Table 3.4 of this udometer, will still be used to correct the precipitation maps of 2016.

Since these equations are solely connected with one udometer, the IDW method was used to calculate the weight, inverse squared distance, that each pixel has on the final transformed precipitation map.

The interpolation method assumes that values closer to the unknown point have greater weight than those that are further, i.e., the influence of the known points towards the unknown ones, declines with distance. This interpolation function is given by:

$$Pcorr = \sum_{j=0}^{n} wj.P_{ME} \tag{3.4}$$

where wj, represents the weight function. This function is given by:

$$wi = \frac{{h_i}^{-2}}{\sum_{j=0}^{n} {h_j}^{-2}} \tag{3.5}$$

In this function, the h_j represents the distance from the dispersion points to the interpolation point, given by:

$$h_{ij} = \sqrt{(x - x_{ij})^2 + (y - yj)^2} \tag{3.6}$$

where (x, y) are the coordinates of the interpolation point and (x_{ij}, yj) are the coordinates of each dispersion point.

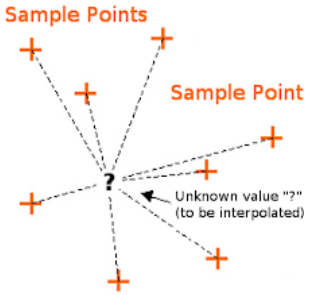

Figure 3.22-Inverse Distance Weighting Method. Souce: https://docs.qgis.org/3.4/en/docs/gentle_gis_introduction/spatial_analysis_interpolation.html

The resulting raster files are intersected with the watershed file and the new and the new average values of precipitation per subcatchment are calculated. These corrected values per subcatchment will then be used as an input on the modelling program HEC-HMS.

Table 3.5 presents the determination coefficient of the equation generated for the selected udometers.

Table 3.5 - Coefficient of determination for each udometer corrective equation of the Multiple Equations Method, on the events of 2016 and 2019.

Udometers	r^2
Anadia	0,70
Aveiro	0,71
Bouçã (Pessegueiro do Vouga)	0,66
Campia	0,87
Varzielas	0,26

On a statistical level this analysis is quite inconclusive since the performance of this method is deemed as unsatisfactory for the stations of Varzielas, and good for the rest. The fact that the r^2 value is so small for the rain gauge of Varzielas is quite concerning because this is a station that is located within the watershed boundaries and will have a big impact on the final data, especially for the subcatchments of Ponte Redonda and Ribeiro.

3.3.3.4 Considerations about the quality of radar data

Effects of precipitation regime and sources of error

Raw radar data underestimates precipitation in both 2016 and 2019 events. This problem is a lot more evident in the event of 2016. According to IPMA, both precipitation events were the result of the passage of frontal perturbations, however, different precipitation regimes characterized each phenomenon. While in 2016 the rainfall regime was defined as stratified, in 2019 it was classified as convective.

The divergent regimes also affect the difference between the precipitation estimates of the radar and the measurements of the rain gauges, the event of December 2019 presents more expressive values in both measuring instruments than in February 2016, due to intense vertical movements and higher precipitation intensity. Therefore, it is possible to verify that there was a decrease of precipitation underestimation from February 2016 to December 2019, part of the credit of this observation is due to the use of the same Z-R relationship applied, $Z=200R^{1,6}$,to estimate the value of precipitation intensity per hour, independently of the precipitation regime, which is a common practice in operational environment.

Even though it is usual to observe an underestimation of the estimates by the radar, there were some occasions were an overestimation is noticed, these fewer common observations are usually associated with the existence of fixed clutter. The overestimation of precipitation measurements on the location of the udometric stations of Barragem de Castelo Burgães, Coimbra/Aeródromo and Nelas was partially attributed to the presence of moderate to strong (> 15dBZ) fixed echoes. This circumstance can justify the presence of non-filtered residual clutter that can lead to the measurements of accumulated values that overestimate the rainfall estimates made by the udometers, particularly in situations with low real precipitation.

Impacts on the quality of the Single Equation method

The single equation method considers a general factor that is to be multiplied by all hourly precipitation maps. The results of this multiplication are then used as input on the hydrological model.

This factor is dependent on the information collected by the weather radar and the udometers during the whole event. However, when considering the relations between these devices for each udometer and event, it is possible to note that they are extremely variable, Annex K.

When considering the event of 2016, the equation coefficients can have values from 1,2 to 4,3. Within the same event this is a relevant variation that will have a big impact on the general factor to be used. This variation may be connected with the type of precipitation regime associated with the event, a stratiform regime indicates widespread coverage and weak reflectivity gradients that affect the radar precipitation estimated by the radar and therefore affect the factors. For the event of 2019, these individual factors were not as variable, fluctuating between 1,5 and 2,3, except for Varzielas where the corrective factor is only 0,4, which will be explained further on. The limited variability may also relate to the regime, since a convective regime is related with higher reflectivity values, therefore, less probability of the radar missing the precipitation. The precipitation regime along with other factors, such as the presence of clutter or the orography, may affect the performance of the weather radar and therefore affect the pixel value considered.

When joining the precipitation data of both events, the relations previously mentioned will influence each other. While only considering the event of 2016 the general fact to be used would be 2,6, however, the event of 2019 does not have individual factor values as high as the previously mentioned event, which means that the general correction equation used will have a lower constant, in this case, 2,0431. The decrease of the factor used contributes to the underestimation of the precipitation values, since the correction applied will be insufficient for the radar to achieve the rain gauge results.

Impacts on the quality of udometer factors for the Multiple Equation method

The multiple equations method uses a factor that only takes into consideration the data measured at the selected udometers and on the correspondent pixel, as mentioned in chapter 3.3.3.3.

Once again, the consideration of the precipitation that fell on both events, affects the factors used. Similarly to the previous situation, when considering the individual equations from each event separately, the factor reduces from 2016 to 2019, in most of the cases. This decrease leads to an insufficient correction of the radar precipitation for the first event, that is especially felt due to Varzielas. On this station, the factor from 2016 is equal to 2,9, while the factor from 2019 only reaches 0,4, resulting in a general corrective equation for both events with a factor of 0,84. Since it is one of the stations with most weight within the basin, a final factor under 1, can have a great impact on the precipitation results.

Due to the extreme decrease between factor values from one event to the other, the station of Varzielas was carefully analysed. It was observed that the pixel where this udometer is located was affected by different phenomena in both events.

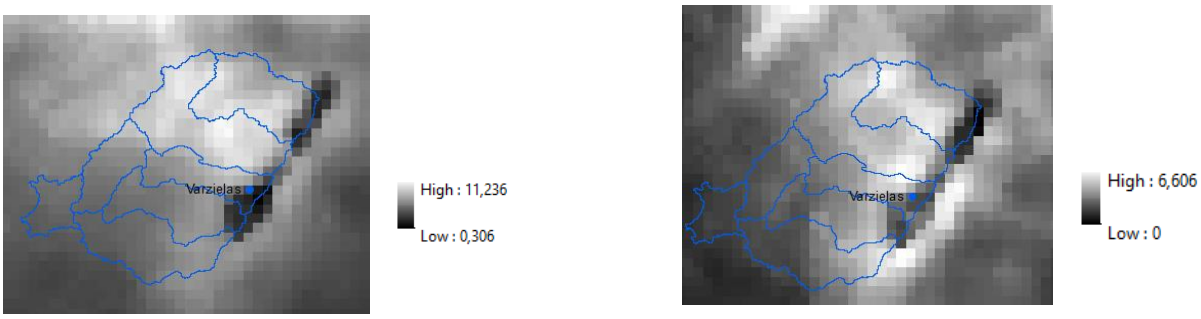

Figure 3.23-Accumulated Precipitation Map of the 9th (left) and 11th (right) of February 2016.

In 2016, an anomaly was detected that affected the Varzielas pixel. Figure 3.23 presents two days, 9th For the event of 2019, the opposite was detected. It was found that during some periods of time, mainly on the 17th of December 2019, there were some interferences or maybe even clutter on the basin that caused the radar to detect excessive precipitation on the basin when the udometers wither have no collection of these precipitation or the precipitation measured by this device is quite lower, Figure 3.24.

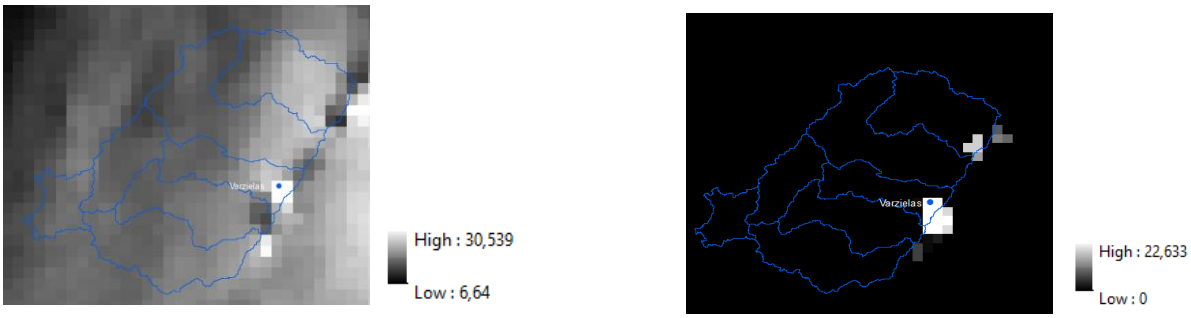

Figure 3.24- Accumulated Precipitation Map of the 16th (left) and 17th (right) of December 2019.

These effects that occur and affect the precipitation correction value are very important to be accounted, especially when they occur in one of the most important rain gauges that are being considered. The station of Varzielas is one of two that is located within the basin and has a heavy weight on the correction of data, with its ration affecting multiple subcatchments. The corruption of the data measured at this pixel alerts for the dangers of only considering a pixel to as the sole data provider.

3.3.4 River Gauge Data

The river gauge data relevant to this work was collected at three river gauge stations: Ponte Redonda, Ponte Águeda and Ribeiro, whose characteristics are presented in Table 3.6. These stations are equipped with automatic sensors which measure the river gauge level at every hour, except when a critical threshold is reached, and the measurement time step is reduced. The hourly records obtained from APA (Annex E and F) present the hourly averages of the values above the critical threshold. The discharge values were obtained from these records, using the rating curves presented in snirh.pt.

Table 3.6 - Main Characteristics of the river gauge stations

SNIRH River gauge Station	Code	Latitude(ºN)*	Longitude(ºW)**	City	Hydrographic Watershed	River
Ponte Águeda	10G/02H	40,571	-8,448	Águeda	Vouga/ Ribeiras Costeiras	Águeda
Ponte Redonda	10G/05H	40,566	-8,398	Águeda	Vouga/ Ribeiras Costeiras	Águeda
Ribeiro	10G/03H	40,546	-8,378	Águeda	Vouga/ Ribeiras Costeiras	Alfusqueiro

*Geographical system: EPSG:3763 - ETRS89 / Portugal TM06 - Projetado

A verification of the occurrence of data failure was carried out and the results are displayed on Table 3.7.

Table 3.7-Failure to measure the river gauge level by river gauge stations on the events of 2016 and 2019.

SNIRH River gauge Station	Code	Event of 2016	Event of 2019
Ponte Águeda	10G/02H	No data failure	No data failure
Ponte Redonda	10G/05H	No data failure	Data failure: 16/12/2019 (00h-10h)
			16/12/2019 (17h) - 17/12/2019 (08h)
			18/12/2019 (17h) - 19/12/2019 (12h)
			19/12/2019 (14h) - 20/12/2019 (10h)
Ribeiro	10G/03H	Data failure: 14/02/2016 (00h – 17h) 15/2/2016 (17h) - 16/2/2016 (14h)	Data failure: 19/12/2019 (20h) - 23/12/2019 (22h)

The river gauge records contain some gaps. Considering in particular, the event of December 2019 possesses multiple data failures, due to data collection failure of the Ponte Redonda station and damage of the river gauge station of Ribeiro.

Each of the river gauge stations previously mentioned has a rating equation or equations, associated with it, Table 3.8.

Table 3.8 -Table with the rating equations and the criteria validity for each of the river gauge stations. Legend: Q= discharge (m3/s), h(m)=height, H0=river gauge height for which the discharge is zero, Hmin/max= minimum/maximum height for the application of the equation/reach

River gauge Station	Rating Equation	Validity Criteria			Origin
	$Q=a\times(h-h0)^{b}$	H0 (m)	Hmin(m)	Hmax(m)	
Ponte Águeda	$Q=10{,}065\times (h + 0{,}384)^{1{,}538}$	-0,384	-0,384	2,3	Autoridade Nacional da Água
Ponte Redonda	1st Reach $Q= 11.07945 \times (h – 0{,}877)^{2{,}35134}$	0.877	0,877	2,2	Direção Geral dos Recursos Naturais
	2nd Reach $Q= 1{,}1235 \times (h + 0{,}64)^{2{,}83784}$	-0.64	2,22	5	
Ribeiro	1st Reach $Q = 16{,}22209 \times (h – 0{,}80482)^{2{,}39444}$	0,80482	0,80482	1,82761	Direção Geral dos Recursos Naturais
	2nd Reach $Q = 4{,}63162 \times (h - 0)^{2{,}16824}$	0	1,82761	4,5	

Table 3.9 identifies the periods when the river gauge level exceeds the validity range of the rating curves and when the discharge estimates become less accurate.

Table 3.9 -Identification of the time periods where the rating equation is invalid due to water height being superior to equation's Hmax.

River gauge Station	Situations where h>hmax	
	Event of 2016	**Event of 2019**
Ponte Águeda	09/02/2016 (16h35) - 16/02/2016 (22h45)	16/12/2019 (00h)-18/12/2019 (16h)
		18/12/2019 (23h) - 19/12/2019 (22h)
Ponte Redonda	12/02/2016 (09h) - 13/02/2016 (01h)	20/12/2019 (16h)
	13/02/2016 (04h - 19h)	21/12 (06h)
Ribeiro	10/02/2016 (13h - 16h)	16/12/2019(02h - 07h)
	11/02/2016 (09h - 11h)	
	12/02/2016 (10h) - 13/02/2016 (22h)	19/12/2019 (08h - 19h)

The Figures 3.25 to 3.28 display in red the time intervals where the water height measured is higher than the maximum height valid for the equation used. It is possible to verify that this circumstance occurs mainly on the peak discharges, inferring that the discharge resulting from the rating equation is no longer accurate. However, since there is no information about an adequate equation for these occasions, the presented equations will still be used to transform water height into discharge, acknowledging, however that the uncertainty in the values of discharge is higher.

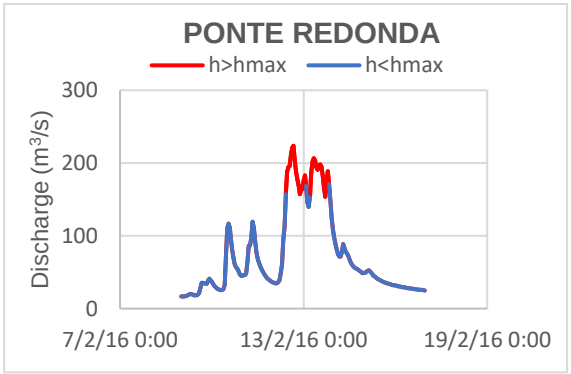

Figure 3.25-Graph of the observed discharge in Ponte Redonda, in 2016

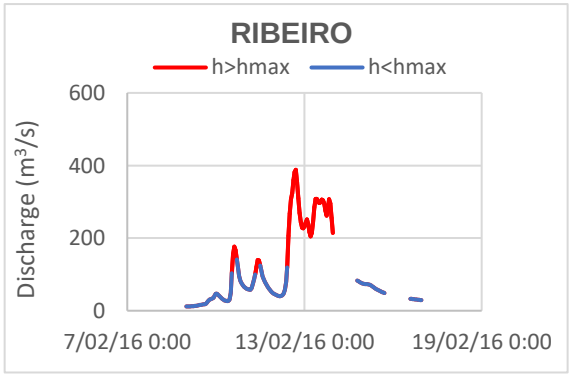

Figure 3.26-Graph of the observed discharge in Ribeiro, in 2016

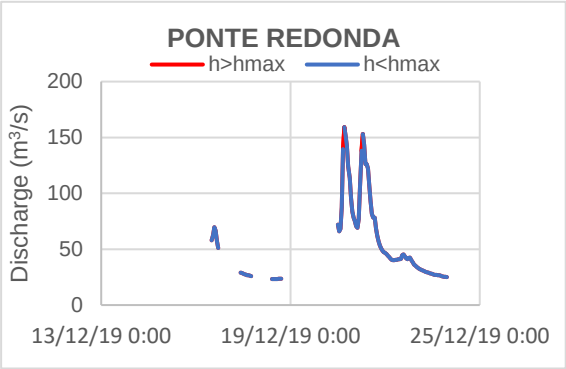

Figure 3.27 -Graph of the observed discharge in Ponte Redonda, in 2019.

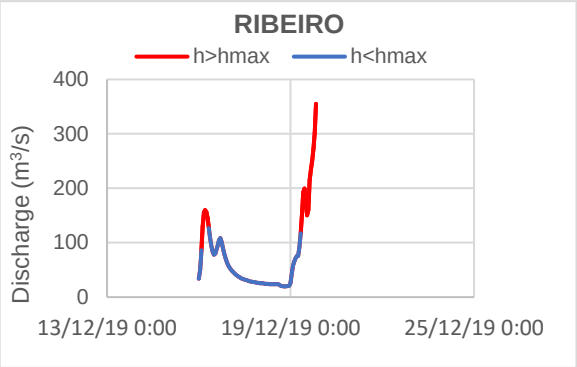

Figure 3.28-Graph of the observed discharge in Ribeiro, in 2019.

It is also important to note that according to data available at snirh.pt on July 2020, Ponte de Águeda rating curve has not been updated since 2014. This indicates that the estimated discharges using this curve may be associated with significant errors. However, since no other alternative equation was provided, this rating curve was still used to transform river gauge levels into observed discharges. As a result of this situation, the discharge simulated by the program HEC-HMS will suffer no parameter calibration, unlike the other stations that will be calibrated according to the observed values.

4. Results and Discussion

4.1 Precipitation

4.1.1 Event of 2016

4.1.1.1 Results of the 2016 Event

The resulting precipitation values of the application of the corrective equations, mentioned in chapter 3 (equation 3.2 and equations of the Table 3.4), are presented in the Figures, 4.1 to 4.7. The numeric data can be found in Annex G. These graphs display the cumulative average daily precipitation per subcatchment calculated using the udometric information (IDW and Thiessen), the original radar values (raw radar) and the corrected radar data (Single Equation and Multiple Equation). The observation of These figures reveal that the radar values (original and corrected) underestimate the precipitation that fell over a subcatchment.

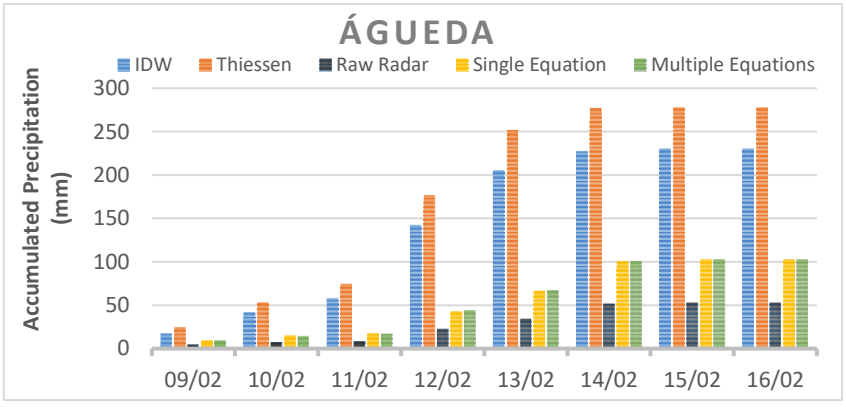

Figure 4.1-Accumulated Precipitation on the Águeda subcatchment.

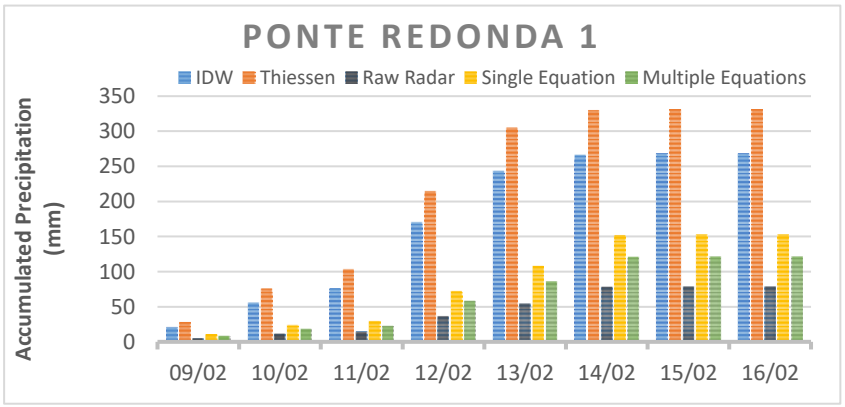

Figure 4.2-Accumulated Precipitation on the Ponte Redonda 1 subcatchment.

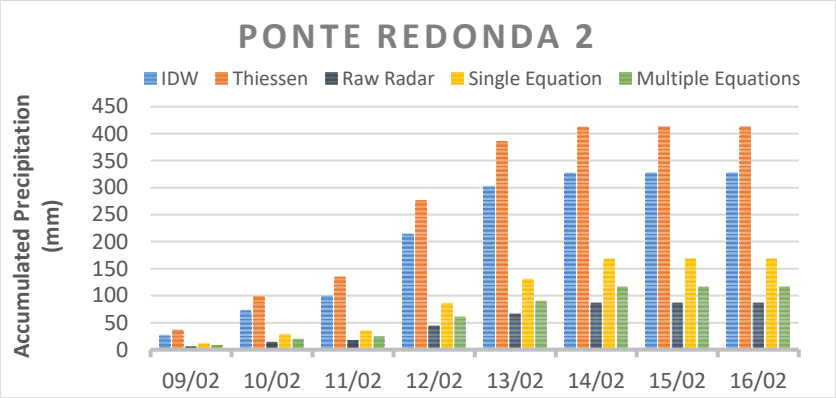

Figure 4.3-Accumulated Precipitation on the Ponte Redonda 2 subcatchment.

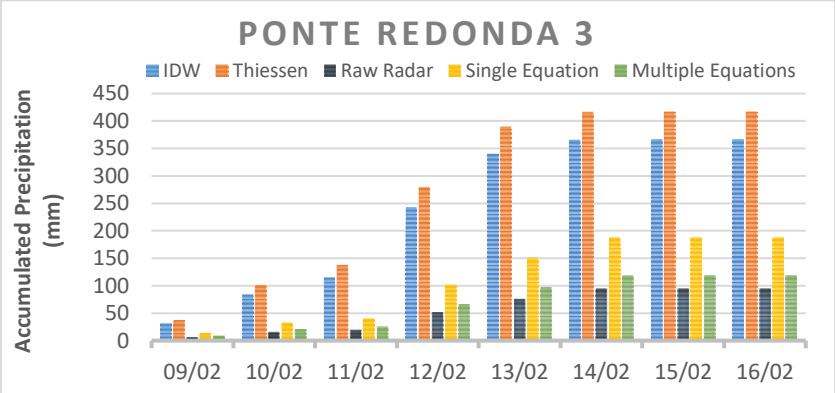

Figure 4.4-Accumulated Precipitation on the Ponte Redonda 3 subcatchment.

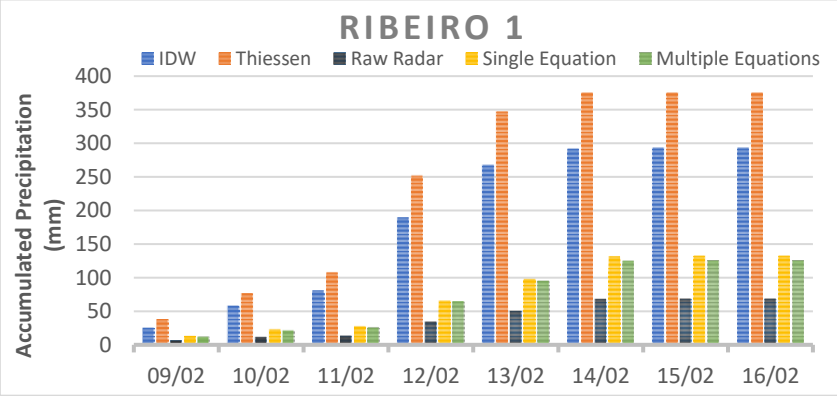

Figure 4.5-Accumulated Precipitation on the Ribeiro 1 subcatchment.

.

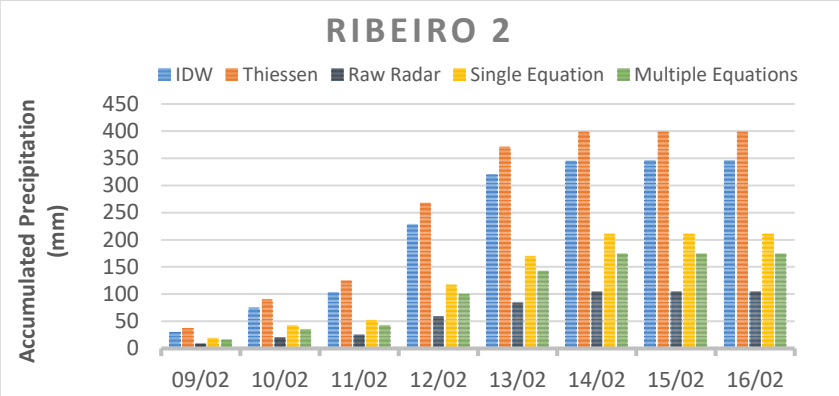

Figure 4.6-Accumulated Precipitation on the Ribeiro 2 subcatchment.

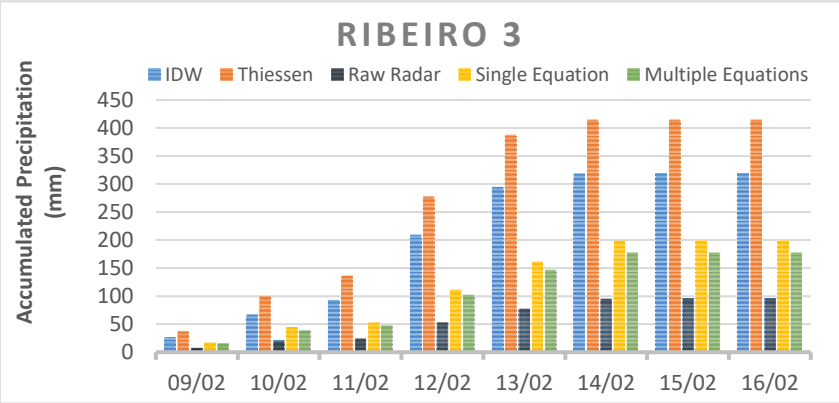

Figure 4.7-Accumulated Precipitation on the Ribeiro 3 subcatchment.

4.1.1.2 Discussion of the 2016 Event

General Discussion

The application of the gauge adjustment methods, Single Equation and Multiple Equations, originated results that react differently between subcatchments, as it can be observed by the graphics 4.1 to 4.7.

Focusing on the data used as the ground truth, the two interpolation methods permitted to comprehend that the areal interpolation method considered can affect the volume of precipitation that will be accounted to have reached the surface. In this method, the Thiessen method measures higher total volume of rainfall for this event. This occurs probably because the Thiessen method fixes the precipitation value over the subcatchment, while the IDW considers the information of more udometers and how the distance affects the pixel values.

The comparison between original weather radar estimates and the measurements executed by the udometric stations permits to conclude that the radar underestimates the total volume of rainfall during either event. This underestimation is extremely evident in situations when the precipitation intensity is higher, and more subdued when it is low, mainly when the storm is reaching its end. This result agrees

with what many authors such as Gjertsen, Šálek & Michelson, 2004; Wilson & Brandes, (1979), had already noted, which is that the radar tends to underestimate the heavy precipitation period and sometimes overestimates the final light rain phase, if no correction is applied.

As mentioned on the third chapter, the degree of underestimation suffered by the weather radar data, in this event, is believed to be strongly related with the precipitation regime observed. Since this precipitation event is characterized by its stratified regime, which is a regime that is susceptible to cause systematic errors due to bright band effect, attenuation over areas of continuous precipitation and a steep vertical gradient of reflectivity that causes range dependent bias, causing the underestimation of precipitation estimates by the weather radar, (Šálek et al., 2004).

As expected, the application of the corrective equation methods increases the estimation values of the weather radar, reducing the difference between the ground truth and altitude measurement. This decrease, even if small, is variable depending on the subcatchment considered, supporting the statements that the spatial distribution of the rainfall is usually irregular, (Hillel and Hatfield, 2005). Nonetheless, the application of these gauge adjustment methods is clearly insufficient to reduce the difference between measurements for a neglectful value.

Method 1 – Single Equation

The implementation of the single equation method doubled the total amount of precipitation estimated by the weather radar, accordingly to the 2.0431 factor used to correct the original values.

The difference between the corrected radar data and the rain gauge measurements, accounting for either spatial interpolation technique, is variable along the event. It relates to the original radar data and how close the estimate was to the udometric value. Thus, it was observed that in situations where the original radar estimates are similar to the udometers measurements, mostly when the event is reaching its end and the rainfall is starting to dwindle, this corrective equation causes a slight overestimation of the precipitation calculated, but considering the low values, it is not very significant. On the other hand, during periods of increasing and high precipitation, the corrected values are unable to reach the values measured at the rain gauges, resulting in visible underestimation.

Some of this underestimation is attributed to the use of a single corrective factor for both events. As previously mentioned in the general considerations, the events have different characteristics, when considering an equation that accrues from both case studies there is a loss of the individual characteristics, resulting in an ineffective correction. Since the event if 2016 has a bigger difference between the rainfall data measured by both devices, this implies that this event would require a higher corrective factor than the one used.

In conclusion, the application of this method was insufficient to reach acceptable representative values.

Method 2 – Multiple Equations

Similarly to the previous method, this one also led to a small increase of the precipitation volume that is attributed to the original weather radar estimates, even if less evident for some subcatchments.

The difference between the corrected radar data and the rain gauge measurements, accounting for either spatial interpolation technique, is even more variable along the event, due to the IDW technique used in this method. Ergo, it was observed that in subcatchments like Águeda and Ponte Redonda 1 this method offers values quite similar to the ones presented by the single equation method, while the remaining subcatchments present an even lower total of rainfall per subcatchment.

Once again, some of this underestimation is attributed to the use of a single corrective factor, per chosen udometric station, for both events. Another aspect that influenced the corrected values, and even the corrective factor used, was the existence of an attenuated region that crosses over the pixel where the udometric station of Varzielas is located, and that lasts for almost half of the event. This station is one of the most important sources of information, since is the one of the few that is located within the studied watershed, the loss of this data can give origin to an unrepresentative corrective factor, which impacts the whole corrected data, especially when considering that the station of Varzielas is the one that has higher weight overall the watershed. As previously discussed, the station of Varzielas also overestimates the event of 2019, which implies a corrective factor under one. When combining the events data, the final factor is also under one, resulting an underestimation of an already underestimated event.

In conclusion, the application of this method has also demonstrated to be insufficient to reach representative radar precipitation estimates.

4.1.2 Event of 2019

4.1.2.1 Results of the 2019 Event

Similarly, to the event of 2016, the results from the application of the corrective equations, mentioned in chapter 3 (equation 3.2 and equations of the Table 3.4), are presented in Figures 4.8 to 4.14. These graphs display the cumulative average precipitation per subcatchment calculated using the udometric information (IDW and Thiessen), the original radar values (raw radar) and the corrected radar data (Single Equation and Multiple Equation). Even though they do not allow the monitoring of the precipitation along the event, these graphics permit the understanding of when radar values (original and corrected) underestimate and overestimate the precipitation considered to have fallen on the subcatchments.

The precipitation data can be found in Annex H.

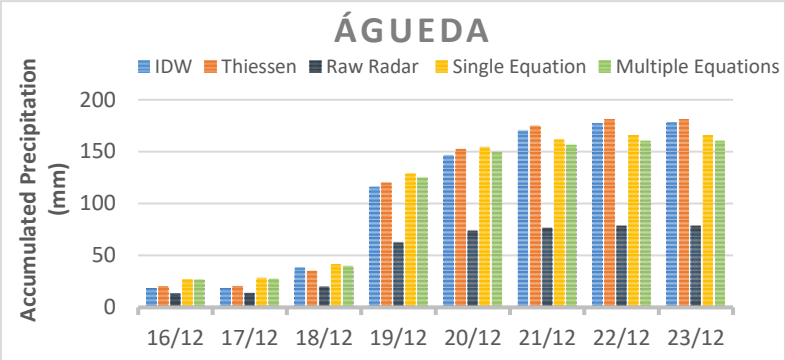

Figure 4.8-Accumulated Precipitation on the Águeda subcatchment.

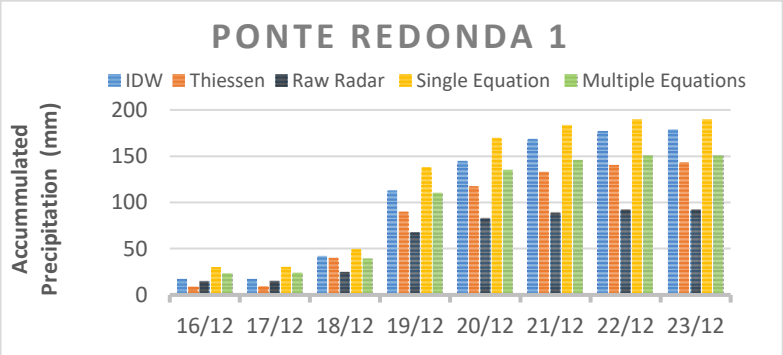

Figure 4.9-Accumulated Precipitation on the Ponte Redonda 1 subcatchment.

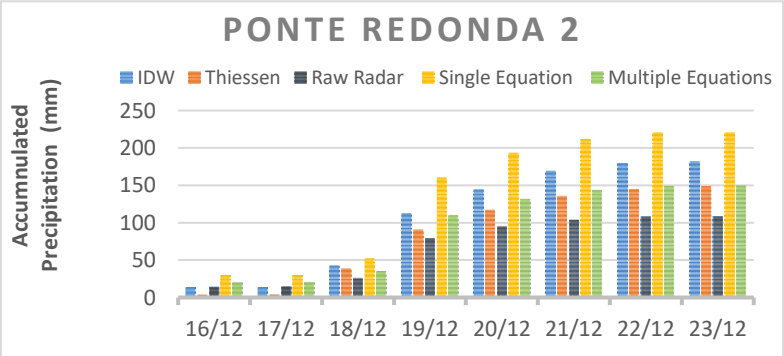

Figure 4.10-Accumulated Precipitation on the Ponte Redonda 2 subcatchment.

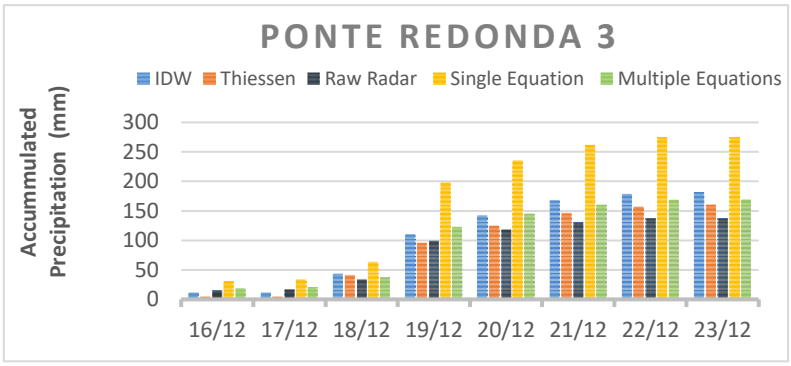

Figure 4.11-Accumulated Precipitation on the Ponte Redonda 3 subcatchment.

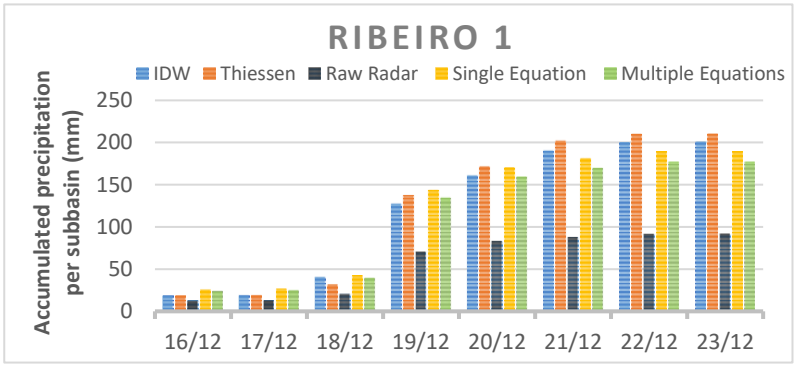

Figure 4.12-Accumulated Precipitation on the Ribeiro 1 subcatchment.

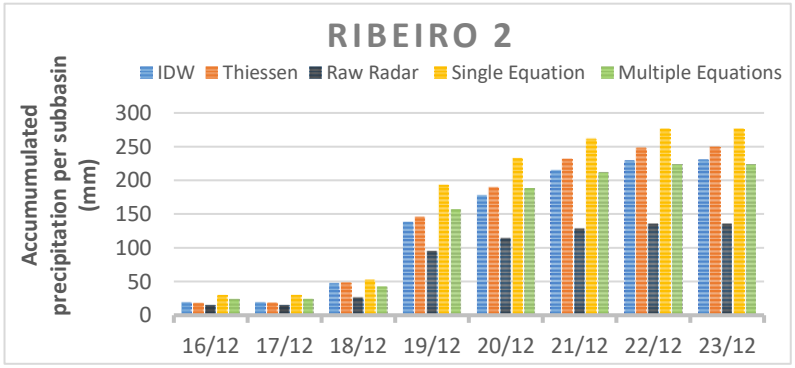

Figure 4.13-Accumulated Precipitation on the Ribeiro 2 subcatchment.

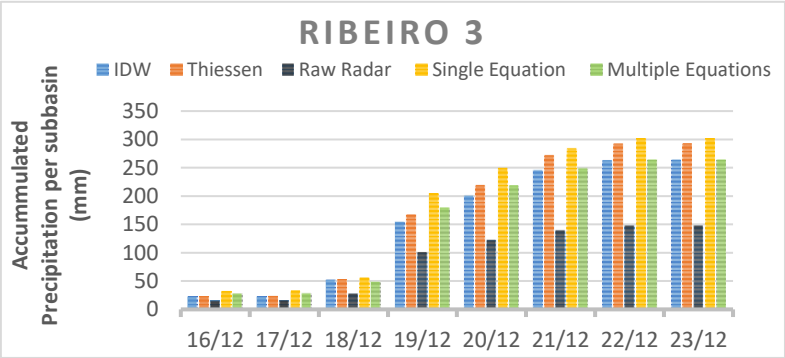

Figure 4.14-Accumulated Precipitation on the Ribeiro 3 subcatchment.

4.1.2.2 Discussion of the event

General Discussion

Contrarily to the event previously presented, the performance of the corrective methods is not as clear or homogenous, as proven by the graphs presented on the Figures 4.8 to 4.14. When considering accumulated rain that fell on the watershed, the conclusion that the weather radar underestimates the total rainfall stands truth, even if the difference between the radar and udometers is less evident. Along the event, it is possible to observe instances where the radar overestimates the precipitation measured by the rain gauges and other instances where the radar underestimates the rainfall values. In short, the approximation between radar data and the udometer data is extremely variable. This variation might be related to the type of precipitation regime observed. This event has a convective regime, associated with the vertical movements, depending on updrafts and downdrafts, the overestimating of surface precipitation rate is expected, (Šálek et al., 2004).

Method 1 – Single Equation

The application of this corrective equation to the original radar values proved to be mostly successful in approximating the estimates to the precipitation measurements executed by the udometers.

When comparing the increase in values between events, the event of 2019 presents the same increase of values, since the corrective equation used is the same, but better results. A big part of the improvement on the corrected estimations is due to the original estimates performed by the weather radar already being closer to the ground truth values, since this tool performs better in convective events, according to IPMA.

This event also displays a lot more overestimation, that was attributed to the fact that the original weather radar estimates already presented multiple periods were the estimates made by the radar were already very close or higher than the ones measured at ground height. In the subcatchment Ponte Redonda 3, there is an evident overestimation of the corrected values, this problem was recurrent throughout the event and is expressly noticeable when considering the total volume of precipitation measured, graphic 4.13, which is almost 1.3 times higher than the other methods. Another reason for

this overestimation, is that the use of a single corrective equation leads to an increase of the factor that would be used if only the data from this event was considered, due to the difference between measurements on the previous event.

Method 2 – Multiple Equations

When analysing the impact that the multiple equations method has on the radar estimates, it is possible to ascertain that the main goal of approximating the radar and udometric values is generally fruitful and more homogeneously observed, instead of the multiple spikes of overestimation presented by the previous method.

Taking into consideration the total precipitation graphs, graph 4.8 to 4.14, it is possible to notice that this method presents values that are similar to the IDW method, suggesting that the approximation of the radar and udometric values at the udometric station was effective.

However, and taking into consideration the critics previously made concerning the use of a single correction factor, the good results from this event are actually linked with this factor. Aforementioned, on the event of 2019 the calculated corrective expression for Varzielas would be $Pcorr = 0{,}3957Pr$, when in reality the factor used was 0,8358, if the first equation was to be used, it would be detected an underestimation of this corrected precipitation for some of the subcatchments of Ribeiro and Ponte Redonda. This would happen because these are the subcatchments where the Varzielas station has more weight, and the precipitation measured at this station pixel is usually higher than on the rest of the watershed.

4.2 Discharges

4.2.1 Introduction

The goal of this thesis is to understand if the corrected values of radar can offer a better understanding of the flooding phenomena that transpired during these events.

Two types of discharges were generated: discharges that use udometric information as input and discharges that use the corrected radar precipitation values as input. The first type uses two of the most common spatial interpolation methods, IDW and Thiessen, to generate the input for the hydrological models. The second type generates two different discharge values, one that uses the radar precipitation values corrected by the single equation method and another one that uses the rainfall values corrected using the multiple equations method.

This transformation from precipitation to discharge is executed using the program HEC-HMS. As previously mentioned, the input precipitation, temperature and observed discharges data is inserted on the time series section, the watershed model section required the input of the general characteristics of the watershed and the parameters for the different methods chosen, these methods influence how complementary hydrological processes are simulated. The general characteristics of the watershed are automatically inserted by the ArcGIS extension, HEC-geoHMS. Considering that the loss method

chosen was Green & Ampt, (U.S. Army Corps of Engineers, 2018), the model parameters are : the initial content of water in the soil(-), the saturated water content (-) , the suction head (mm), the conductivity(mm/hr) and the imperviousness(%), the transform method selected was the Clark Unit Hydrograph method that uses as input the concentration time (h) and the storage coefficient. The method to estimate the baseflow is the linear reservoir, for which the groundwater initial discharge and the groundwater coefficient for each reservoir needs specification. The routing and loss/ gain methods chosen were, respectively, Muskingum-Cunge and Percolation, (U.S. Army Corps of Engineers, 2018).

For all the methods mentioned above, the same set of parameters were used to calibrate the models, Annex L. These parameters were firstly calculated considering the texture maps available at sniamb.apambiente.pt, and the correspondent parameter tables. The next step was to adjust the parameters, in order to achieve discharge values similar to the observed ones. For this calibration, the IDW method was used.

4.2.2 Event of 2016

4.2.2.1 Results of the Event

Figures 4.15,4.16 and 4.17, present the measured and simulated discharges on the stations of Ponte Redonda, Ribeiro and Ponte Águeda, respectively.

As mentioned in chapter 3, the rating equation available for the station of Ponte Águeda is incorrect, therefore, the use of normalized values, ($\frac{Discharge\ i}{Max\ Discharge}$), of discharge data, (Figure 4.17), was adopted instead of comparison between discharge values.

The discharge values are reported in Annex I.

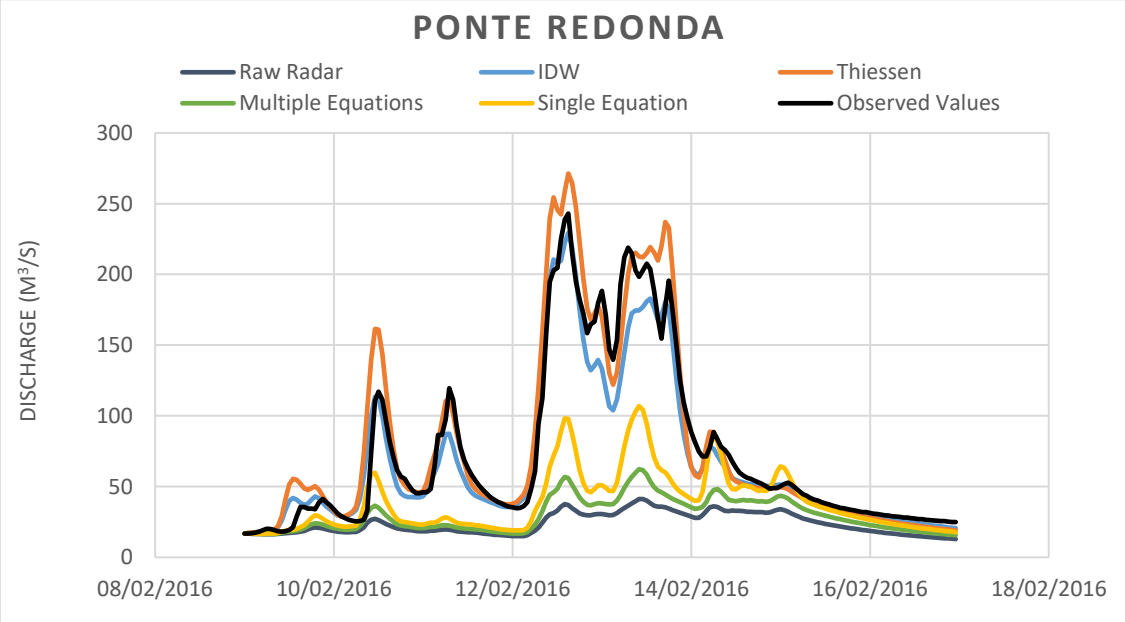

Figure 4.15-Observed and Simulated Discharge Results at Ponte Redonda river gauge station.

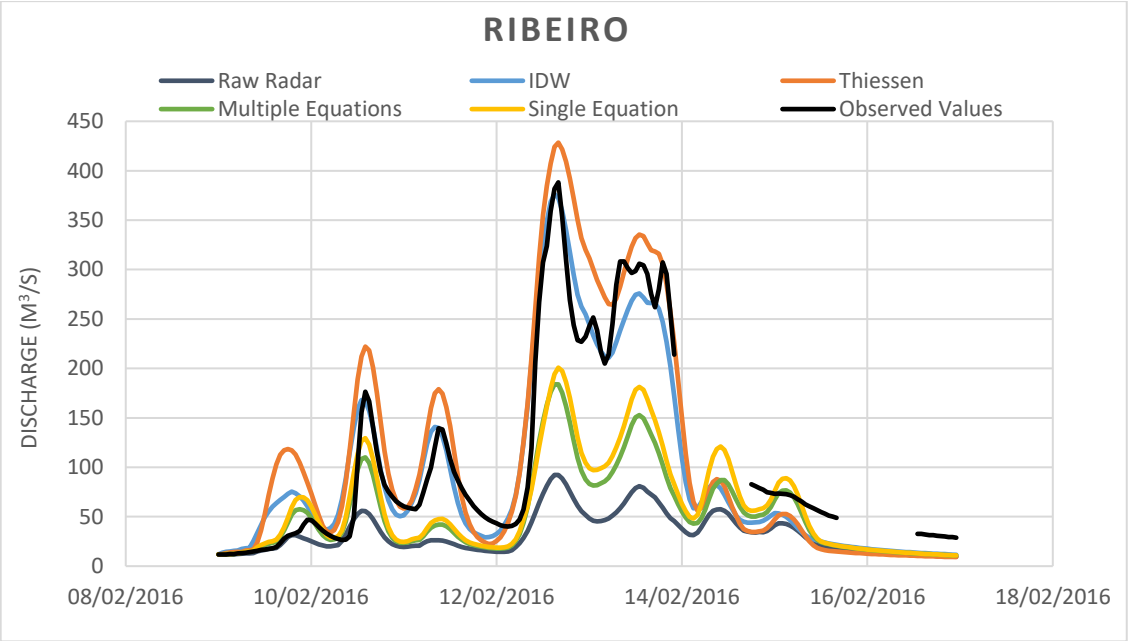

Figure 4.16-Observed and Simulated Discharge Results at Ribeiro river gauge station.

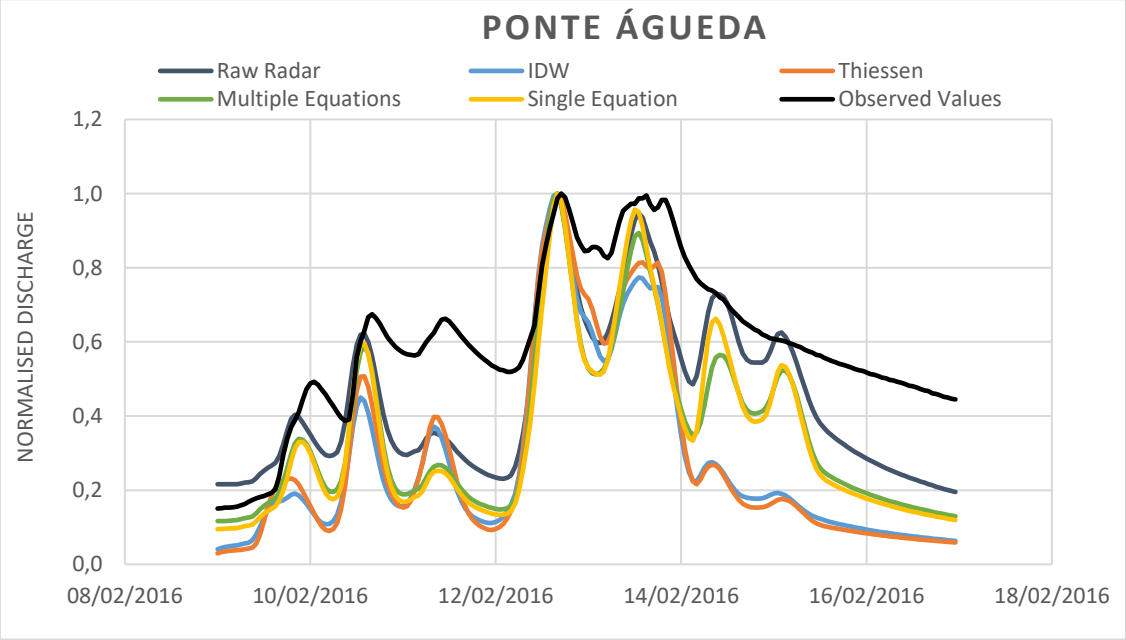

Figure 4.17- Simulated and Observed Normalized Discharge at the river gauge stations of Ponte Águeda.

A statistical analysis was performed, using the HEC-HMS statistics tools. The results for the different considered statistics are presented in Table 4.1.

Table 4.1-Statistical Analysis of the modelled data.

	RMSE Std Dev	Percent Bias	Nash-Sutcliffe
IDW			
Ponte Redonda	0,3	- 8,20%	0,930
Ribeiro	0,4	9,38%	0,870
Thiessen			
Ponte Redonda	0.4	6,94%	0,851
Ribeiro	0,5	28,01%	0,748
Raw Radar			
Ponte Redonda	1,2	-67,92%	-0,525
Ribeiro	1,0	-62,63%	-0,004
Single Equation			
Ponte Redonda	0,9	-47,64%	0,109
Ribeiro	0,7	-30,56%	0,497
Multiple Equations			
Ponte Redonda	1,1	-60,06%	-0,270
Ribeiro	0,8	-39,24%	0,420

4.2.2.2 Discussion of the Event

Udometric Methods

The analysis of the performance indicator, i.e., the two discharges that were generated using as input the udometric precipitation calculated through the spatial interpolation methods IDW and Thiessen, set the bar on what to expect on an operational situation.

Both discharges generated from the udometric methods (IDW and Thiessen) present very adequate simulations of the event.

The performance of the IDW method is marked by its ability to follow the trend of the observed discharges. For the stations of Ponte Redonda and Ribeiro, it was observed that there was an overestimation of the initial discharge peak. The peak discharge of the event was accurately simulated by this method for the station of Ponte Redonda but not reached for the station of Ribeiro. After the peak discharge, the IDW method tends to underestimate the smaller discharge peaks that occur. Qualitatively, the simulated discharges presents an evolution of the event very similar to the one observed in Ponte Águeda, capturing most of the discharge variations. However, the simulated watershed generates discharges whose variation is more abrupt. It was also observed that there is an anticipation of the generated discharges in comparison with the original ones, this might suggest that the simulated watershed is also reacting quicker.

The Thiessen method also displays great ability to follow the trend. In this method, the Ponte Redonda discharges were better simulated than the discharges measured in Ribeiro. In Ponte Redonda, there was an overestimation of the initial discharge peaks detected on the 9th and 10th of February and of the

event peak discharge, as well as, of the discharge peaks that occurred in the 13th of February, while the rest of the event was accurately simulated, while in Ribeiro, the Thiessen method overestimates most of the event. Some of this overestimation could be mitigated if the parameters resulted from the calibration of this method and not of the previous one. The behaviour of this method in Ponte Águeda is very similar to the one observed for the IDW method.
On a statistical level, Table 4.1, both methods presented mainly very good results, indicating a high-performance model.
Regarding these methods, it is possible to declare that both methods originate good simulations of the event.

Method 1 – Single Equation

In accordance with the precipitation results, this method displays an inability to accurately simulate the event discharges due to its inaptitude to generate discharges that reach the necessary levels to adequately simulate the event.

From a qualitative point of view, this method can mostly display the main discharge variations for the station of Ponte Redonda, not so much for the station of Ribeiro, where the original discharge variation is more noticeable.

On Ponte Águeda, it was observed that the simulated discharge produces results that follow the trend, however, the generated discharges are reaching the watershed earlier than the real discharges, this indicates that the simulated watershed is responding to the rainfall faster than the real one, probably because the simulated watershed has limited consideration for the hydraulic processes that occur. Additionally, the descending limb of the observed results are a lot smoother that the generated ones, even the rain gauge methods present a smoother discharge variation. The sharp results may also be connected with the period of precipitation overestimation associated with the end of the event.

The statistical analysis, Table 4.1, results are pretty homogeneous, indicating that the event is not accurately simulated. The RMSE is higher than 0,5, indicating that the model has poor ability to accurately predict the data, the Percentage Bias, is unsatisfactory for Ponte Redonda since the simulated values tend to underestimate the values, meaning that the average tendency of the generated results is to present lower discharges than observed, the Ribeiro watershed also possesses a very bad PBIAS value which indicates that the tendency to simulate lower discharge values than the observed ones is lower. Lastly, the values of the statistic Nash- Suctcliffe, are satisfactory for the Ribeiro watershed, which indicates that the residual variance, when compared with the measured data is quite high but still acceptable The watershed of Ponte Águeda was not contemplated on the statistics due to the uncertainty associated with the original discharge values.

All of the observations above indicate that this method does not provide additional information to the one provided by the discharges generated by Thiessen method, or even the IDW.

Method 2 – Multiple Equations

Identically to the previous events, the discharge simulation results of this method are a perfect example of the importance of using representative precipitation measurements as inputs on hydrological simulation models. The extreme underestimation of the precipitation values used is very well displayed on the results of the multiple equations method.

It was observed that for both methods, the generated discharge can only keep up with the discharges at the beginning and end of the event, because these are the periods when the rainfall was less intense.

Considering these results merely from a qualitative point of view, it is once again possible to observe that the generated discharge can mostly follow the trend of the event for the stations of Ponte Redonda and Ribeiro.

On Ponte Águeda, it was observed that the simulated discharge produces results that follow the trend, however, the generated discharges are reaching the watershed earlier than the real discharges, this indicates that the simulated watershed is responding to the rainfall faster than the real one. Additionally, this event is also incapable of displaying the small discharge variations that occur at the peak discharge and that are simulated by the udometric methods. This method also exaggerates the small discharge peaks that occur in the ending of the event.

On a statistical level, Table 4.1, this method declares a worse performance than the previous one, presenting higher values of RMSE, which indicates a worse ability to predict data, higher values of percent bias, which means that there is a more expressive average difference between the simulated and observed discharges and lower Nash – Sutcliffe values, indicating a worse match between the real and simulated discharges.

In short, the weather radar did not perform well on this event.

4.2.3 Event of 2019

4.2.3.1 Results of the Event

In this section, the discharges simulated using the different precipitation data are presented for the river gauge stations of Ponte Redonda, (Figure 4.18) and Ribeiro, (Figure 4.19). As mentioned in chapter 2, the rating equation available for the station of Ponte Águeda is incorrect, therefore, the use of normalized values, ($\frac{Discharge\ i}{Max\ Discharge}$), of discharge data,(Figure 4.20), was adopted instead of comparison between discharge values.
The numeric results of these graphs are presented in Annex J.

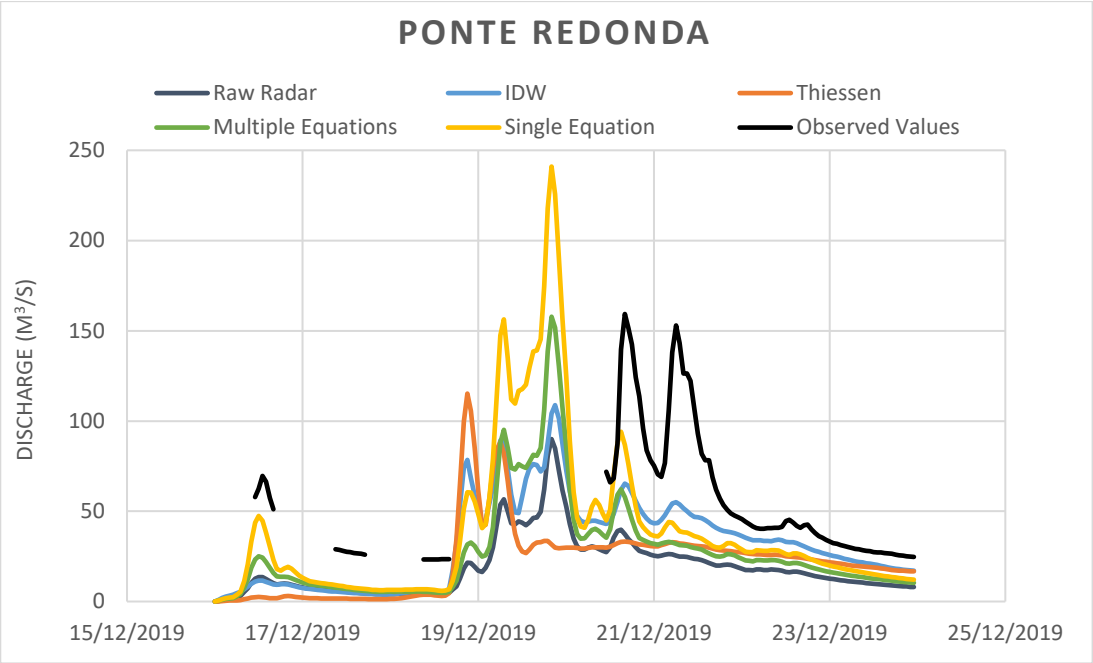

Figure 4.18-Observed and Simulated Discharge at Ponte Redonda river gauge station.

There is some doubt on the legitimacy of the discharge data measured by this river gauge station due to the constant missing data and total incapacity of the simulated discharges (by radar and rain gauges) to achieve discharge values similar to the real ones. Therefore, the results obtained on this river gauge station (Ponte Redonda) were not taken into consideration.

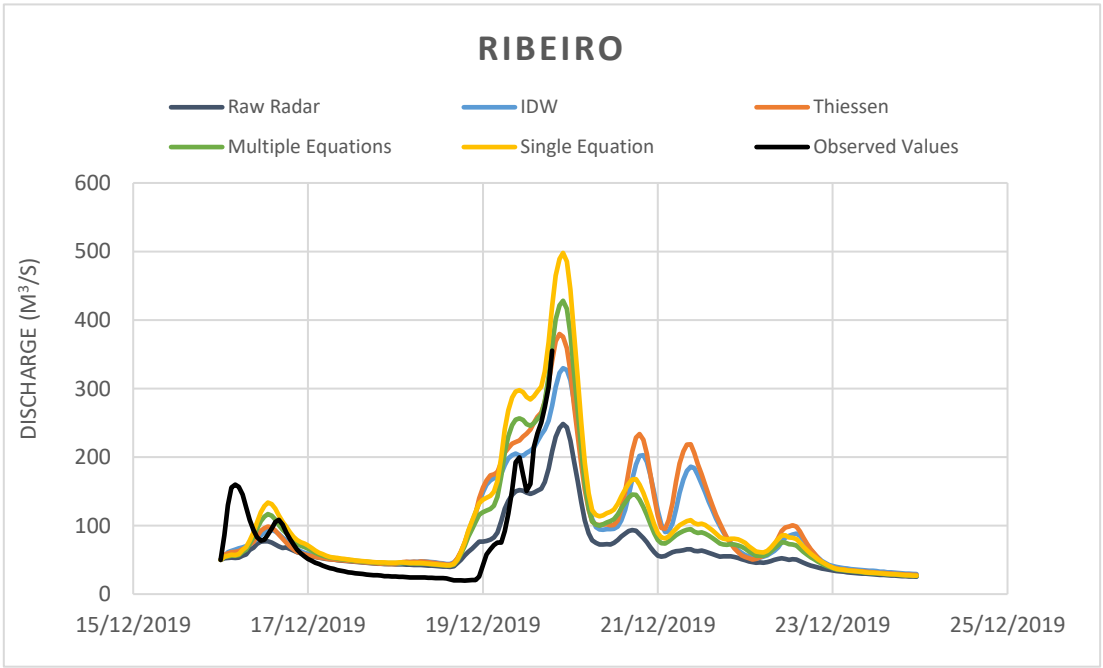

Figure 4.19-Observed and Simulated discharge at Ribeiro river gauge station.

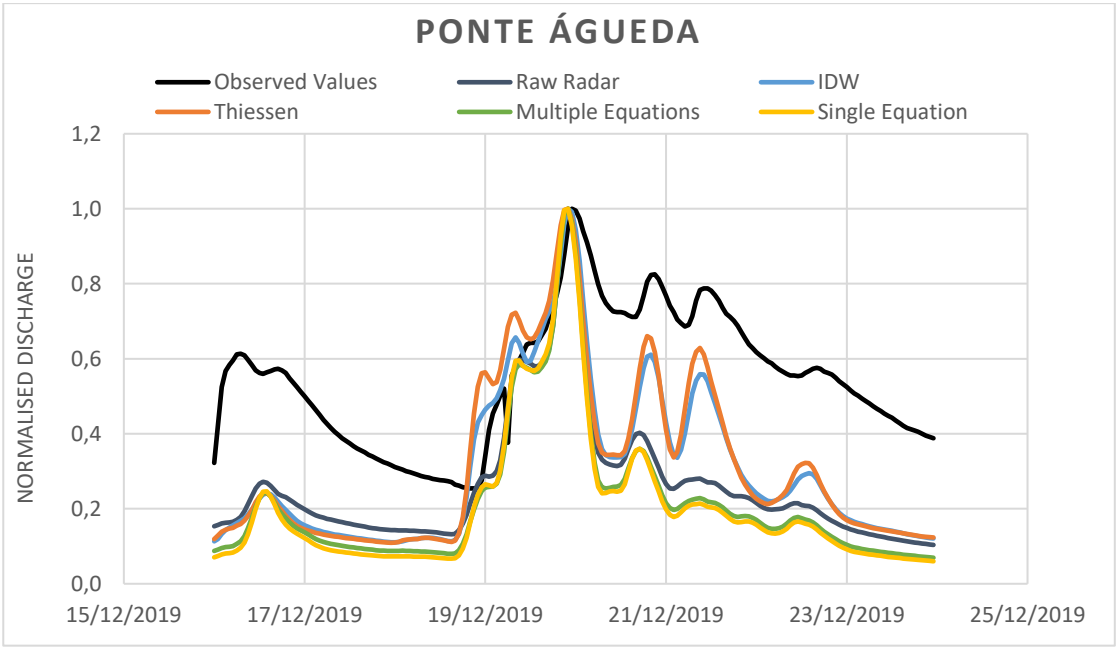

Figure 4.20- Normalised Observed and Simulated discharge at Ponte Águeda river gauge station.

Since there was a lot of data failure collection on the event of 2019, no statistical analysis was performed for this event.

4.2.3.2 Discussion of the Event

Udometric Methods

On the event of 2019, the general ability that these discharges posse to follow the trend in Ribeiro is evident.

Both events presented very similar numeric values until the ascending limb is reached and after the peak discharge. In the ascending limb it is possible to notice that the Thiessen method presents a higher overestimation and anticipation of the discharge values, that may once again be exacerbated with the chosen approach of using only a set of parameters on the HEC-HMS program.

In Ponte Águeda, both methods follow the general trend of the event. However, there was an abrupt but small discharge variation that occurred in the 19th of December that was only captured by the Thiessen method.

Between these two methods, the use of precipitation interpolated with the Thiessen method generated discharges that compute the event more accurately when compared with the real values.

Method 1 – Single Equation

Unlike the results assessed on the previous event, this method presents better simulated values for the available half of the event.

When comparing this discharge with the observed ones, it is possible to observe that it accurately follows the trend of the event. There is an inability to display the first low discharge peak, that occurs in all the events, however this method is more successful simulating the one that occurs on the 16th of December. Similarly to the udometric ones, there is an anticipation of the discharge values, that may be associated with the choice of using a single set of parameters. However, the display of small discharge variations is a lot more qualitatively accurate.

There is an evident overestimation of the assumed peak discharge, that is in accordance with the overestimation observed in the precipitation results. After the peak discharge, this method displays a different behaviour from the udometric methods, but since there are no observed discharge data available, there is an uncertainty regarding the performance of this method.

In Ponte Águeda, the single equation method has the ability to follow the event general trend, however, this method also struggles to display the small but abrupt dip that the discharge suffers on the 19th of December.

Thus, this method may have a small problem with discharge overestimation but can accurately represent the discharge evolution, on a more detailed scale than the previous analysed methods for the station of Ribeiro.

Method 2 – Multiple Equations

The multiple equations method also provided satisfactory results of the discharge.

When comparing the generated discharged with the observed discharge values, it is possible to observe that this method can accurately follow the general trend of the event for Ribeiro and Ponte Águeda.

When simulating the event on the station of Ribeiro the discharge generated by this method offers similar if somewhat overestimated discharge values that simulate the discharge variation that occurred with precision and without the extreme overestimation displayed by the previous method. The multiple equations method also overestimates the assumed discharge peak, but not as evident as the singular equation method. This overestimation may be connected with the parameters chosen for the case studies, since it is not as evident as on the other method.

The normalized discharge results for the station of Ponte Águeda are extremely similar to the ones observed in the previous method, so the observations made before also apply in this scenario. It is important to note that the only reason that the radar methods have similar results on the graph 4.20 is due to the use of normalized, $(\frac{Q}{Qmax})$, values, since the overestimation observed in the single equation method originates discharge values in Ponte Águeda that are on average 20% higher.

For this case, the radar results suggests that the weather radar data has a good capacity to simulate the events discharge, at least in Ribeiro, due to the perceived superior simulation of the results for the first half of the duration of the event. However, the lack of information regarding the whole event for all stations, hinders the absolute definition of it as an absolute success.

5. Conclusion and Recommendations

5.1 Conclusion

The aim of this thesis is to understand the potential of the precipitation data estimated by the weather radar to forecast flood events.

This goal was attained through the analysis of two case studies, corresponding to two flood events in Rio Águeda, in February 2016 and in December 2019. Good results at a hindcast level are a good indication that the weather radar may be ready or on track to be used as an operational tool; less encouraging performance accentuates the need to invest in further scientific studies.

Measured discharges of these flood events were compared with discharges computed with the hydrological model HEC HMS, using different input precipitation data. The latter included spatialized udometer data and corrected radar data, by two different methods. The resulting simulated discharges were compared with the observed values at the river gauge stations of Ponte Redonda, Ponte Águeda and Ribeiro. Due to uncertainty associated with the use the rating equation of Ponte Águeda, the discharge that reaches the subcatchment of Águeda is compared on a qualitative level, by considering normalized discharges. On the event of 2019, the subcatchment of Ponte Redonda was also excluded from analysis due to the lack of river gauge data.

The weather radar generally underestimates the actual precipitation, a result that has been observed in many previous studies for different precipitation regimes, and that has been confirmed in this dissertation. Thus, it is proposed that the weather radar should be considered in operational forecasting systems only within a framework of redundancy. Udometric precipitation data has been seen to allow for good discharge forecasts, always better, in this dissertation, than raw radar data. Hence, the estimates of the weather radar should always be corrected by udometer data, considered “ground truth” in this context.

The application of the precipitation corrective methods, single equation and multiple equations conducted to the approximation of the original weather radar estimates to the udometers measurements. For the event of 2016, neither methods presented a reasonable improvement on the discharge estimates. This case study is the perfect example of a situation where the weather radar would have not been useful in an operational context. This was mainly due to radar measurement errors, the nature of which was impossible to establish beyond doubt. However, it has been observed that the weather radar had exhibited difficulties in capturing accurate reflectivity information in the precipitation conditions that occurred, considering the fact that the corrective equations were insufficient to correct. There was also pixel corruption, as it occurred in Varzielas, that had a great negative impact on the multiple equation method. This 2016 case study thus reveals that the use of the weather radar in an operational forecasting context, even if corrected by some kind of “ground truth”, is still problematic. As a corollary, using radar data in, for instance, ungauged basins, may not be advisable for the current state of art.

In the 2019 case study, both (single and multiple equation) methods offered better estimates of discharges in River Águeda. The event of 2019 had different characteristics, including a different precipitation regime. In this event there was also a catastrophic failure of river gauge stations, destroyed by the flood itself. The fact that the discharge results were good, and coherent with registered data before river gauge stations malfunctioned, allowed to verify the operational potential of the radar, as a redundancy operational alternative. The fact that the correlation between the udometers and the radar were less variable in this event, also indicates that these methods would work in 2019.

The evaluation of the performance of the weather radar for each case-study led to different but complementary conclusions. The event of 2016 lays the argument for the need to carefully analyse the precipitation maps generated by the weather radar, since they may induce the operator in error. To avoid major forecasting errors, it is advisable to use the weather radar within a framework of redundancy, complementary to with other precipitation gauges, namely udometers.

The event of 2019, suggests that even a simplistic methodology, as that adopted in this dissertation, may be sufficient to correct the estimates of weather radar and render them useful at operational context, as a redundancy alternative, when there is lack of river gauge data and in the event of failure of udometric stations.

5.2 Recommendations

Although the case studies used in this thesis suggest that the weather radar does not consistently provide extra relevant information for flood modelling and forecast, it must be recognised that there is still significant room for improving the methods to validate and correct the weather radar precipitation measurements.

An improvement on the core of the methodology is an aspect to be explored. The precipitation correction results indicate a need to find a methodology that analyses the precipitation maps and detects corrupted pixels, minimizing the impacts that these can have on the results, for instance by replacing the pixel measurement from the radar surface by a statistic of the pixels within a window. The use of additional information to condition the application of corrective equations to precipitation events of different characteristics should also be object of research. In addition, the consideration of other Z-R relationships may also improve the original radar estimates.

For the hydrological model, using a set of parameters that are adequate for the method used may also increase the performance of the method, the calculation of a rating curve for the station of Ponte Águeda would allow for a more accurate calibration of the methods and analysis of the event results.

Since hydrological forecast is a process that depends on many factors beyond precipitation, the application of the method to other watersheds and events can also offer great advances on this subject. Some aspects that should be taken into consideration are the watershed size, watershed orography, density of udometers network and radar beam measurement height. Watersheds that possess small areas, display immense spatial variability of the precipitation distribution that is easily captured by the weather radar but that the rain gauge has low sensibility to accurately exhibit, (Biggs & Atkinson, 2010).

The orography of the terrain can also affect the measurements of reflectivity executed by the weather radar, as previously explained in the state of art. Lastly, in this work, the measurement of the reflectivity performed by the weather radar of Arouca was executed at a height of approximately 1000m, this vertical length is considered the maximum acceptable, meaning that the precipitation measured is on the verge of displaying serious inaccuracies, which means that having the radar beam at less bordering height may also affect the radar performance.

At last, it was also noted that the methodology used in this dissertation would benefit from the consideration of additional precipitation data, both from udometers and radar, which would increase the statistical confidence of the correlation models.

6. References

Alfieri, L., Claps, P., & Laio, F. (2010). Time-dependent Z-R relationships for estimating rainfall fields from radar measurements. *Nat. Hazards Earth Syst. Sci*, (10), 149-158.

Alpuim, T., & Barbosa, S. (1999). The Kalman filter in the estimation of area precipitation. *Environmetrics*, *10*(4),377-394. https://doi.org/10.1002/(sici)109995x(199907/08)10:4<377: aid-env363>3.0.co;2-l.

Barbosa, S. (2006). *Rede nacional de radares meteorológicos: situaçao actual e desafios futuros.* Retrieved from http://hdl.handle.net/20.500.11765/5214

Barbosa, S., Silva, Á., & Narciso, P. (2017). Analysis of the 1 November 2015 heavy rainfall episode in Algarve by using weather radar and rain gauge data. *Natural Hazards*, *93*(S1), 61-76. https://doi.org/10.1007/s11069-017-3065-2

Berne, A., & Krajewski, W. (2013). Radar for hydrology: Unfulfilled promise or unrecognized potential? *Advances in Water Resources*, *51*, 357-366. https://doi.org/10.1016/j.advwatres.2012.05.005

Beven, K. (2012). *Rainfall-runoff modelling : the primer* (2nd ed.). John Wiley & Sons, Ltd.

Biggs, E., & Atkinson, P. (2010). A comparison of gauge and radar precipitation data for simulating an extreme hydrological event in the Severn Uplands, UK. *Hydrological Processes*, *25*(5), 795-810. https://doi.org/10.1002/hyp.7869

Bonta, J. (2005). *Precipitation Measurement - an overview | ScienceDirect Topics*. Sciencedirect.com. Retrieved from https://www.sciencedirect.com/topics/earth-and-planetary-sciences/precipitation-measurement.

Brandão, C. (2018). *Contribuição para a Previsão de Cheias e para a Diminuição da Vulnerabilidade e Risco. Aplicação na Área Metropolitana de Lisboa* (Ph.D). Instituto Superior de Agronomia - Universidade de Lisboa.

Bringi, V., & Chandrasekar, V. (2001). *Polarimetric Doppler Weather Radar: Principles and Applications*. Cambridge University Press.

Carvalho, C. (2020). Um Mês Depois Das Cheias Em Águeda Comerciantes Falam Em Milhares De Euros De Prejuízos. *SIC Notícias*. Retrieved 18 April 2020, from https://sicnoticias.pt/pais/2020-01-20-Um-mes-depois-das-cheias-em-Agueda-comerciantes-falam-em-milhares-de-euros-de-prejuizos-1.

Ciach, G., & Krajewski, W. (1999). On the estimation of radar rainfall error variance. *Advances In Water Resources, 22(6), 585-595.* doi: 10.1016/s0309-1708(98)00043-8

Chow, V., Maidment, D., & Mays, L. (1988). *Applied hydrology*. McGraw-Hill Professional.

Comstock, K., Wood, R., Yuter, S., & Bretherton, C. (2004). Reflectivity and rain rate in and below drizzling stratocumulus. *Quarterly Journal Of The Royal Meteorological Society, 130(603), 2891-2918.* doi: 10.1256/qj.03.187

Cunha, L., Smith, J., Baeck, M., & Krajewski, W. (2013*). An Early Performance Evaluation of the NEXRAD Dual-Polarization Radar Rainfall Estimates for Urban Flood Applications*. Weather And Forecasting, 28(6), 1478-1497. doi: 10.1175/waf-d-13-00046.1

Cunha, N., Magalhães, M., Domingos, T., Abreu, M., & Küpfer, C. (2017). The land morphology approach to flood risk mapping: An application to Portugal. *Journal Of Environmental Management*, *193*, 172-187. https://doi.org/10.1016/j.jenvman.2017.01.077

Dai, A. (2006). Precipitation Characteristics in Eighteen Coupled Climate Models. *Journal Of Climate*, *19*(18), 4605-4630. https://doi.org/10.1175/jcli3884.1

Devia, G., Ganasri, B., & Dwarakish, G. (2015). A Review on Hydrological Models. *Aquatic Procedia*, *4*, 1001-1007. doi: 10.1016/j.aqpro.2015.02.126

Eldardiry, H., Habib, E., & Zhang, Y. (2015). On the use of radar-based quantitative precipitation estimates for precipitation frequency analysis. *Journal Of Hydrology, 531, 441-453*. doi: 10.1016/j.jhydrol.2015.05.016

Flick, R., Chadwick, D., Briscoe, J., & Harper, K. (2012). “Flooding” versus “inundation”. *Eos, Transactions American Geophysical Union*, *93*(38), 365-366. https://doi.org/10.1029/2012eo380009

Friedrich, K., Hagen, M., & Einfalt, T. (2006). A Quality Control Concept for Radar Reflectivity, Polarimetric Parameters, and Doppler Velocity. *Journal Of Atmospheric And Oceanic Technology*, *23*(7), 865-887. https://doi.org/10.1175/jtech1920.1

Fukao, S., Hamazu, K., & Doviak, R. (2014). *Radar for meteorological and atmospheric observations*. Springer.

Gad, M. (2002). Real-time Rainfall Estimation and Prediction (M.SC). McMaster University.

Gjertsen, U., Šálek, M., & Michelson, D. (2004). *Gauge adjustment of radar-based precipitation estimates in Europe*. NASA/ADS.

Giuli, D., Baldini, L., & Facheris, L. (1994). Simulation and modeling of rainfall radar measurements for hydrological applications. *Natural Hazards*, *9*(1-2), 109-122. https://doi.org/10.1007/bf00662594

Glossary | International Cloud Atlas. International Cloud Atlas. (2020). Retrieved from https://cloudatlas.wmo.int/en/glossary.html#P.

Haddad, Z. S., Smith, E. A., Kummerow C. D., Iguchi T., Farrar M. R., Durden S. L., Alves M., and Olson W. S. (1997). *The TRMM“day-1” radar/radiometer combined rain-profiling algorithm*. J. Meteor. Soc. Japan, 75, 799–809.

Hillel, D. and Hatfield, J. (2005). *Encyclopedia Of Soils In The Environment*. Oxford, UK: Elsevier/Academic Press.

Holleman, I., Michelson, D., Galli, G., Germann, U., & Peura, M. (2006). Quality information for radars and radar data. Retrieved 17 August 2020, from http://opera.radar.tugraz.at/docum/opera_2/OPERA_2005_19_DataQuality.pdf

How Do Radars Work? | Earth Observing Laboratory. Retrieved 3 March 2020, from https://www.eol.ucar.edu/content/how-do-radars-work

Ingraham, N. (1998). Isotopic Variations in Precipitation. *Isotope Tracers In Catchment Hydrology*, 87-118. https://doi.org/10.1016/b978-0-444-81546-0.50010-0

Jacinto, R., Grosso, N., Reis, E., Dias, L., Santos, F., & Garrett, P. (2015). Continental Portuguese Territory Flood Susceptibility Index – contribution to a vulnerability index. *Natural Hazards And Earth System Sciences*, *15*(8), 1907-1919. https://doi.org/10.5194/nhess-15-1907-2015

Jackson, A. (2014). *Flooding*. [online] Geographyas.info.

Joe, P., Crozier, C., Donaldson, N., Etkin, D., Brun, E., & Clodman, S. et al. (1995). Recent progress in the operational forecasting of summer severe weather. *Atmosphere-Ocean, 33(2), 249-302*. doi: 10.1080/07055900.1995.9649534

Joe, P., & Smith, P. (2001). 3.1 *Summary of the Radar Calibration Workshop*. Retrieved 2 June 2020, from https://ams.confex.com/ams/30radar/techprogram/paper_21882.htm

Jurczyk, A., Szturc, J., Otop, I., Ośródka, K., & Struzik, P. (2020). Quality-Based Combination of Multi-Source Precipitation Data. *Remote Sensing*, *12*(11), 1709. https://doi.org/10.3390/rs12111709

Kouwen, N. (1988). *WATFLOOD:* a Micro-Computer Based Flood Forecasting System Based on Real-Time Weather Radar. *Canadian Water Resources Journal, 13(1), 62-77*. doi: 10.4296/cwrj1301062

Krajewski, W., & Smith, J. (2002). Radar hydrology: rainfall estimation. Advances In Water Resources, 25(8-12), 1387-1394. https://doi.org/10.1016/s0309-1708(02)00062

Kummerow, C., Simpson, J., Thiele, O., Barnes, W., Chang, A., & Stocker, E. et al. (2000). *The Status of the Tropical Rainfall Measuring Mission (TRMM) after Two Years in Orbit.* Journal Of Applied Meteorology, 39(12), 1965-1982. doi: 10.1175/1520-0450(2001)040<1965:tsottr>2.0.co;2

Legates, D. (2000). Real-Time Calibration of Radar Precipitation Estimates. *The Professional Geographer*, *52*(2), 235-246. https://doi.org/10.1111/0033-0124.00221

Macedo, M., & Hipólito, J. (1997). Aviso de Cheia em Tempo Real Baseado em Tele-Medição e Radar. 3º Simpósio de Hidráulica e Recursos Hídricos dos Países de Língua Oficial Portuguesa (3º SILUSBA), Maputo, Moçambique, 15-17 abril 1997.

Mapiam, P., & Sriwongsitanon, N. (2008). Climatological Z-R relationship for radar rainfall estimation in the upper Ping river watershed. *Scienceasia*, *34*(2), 215. https://doi.org/10.2306/scienceasia1513-1874.2008.34.215

METAR/TAF Conversion Card. Meteocentre.com. Retrieved 18 April 2020, from http://meteocentre.com/doc/taf.html.

Michelson, D., Einfalt, T., Holleman, I., Gjertsen, U., Friedrich, K., & Haase, G. et al. (2004). COST Action 717 — *Weather Radar Data Quality in Europe: Quality Control and Characterisation*. Belgium

Montopoli, M., & Marzano, F. (2010). Meteorological Radar Systems. *Integrated Ground-Based Observing Systems*, 33-57. https://doi.org/10.1007/978-3-642-12968-1_2

Moore, R., Cole, S., & Robson, A. (2012*).* Weather radar and hydrology: a UK operational perspective. Weather Radar And Hydrology. *International Association of Hydrological Sciences*, 429-434. (IAHS Publ., 351)

Narciso, P., Silva, Á., Moreira, N., & Diogo, D. (2016). Estimativa de precipitação radar-udómetro para casos recentes de precipitação intensa na região de Lisboa. *Conferência Internacional De Riscos Urbanos*. Retrieved from https://www.researchgate.net/publication/306429895

Nadipally, M. (2019). Optimization of Methods for Image-Texture Segmentation Using Ant Colony Optimization. *Intelligent Data Analysis For Biomedical Applications*, 21-47. https://doi.org/10.1016/b978-0-12-815553-0.00002-1

Ochoa-Rodriguez, S., Wang, L., Willems, P., & Onof, C. (2019). A Review of Radar-Rain Gauge Data Merging Methods and Their Potential for Urban Hydrological Applications. *Water Resources Research*, *55*(8), 6356-6391. https://doi.org/10.1029/2018wr023332

Pauthier, B., Bois, B., Castel, T., Thévenin, D., Chateau Smith, C., & Richard, Y. (2016). Mesoscale and Local Scale Evaluations of Quantitative Precipitation Estimates by Weather Radar Products during a Heavy Rainfall Event. *Advances In Meteorology, 2016, 1-9.* doi: 10.1155/2016/6089319

Polger, P., Goldsmith, B., Przywarty, R., & Bocchieri, J. (1994). National Weather Service Warning Performance Based on the WSR-88D. *Bulletin Of The American Meteorological Society, 75(2), 203-214.* doi: 10.1175/1520-0477(1994)075<0203:nwswpb>2.0.co;2

Prior, V., Nunes, L., Barbosa, S., Lopes, A., Neto, J., Mendes, M., & Correia, S. (2008). Sistemas de Observação do Clima Atmosférico e da Composição da Atmosfera. *Conference: Workshop Internacional sobre Clima e Recursos Naturais nos países de língua portuguesa – parcerias na área do clima e ambiente (CRIA 08)* At: Ilha do Sal, Cabo Verde.

Prociv.pt. (2020). [online] Available at: <http://www.prociv.pt/pt-pt/RISCOSPREV/RISCOSNAT/CHEIAS/Paginas/default.aspx> [Accessed 5 March 2020].

Raghavan, S., (2003). *Radar Meteorology*. Springer Netherlands.

Rauber, R., & Nesbitt, S. (2018). Radar Meteorology: A First Course. https://doi.org/10.1002/9781118432662

Šálek, M., Cheze, J., Handwerker, J., Delobbe, L., & Uijlenhoet, R. (2004). Retrieved 13 August 2020, from https://is.muni.cz/el/1431/podzim2012/Z0095/um/radar_precip_COST717.pdf?lang=en

ScienceDaily.(2020). *Precipitation (Meteorology)*. [online]. Retrieved 17 April 2020, from https://www.sciencedaily.com/terms/precipitation_(meteorology).html

Serafin, R., & Wilson, J. (2000). Operational Weather Radar in the United States: Progress and Opportunity. *Bulletin Of The American Meteorological Society, 81(3), 501-518*. doi: 10.1175/1520-0477(2000)081<0501:owritu>2.3.co;2

Sinclair, S., & Pegram, G. (2005). Combining radar and rain gauge rainfall estimates using conditional merging*. Atmospheric Science Letters, 6(1), 19-22.* doi: 10.1002/asl.85

Spilhaus, A. (1947). Raindrop Size, Shape, and Falling Speed. *Journal Of Meteorology,* 5, 108 - 110.

Smith, J., Seo, D., Baeck, M., & Hudlow, M. (1996). An Intercomparison Study of NEXRAD Precipitation Estimates. *Water Resources Research, 32(7), 2035-2045*. doi: 10.1029/96wr00270

Soares, P., Cardoso, R., Ferreira, J., & Miranda, P. (2014). Climate change and the Portuguese precipitation: ENSEMBLES regional climate models results. *Climate Dynamics*, *45*(7-8), 1771-1787. https://doi.org/10.1007/s00382-014-2432-x

Tabary, P., Desplats, J., Do Khac, K., Eideliman, F., Gueguen, C., & Heinrich, J. (2007). The New French Operational Radar Rainfall Product. Part II: Validation. Weather And Forecasting, 22(3), 409-427. doi: 10.1175/waf1005.1

Takayabu, Y. N., T. Iguchi, N. Kachi, A. Shibata, and H. Kanzawa (1999). Abrupt termination of the 1997–98 El Niño in response to a Madden–Julian oscillation. Nature, 402, 279–282.

Tan, L., & Jiang, J. (2019). Digital Signal Processing - 3rd Edition. Retrieved 6 August 2020, from https://www.elsevier.com/books/digital-signal-processing/tan/978-0-12-815071-9

Tenório, R., Moraes, M., & Kwon, B. (2010). Raindrop distribution in the Eastern Coast of Northeastern Brazil using disdrometer data. *Revista Brasileira De Meteorologia*, *25*(4). doi: https://doi.org/10.1590/S0102-77862010000400001

Trigo, R., Pereira, S., Ramos, A., Zêzere, J., & Liberato, M. (2016). Revisiting the outstanding flooding episode of November 1967 in the greater metropolitan Lisbon area. In *ICUR2016 - International Conference on Urban Risks*. Lisbon.

van de Beek, C., Leijnse, H., Hazenberg, P., & Uijlenhoet, R. (2016). Close-range radar rainfall estimation and error analysis. *Atmospheric Measurement Techniques, 9(8),* 3837-3850. doi: 10.5194/amt-9-3837-2016

Vieux, B. (2012). Distributed Hydrologic Modeling Using GIS.

Wilson, J., & Brandes, E. (1979). Radar Measurement of Rainfall—A Summary. *Bulletin Of The American Meteorological Society*, *60*(9), 1048-1058. https://doi.org/10.1175/1520-0477(1979)060<1048:rmors>2.0.co;2

Wu, W., Zou, H., Shan, J., & Wu, S. (2018). A Dynamical Z-R Relationship for Precipitation Estimation Based on Radar Echo-Top Height Classification. *Advances In Meteorology*, *2018*. doi: 10.1155/2018/8202031

Viltard, N., Kummerow, C., Olson, W.S. & Hong, Y. (2000). Combined use of radar and radiometer of TRMM to estimate the influence of drop size distributions on rain retrivals*. J.Appl . Meteor*, 39, 2013-2114

Vogl, S., Laux, P., Qiu, W., Mao, G., & Kunstmann, H. (2012). Copula-based assimilation of radar and gauge information to derive bias-corrected precipitation fields. *Hydrology and Earth System Sciences.* Retrieved 30 April 2020, from https://www.hydrol-earth-syst-sci.net/16/2311/2012/hess-16-2311-2012.html.

World Meteorological Organization. (2018). *Guide to meteorological instruments and methods of observation*.Geneva, Switzerland:WMO.

Wilson, J., & Brandes, E. (1979). Radar Measurement of Rainfall—A Summary. Bulletin Of The American Meteorological Society, 60(9), 1048-1058. https://doi.org/10.1175/1520-0477(1979)060<1048:rmors>2.0.co;2

Wilson, J., & Brandes, E. (1979). Radar Measurement of Rainfall—A Summary. *Bulletin Of The American Meteorological Society*, *60*(9), 1048-1058. https://doi.org/10.1175/1520-0477(1979)060<1048:rmors>2.0.co;2

Xumin, L., & Xue, Y. (2011). Research on Vectorization of Weather Radar Image. *Procedia Engineering*, *15*, 1298-1302. https://doi.org/10.1016/j.proeng.2011.08.240

Yuter, S. *Precipitation Radar* (Masters). University of Washington.

Annex A – Graphs that represent the relationship between the precipitation data measured by the udometer and the data resulting from the application of the median filter (3x3) to the weather radar data of Arouca and Coruche, on the event of 2016.

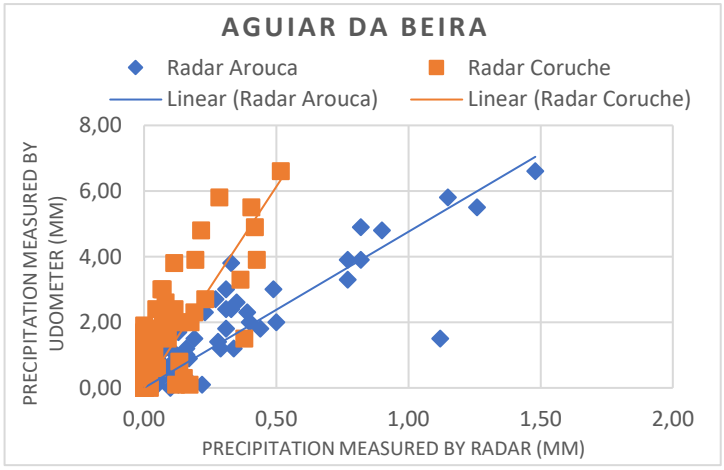

Figure A1- Relationship between precipitation data measured by Aguiar da Beira and the two weather radars, on the event of 2016.

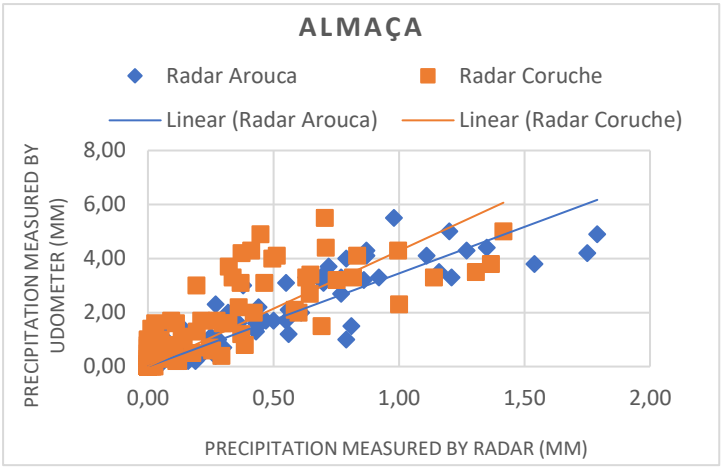

Figure A2- Relationship between precipitation data measured Almaça and the two weather radars, on the event of 2016.

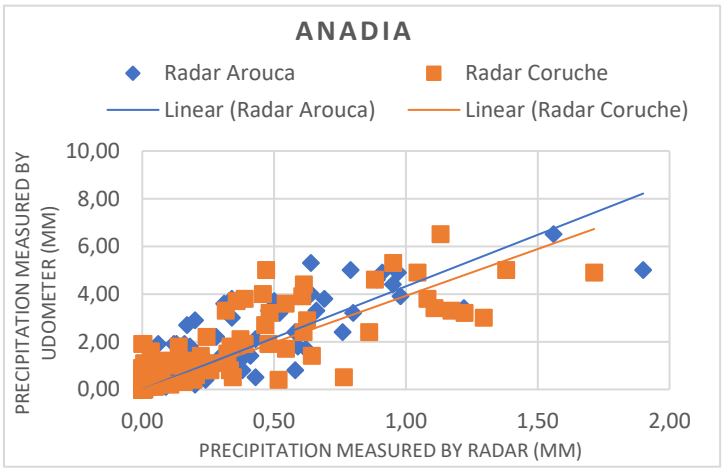

Figure A3- Relationship between precipitation data measured Anadia and the two weather radars, on the event of 2016.

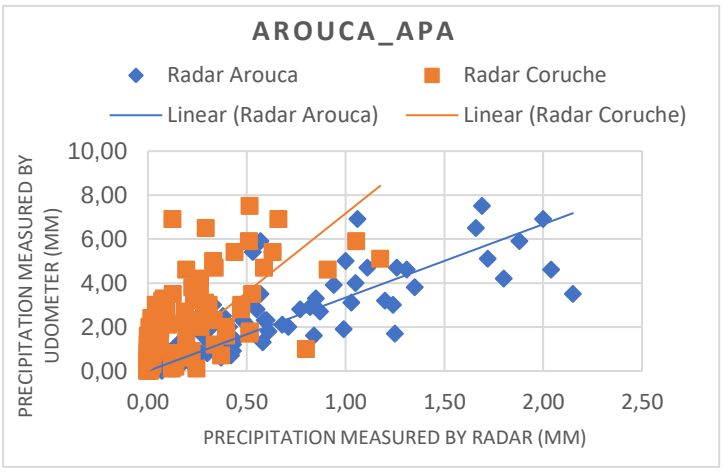

Figure A4- Relationship between precipitation data measured Arouca (APA) and the two weather radars, on the event of 2016.

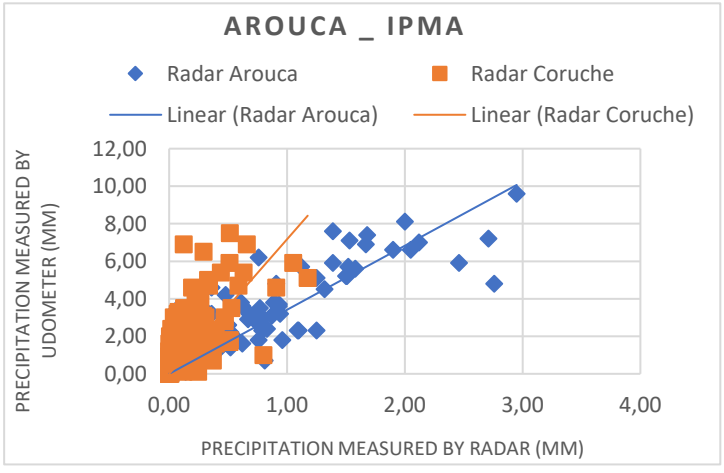

Figure A5- Relationship between precipitation data measured Arouca (IPMA) and the two weather radars, on the event of 2016.

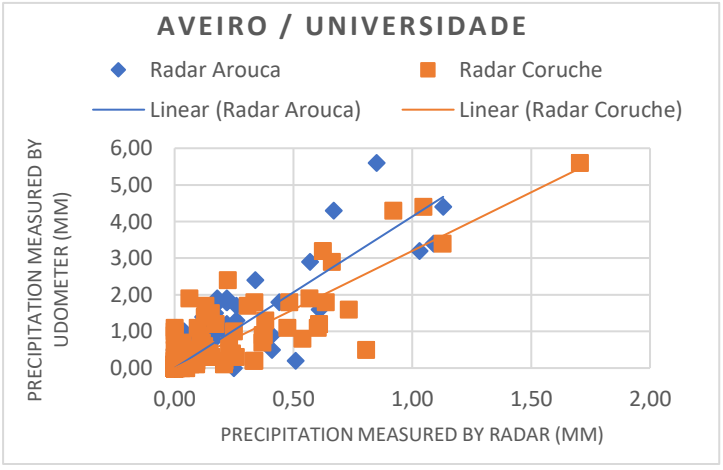

Figure A6- Relationship between precipitation data measured Aveiro (Universidade) and the two weather radars, on the event of 2016.

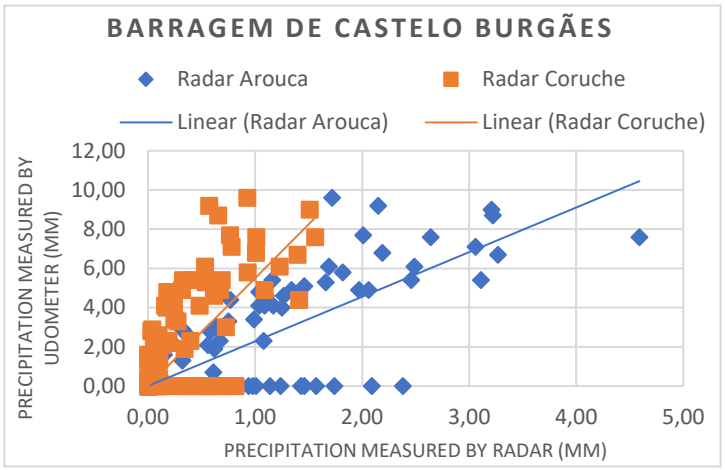

Figure A7- Relationship between precipitation data Barragem de Castelo Burgães and the two weather radars, on the event of 2016.

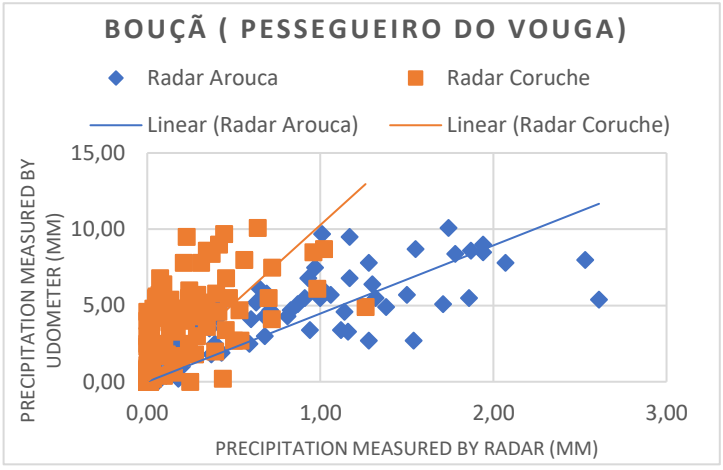

Figure A8- Relationship between precipitation data Bouçã and the two weather radars, on the event of 2016.

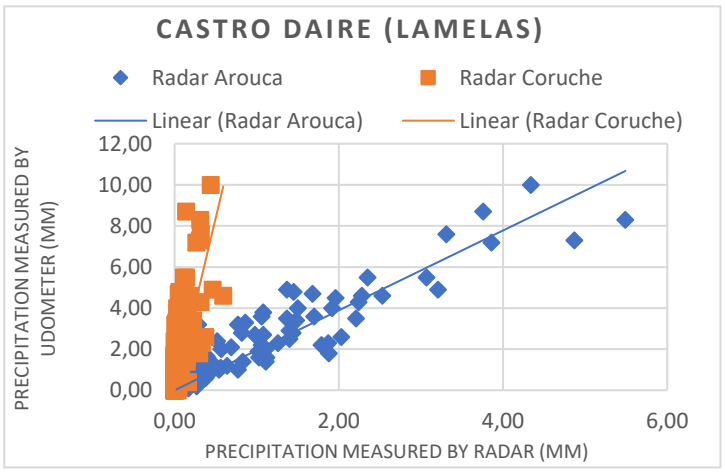

Figure A9- Relationship between precipitation data measured Castro Daire and the two weather radars, on the event of 2016.

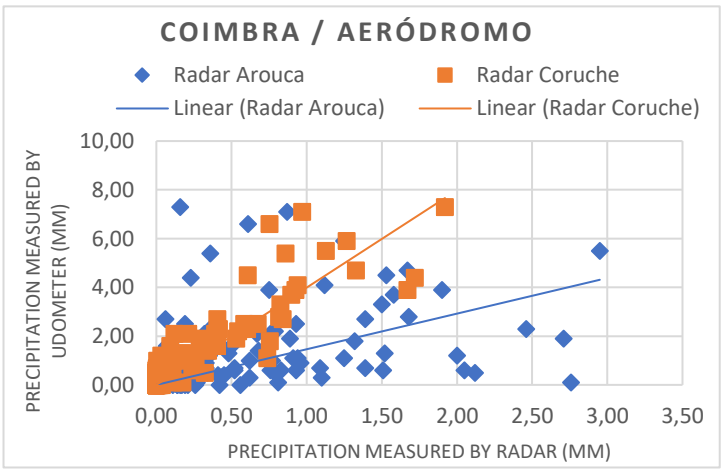

Figure A10- Relationship between precipitation data Coimbra (Aérodromo) and the two weather radars, on the event of 2016.

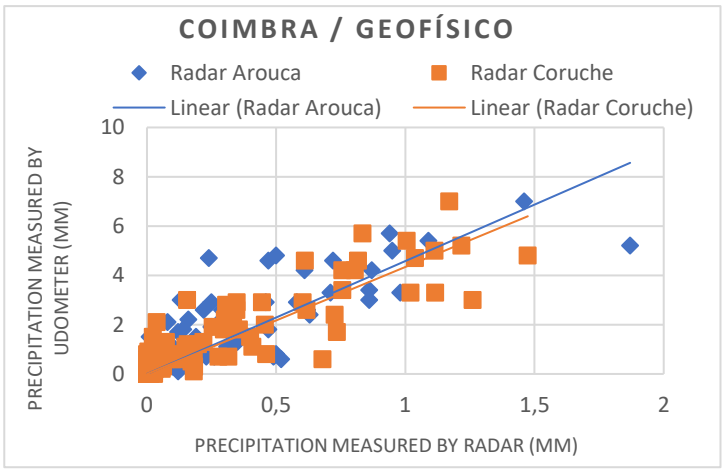

Figure A11- Relationship between precipitation data Coimbra (Geofísico) and the two weather radars, on the event of 2016.

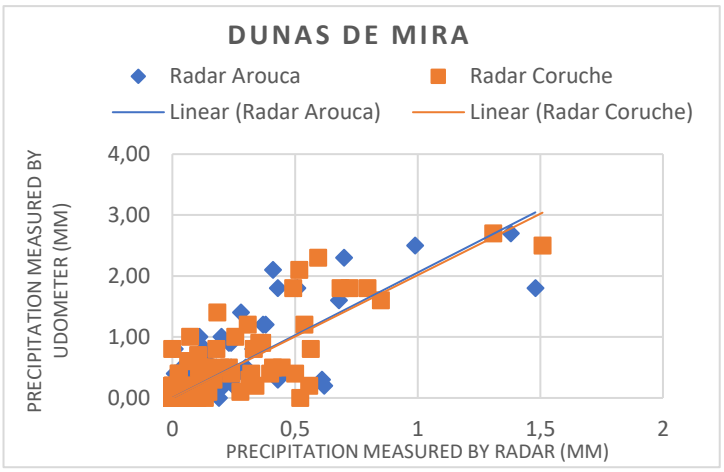

Figure A12- Relationship between precipitation data Dunas de Mira and the two weather radars, on the event of 2016.

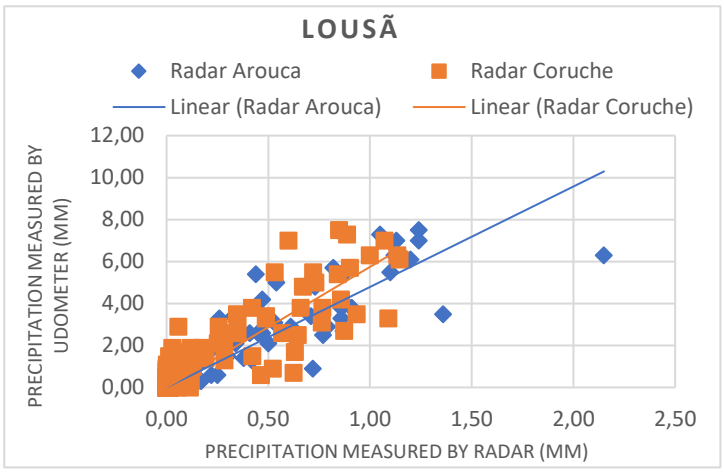

Figure A13- Relationship between precipitation data Lousã and the two weather radars, on the event of 2016.

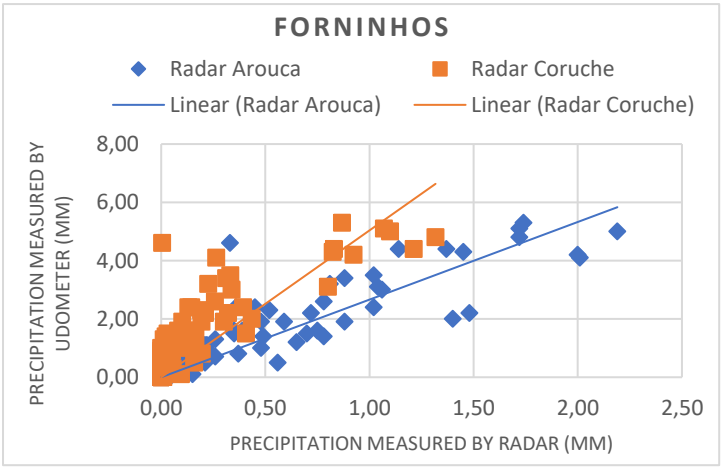

Figure A14- Relationship between precipitation data Forninhos and the two weather radars, on the event of 2016.

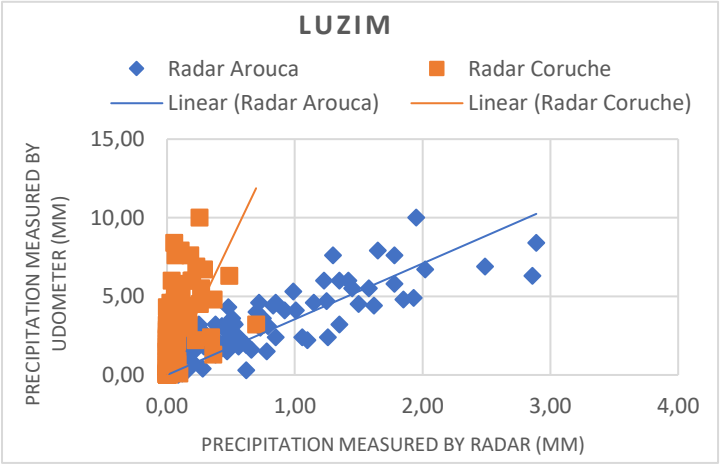

Figure A15- Relationship between precipitation data Luzim and the two weather radars, on the event of 2016.

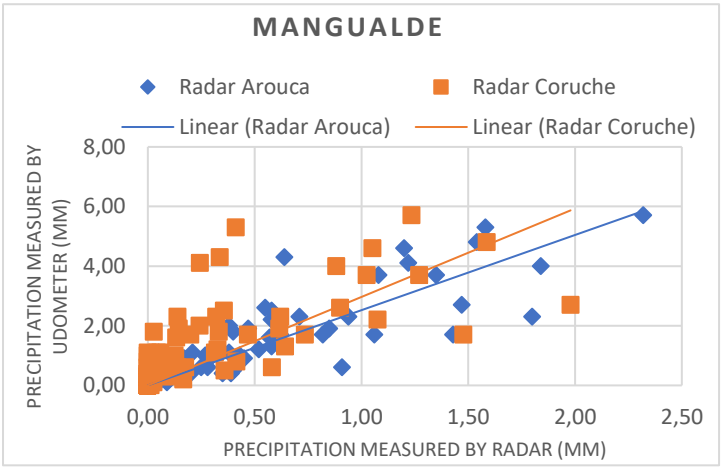

Figure A16- Relationship between precipitation data Mangualde and the two weather radars, on the event of 2016.

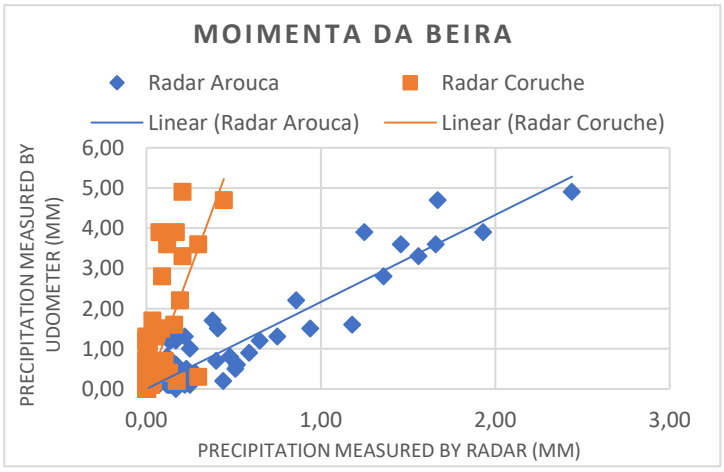

Figure A17- Relationship between precipitation data Moimenta da Beira and the two weather radars, on the event of 2016.

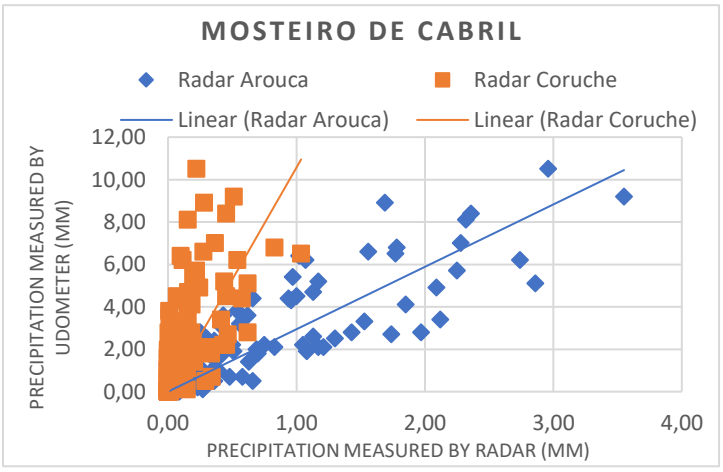

Figure A18- Relationship between precipitation data Mosteiro de Cabril and the two weather radars, on the event of 2016.

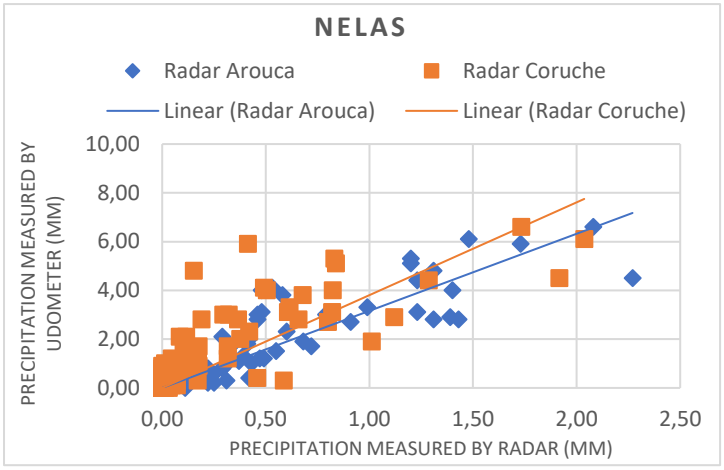

Figure A19- Relationship between precipitation data Nelas and the two weather radars, on the event of 2016.

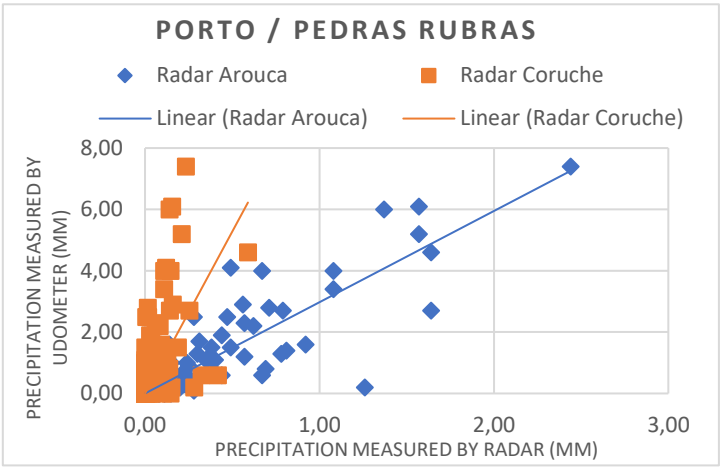

Figure A20- Relationship between precipitation data Porto (Pedras Rubras) and the two weather radars, on the event of 2016.

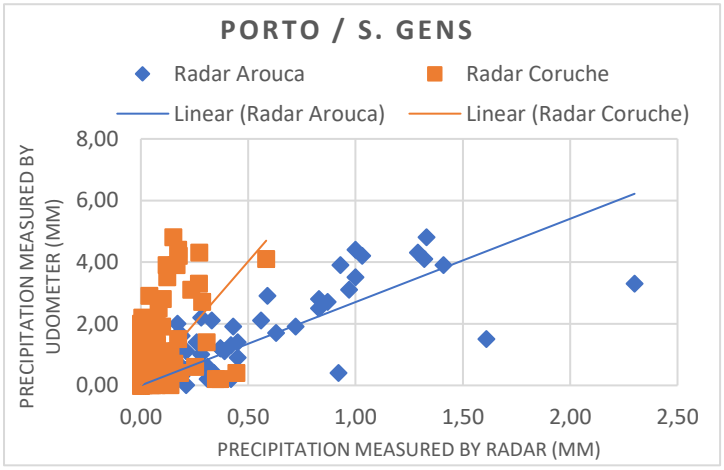

Figure A21- Relationship between precipitation data Porto (S. Gens) and the two weather radars, on the event of 2016.

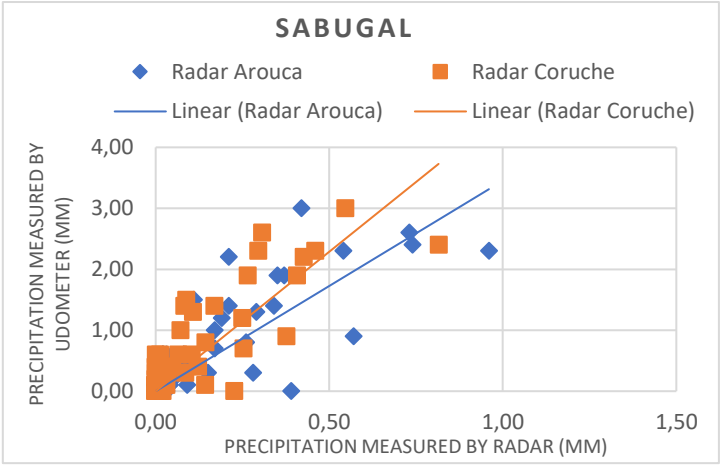

Figure A22- Relationship between precipitation data Sabugal and the two weather radars, on the event of 2016.

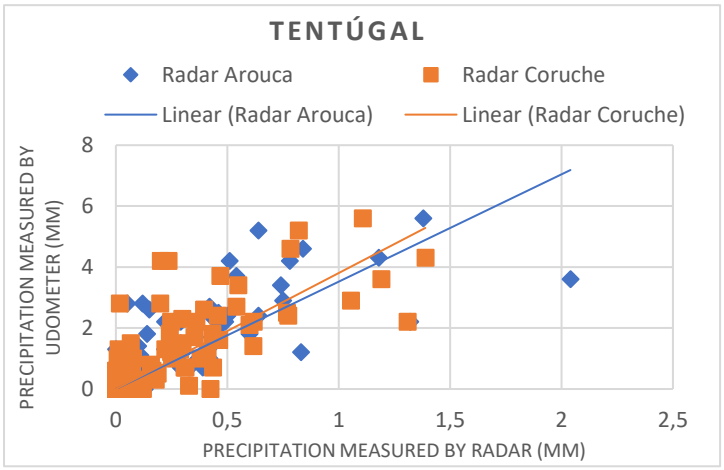

Figure A23- Relationship between precipitation data Tentúgal and the two weather radars, on the event of 2016.

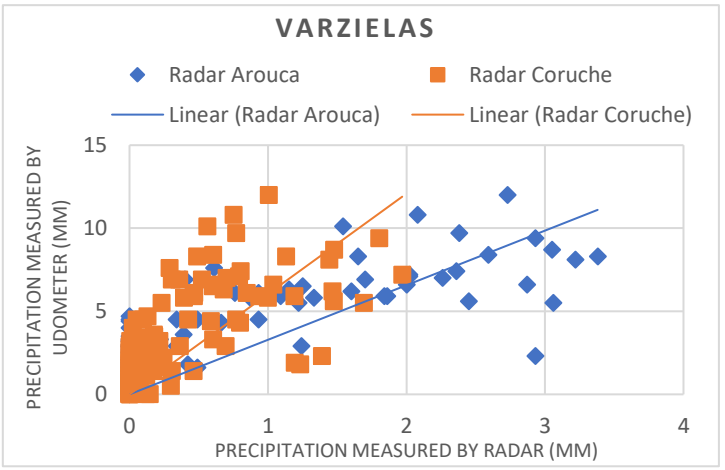

Figure A24- Relationship between precipitation data Varzielas and the two weather radars, on the event of 2016.

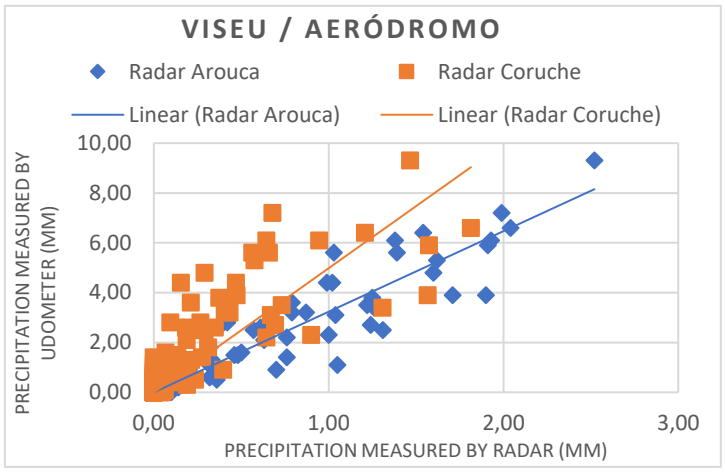

Figure A25- Relationship between precipitation data Viseu (Aeródromo) and the two weather radars, on the event of 2016.

Annex B – Graphs that represent the relationship between the precipitation data measured by the udometer and the data resulting from the application of the median filter (3x3) to the weather radar data of Arouca and Coruche, on the event of 2019.

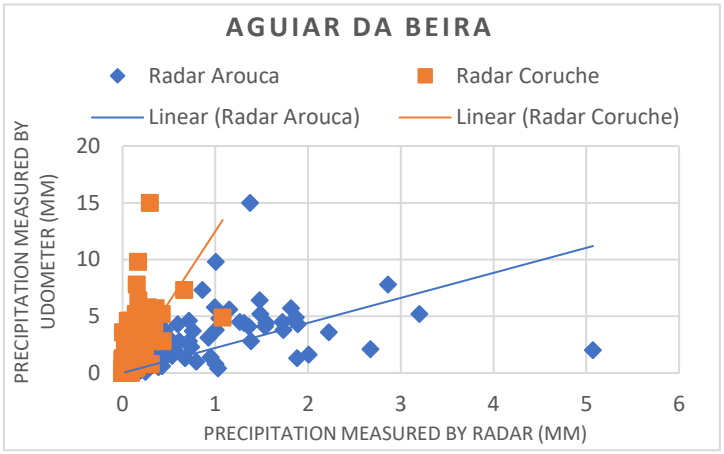

Figure B1- Relationship between precipitation data Aguiar da Beira and the two weather radars, on the event of 2019.

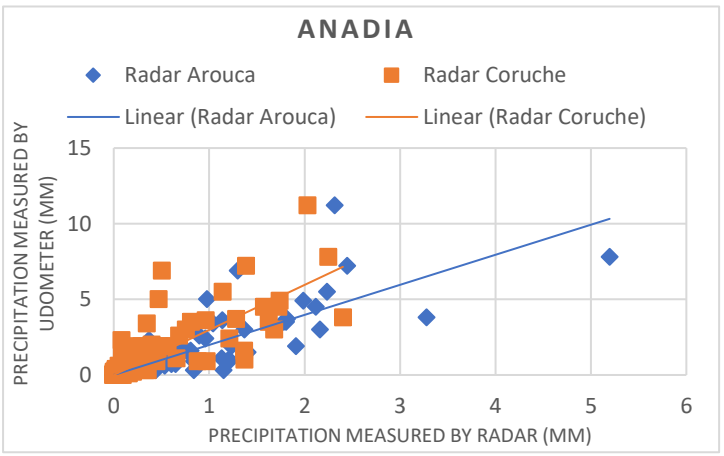

Figure B2- Relationship between precipitation data Anadia and the two weather radars, on the event of 2019.

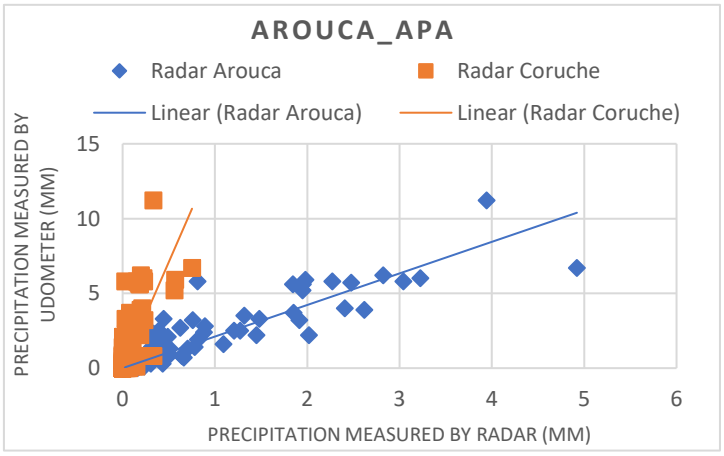

Figure B3- Relationship between precipitation data Arouca (APA) and the two weather radars, on the event of 2019.

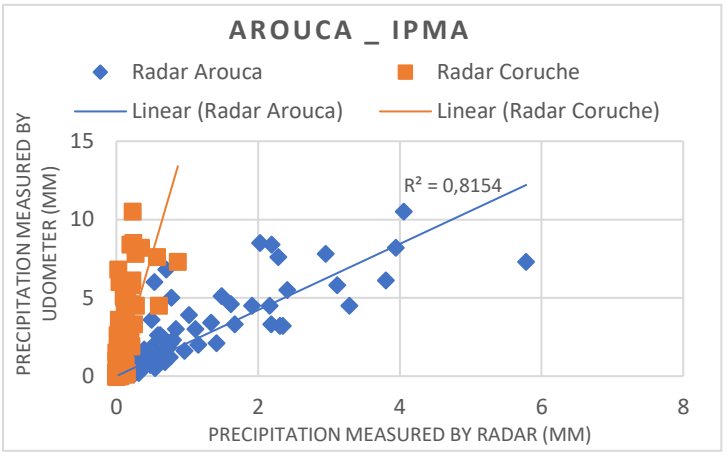

Figure B4- Relationship between precipitation data Arouca (IPMA) and the two weather radars, on the event of 2019.

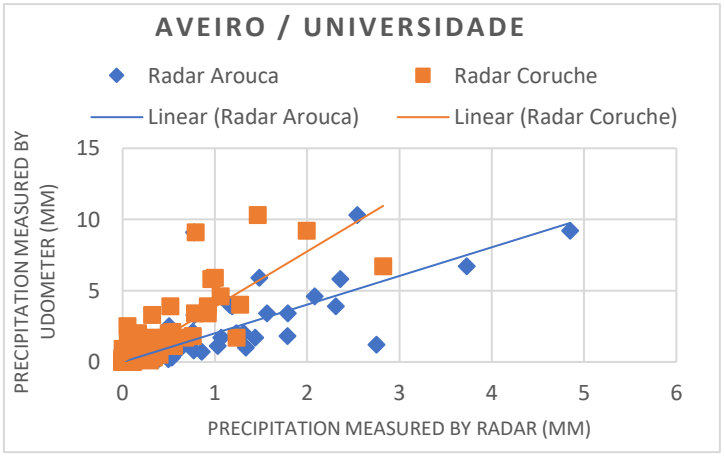

Figure B5- Relationship between precipitation data Aveiro (Universidade) and the two weather radars, on the event of 2019.

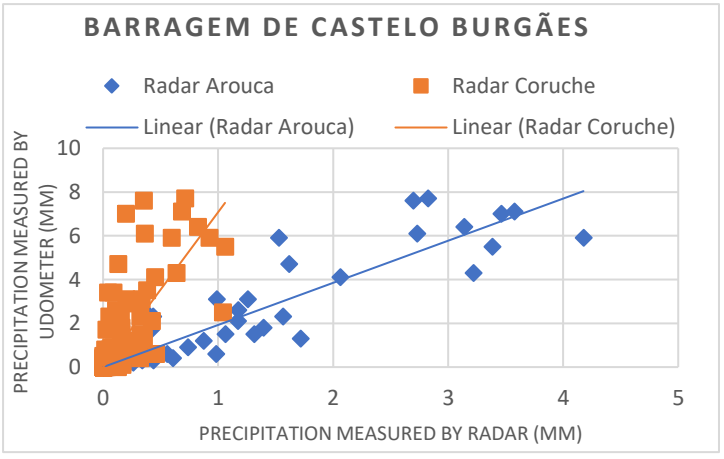

Figure B6- Relationship between precipitation data Barragem de Castelo Burgães and the two weather radars, on the event of 2019.

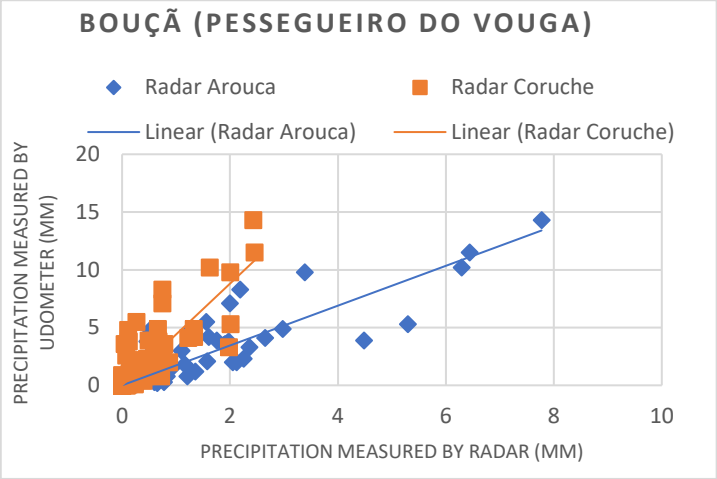

Figure B7- Relationship between precipitation Bouçã and the two weather radars, on the event of 2019.

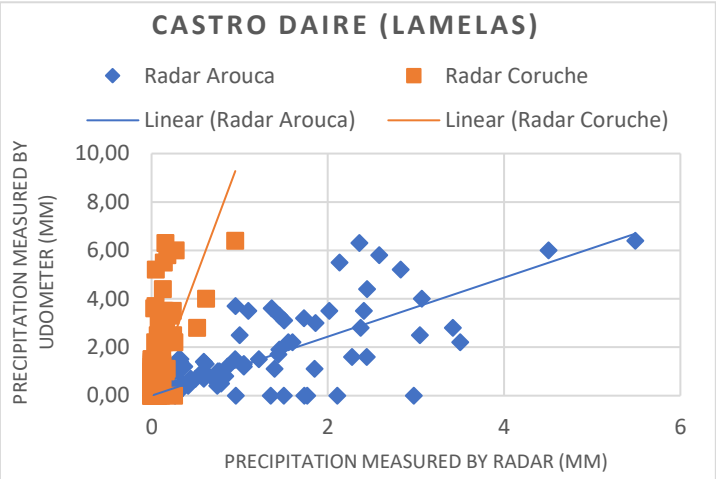

Figure B8- Relationship between precipitation data Castro Daire and the two weather radars, on the event of 2019.

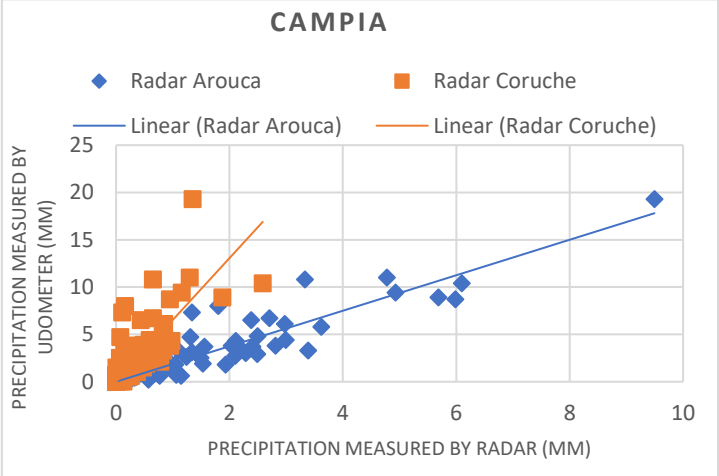

Figure B9- Relationship between precipitation data Campia) and the two weather radars, on the event of 2019.

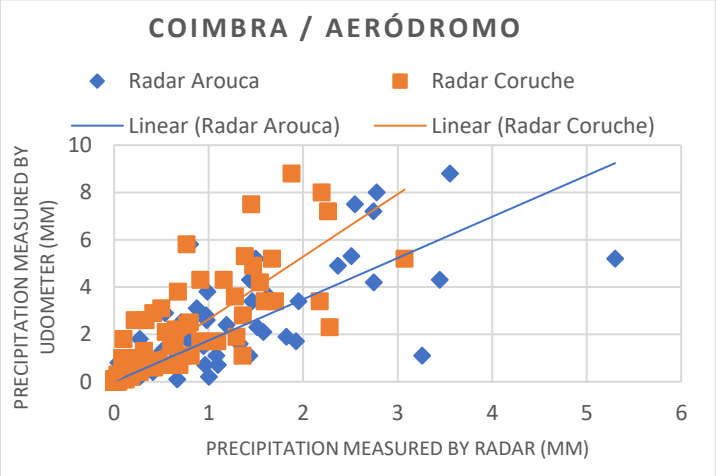

Figure B10- Relationship between precipitation data Coimbra (Aeródromo) and the two weather radars, on the event of 2019.

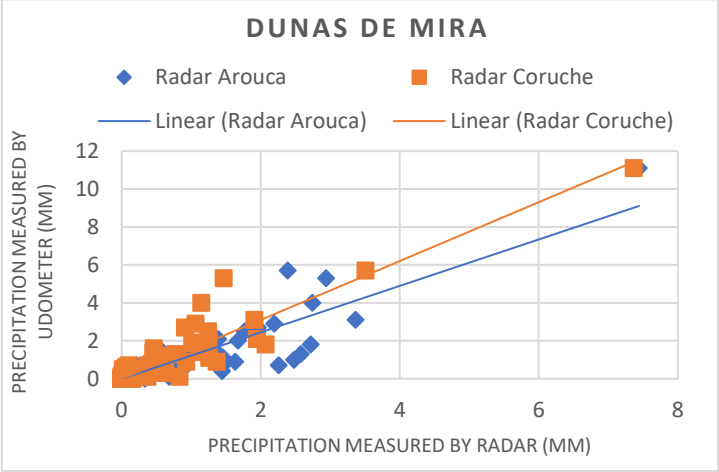

Figure B11- Relationship between precipitation data Dunas de Mira and the two weather radars, on the event of 2019.

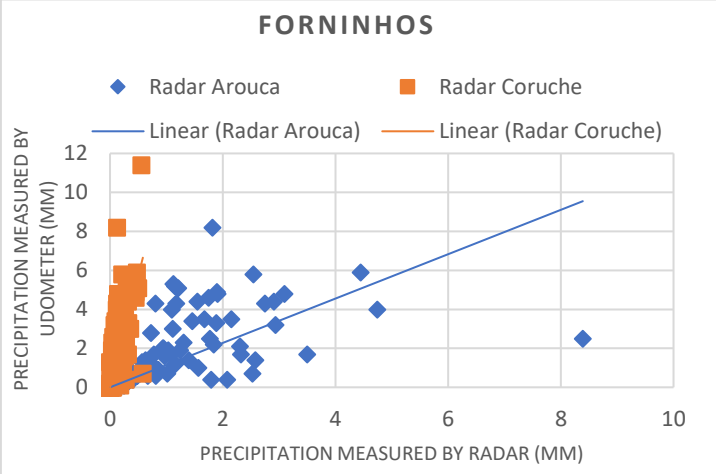

Figure B12- Relationship between precipitation data Forninhos and the two weather radars, on the event of 2019.

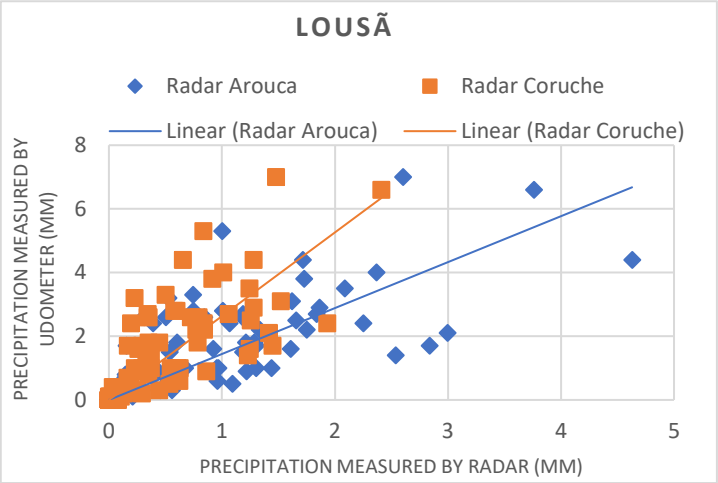

Figure B13- Relationship between precipitation data Lousã and the two weather radars, on the event of 2019.

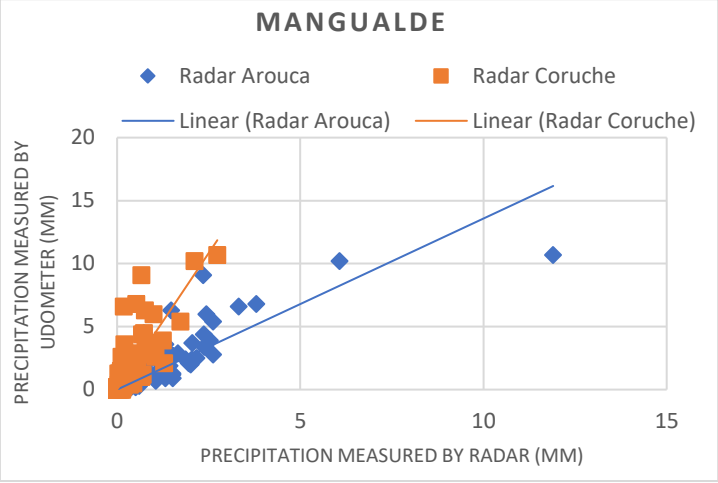

Figure B14- Relationship between precipitation data Mangualde and the two weather radars, on the event of 2019.

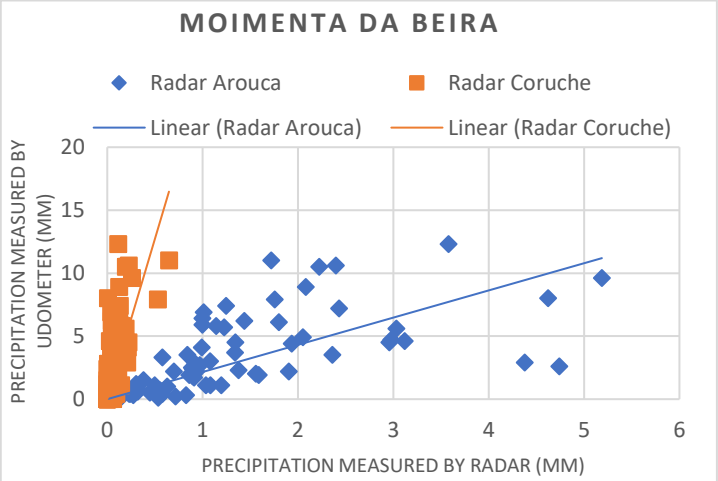

Figure B15- Relationship between precipitation data Moimenta da Beira and the two weather radars, on the event of 2019.

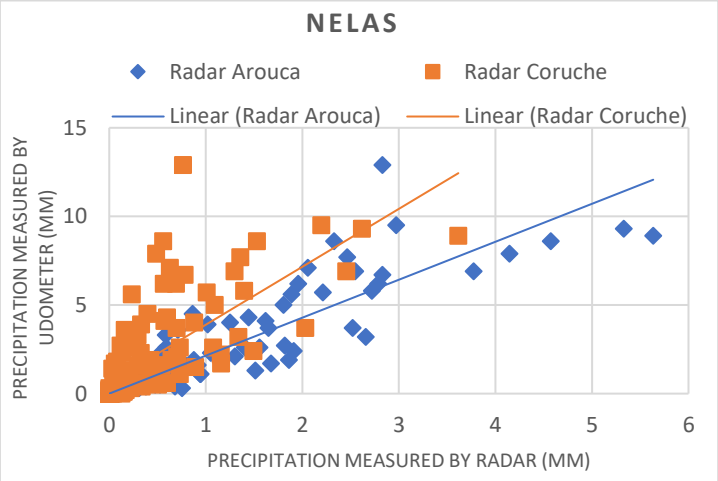

Figure B16- Relationship between precipitation data Nelas and the two weather radars, on the event of 2019.

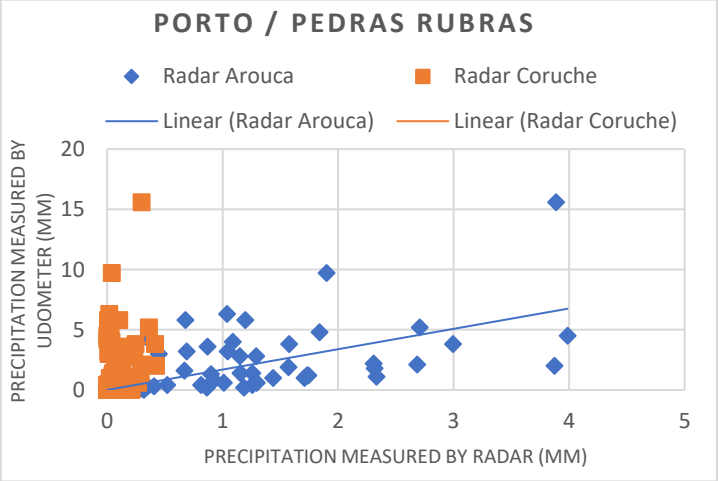

Figure B17- Relationship between precipitation data Porto (Pedras Rubras) and the two weather radars, on the event of 2019.

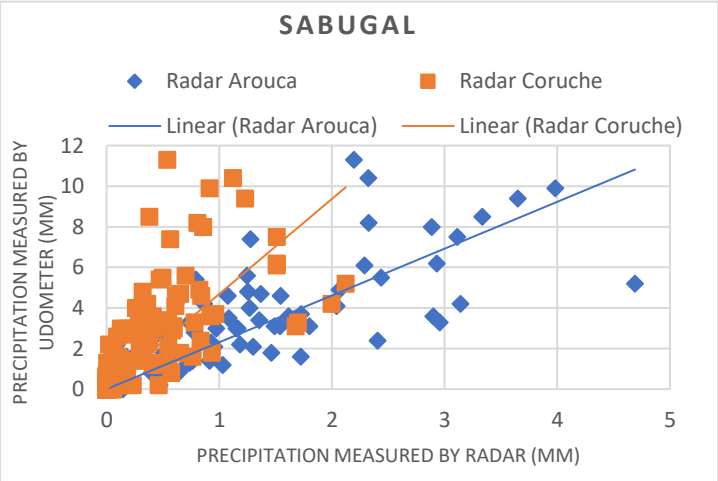

Figure B18- Relationship between precipitation data Sabugal and the two weather radars, on the event of 2019.

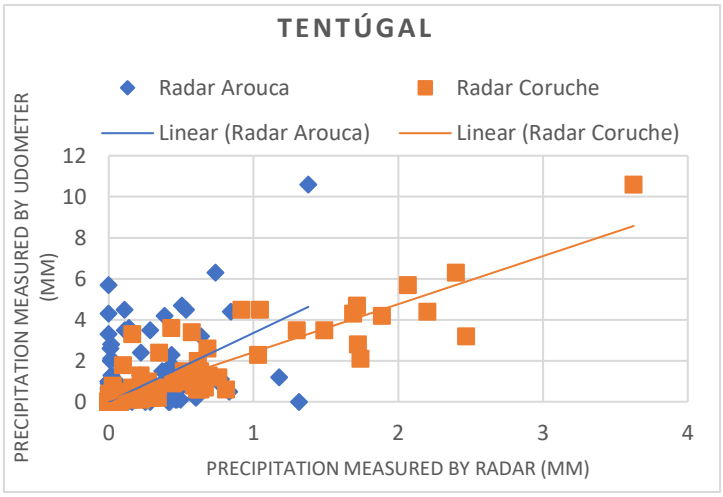

Figure B19- Relationship between precipitation data Tentúgal and the two weather radars, on the event of 2019.

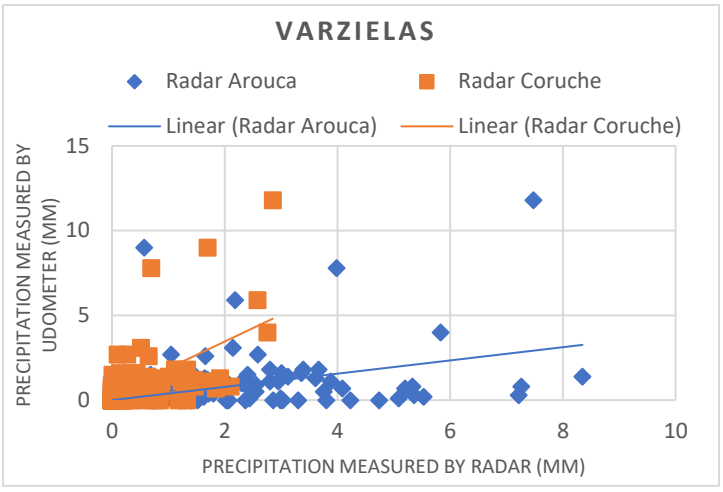

Figure B20- Relationship between precipitation data Varzielas and the two weather radars, on the event of 2019.

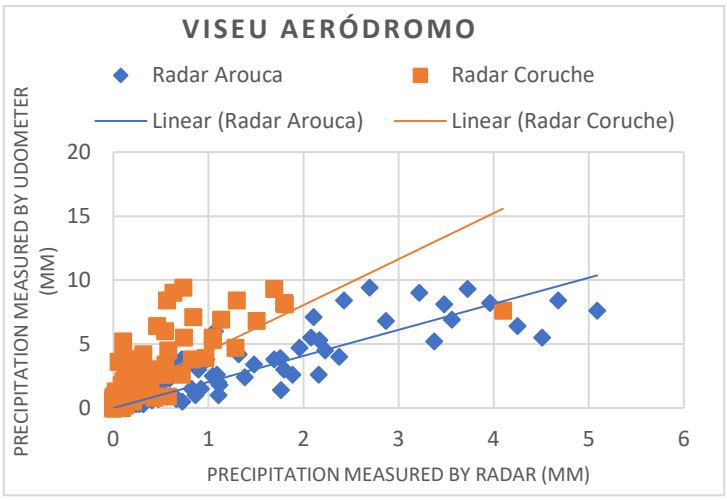

Figure B21- Relationship between precipitation data Viseu (Aeródromo) and the two weather radars, on the event of 2019.

Annex D – Graphs that represent the relationship between the precipitation data measured by the udometer and the data resulting from the application of the median filter (3x3) to the weather radar data.

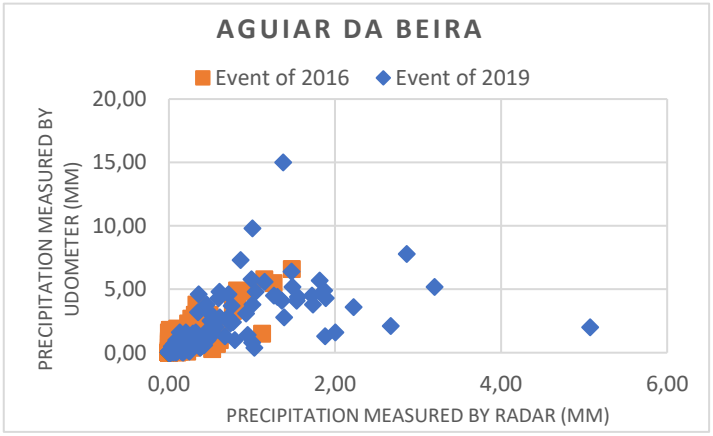

Figure D1- Relationship between precipitation data measured by Aguiar da Beira and the weather radar of Arouca.

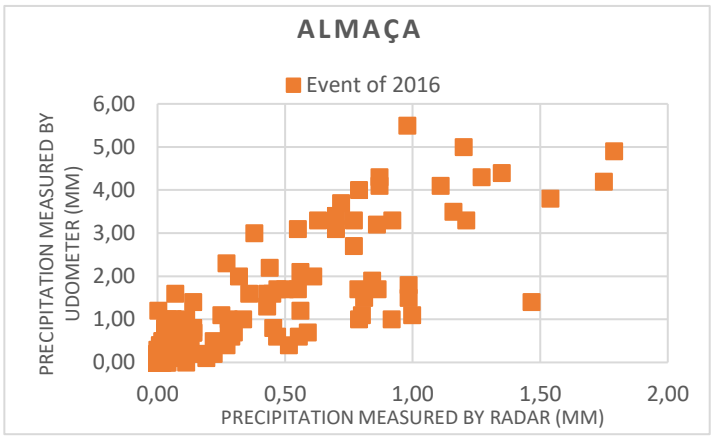

Figure D2- Relationship between precipitation data measured by Almaça and the weather radar of Arouca.

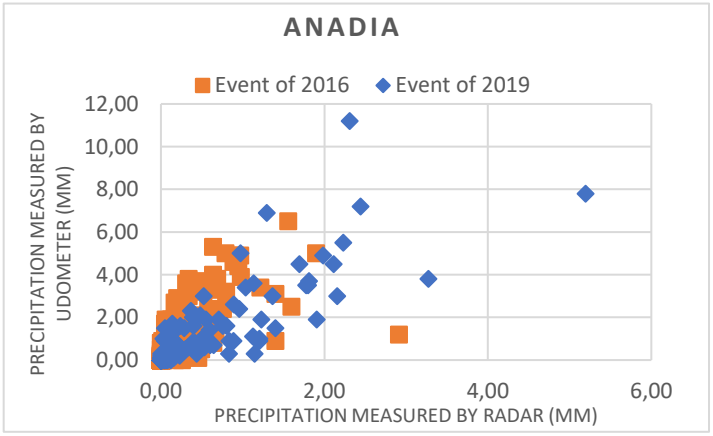

Figure D3- Relationship between precipitation data measured by Anadia and the weather radar of Arouca.

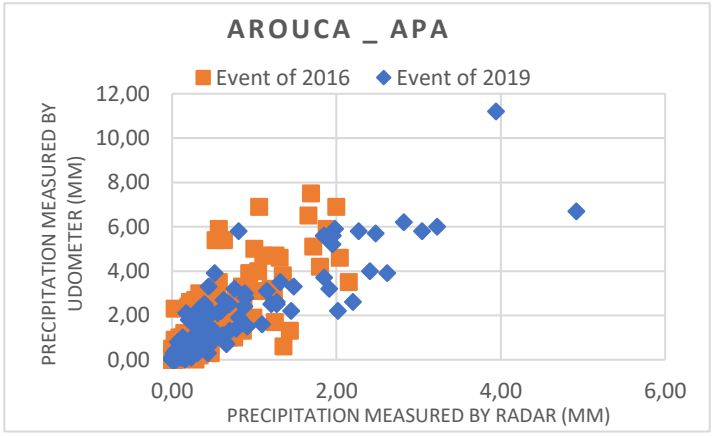

Figure D4- Relationship between precipitation data measured by Arouca (APA) and the weather radar of Arouca.

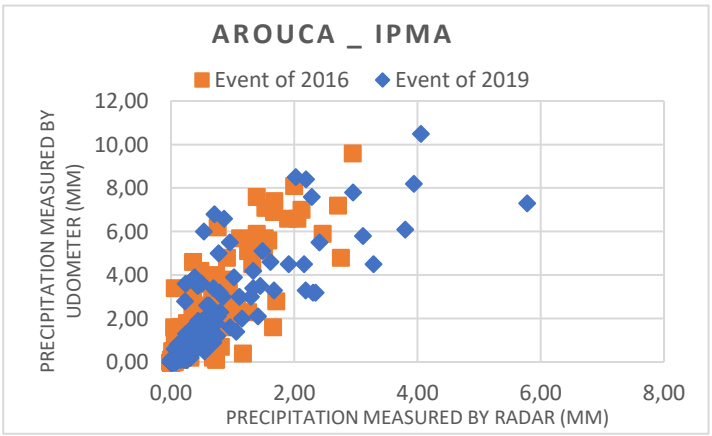

Figure D5- Relationship between precipitation data measured by Arouca (IPMA) and the weather radar of Arouca.

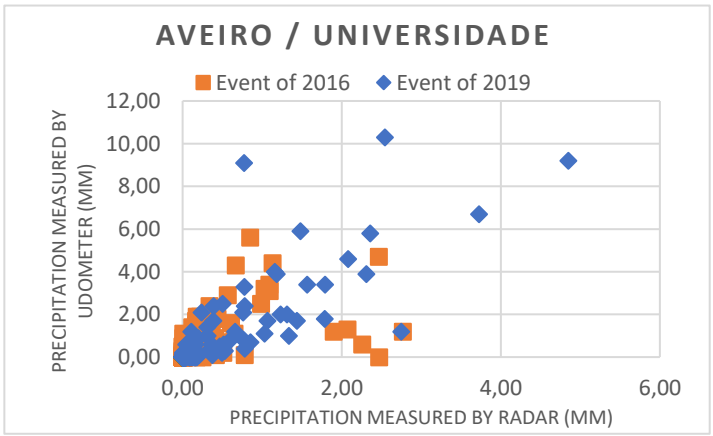

Figure D6- Relationship between precipitation data measured by Aveiro (Universidade) and the weather radar of Arouca.

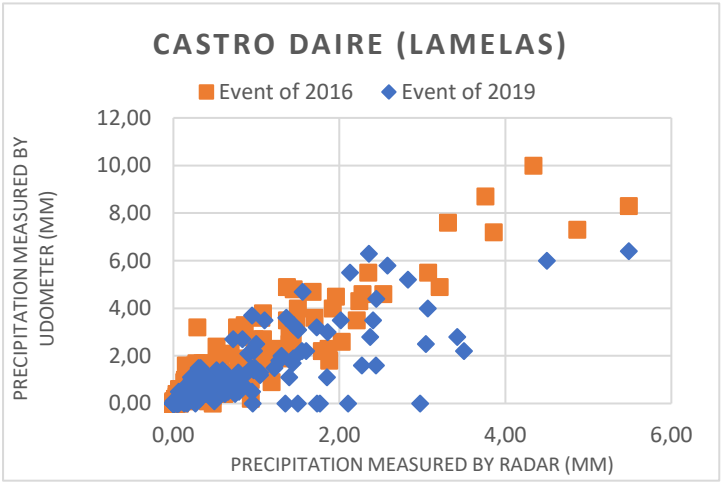

Figure D7- Relationship between precipitation data measured by Castro Daire and the weather radar of Arouca.

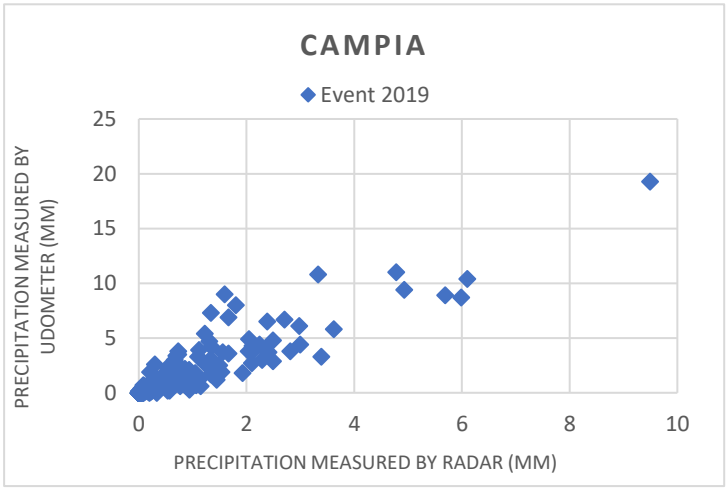

Figure D8- Relationship between precipitation data measured by Campia and the weather radar of Arouca.

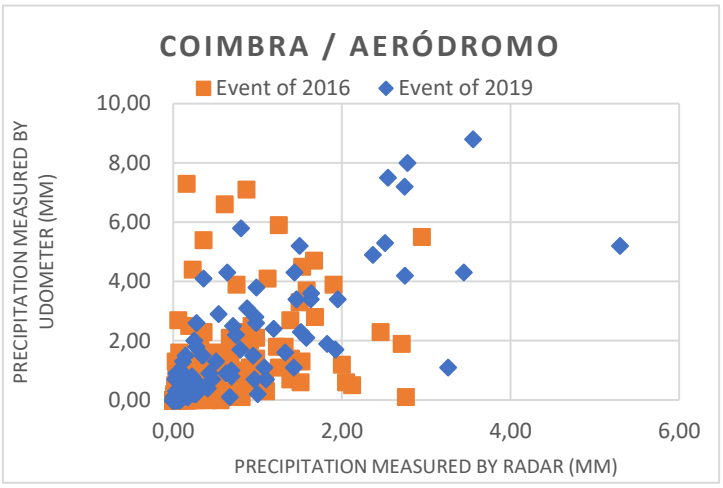

Figure D9- Relationship between precipitation data measured by Castro Daire and the weather radar of Arouca.

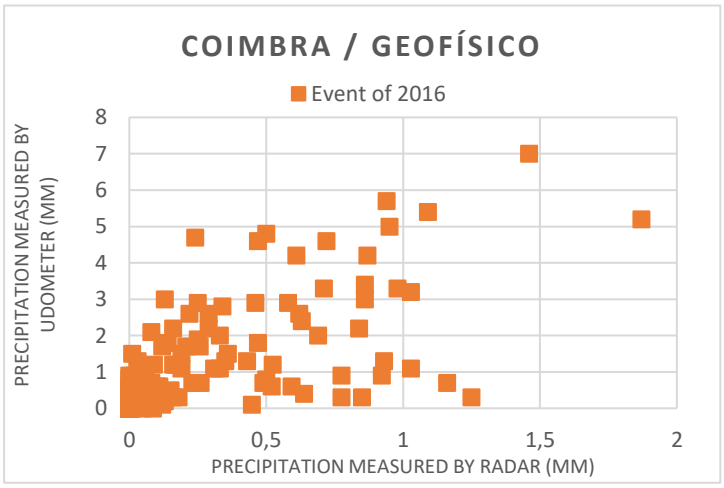

Figure D10- Relationship between precipitation data measured by Castro Daire and the weather radar of Arouca.

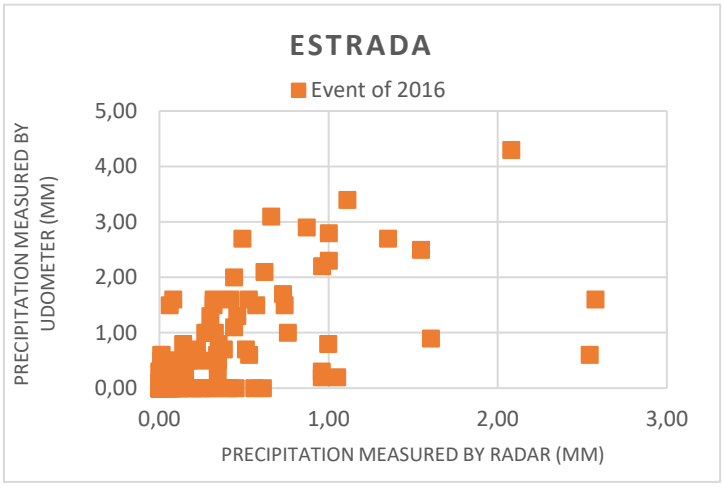

Figure D11- Relationship between precipitation data measured by Estrada and the weather radar of Arouca.

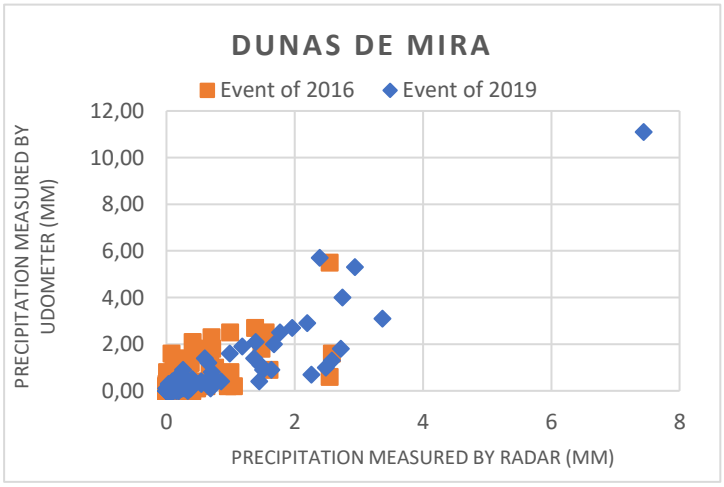

Figure D12- Relationship between precipitation data measured by Dunas de Mira and the weather radar of Arouca.

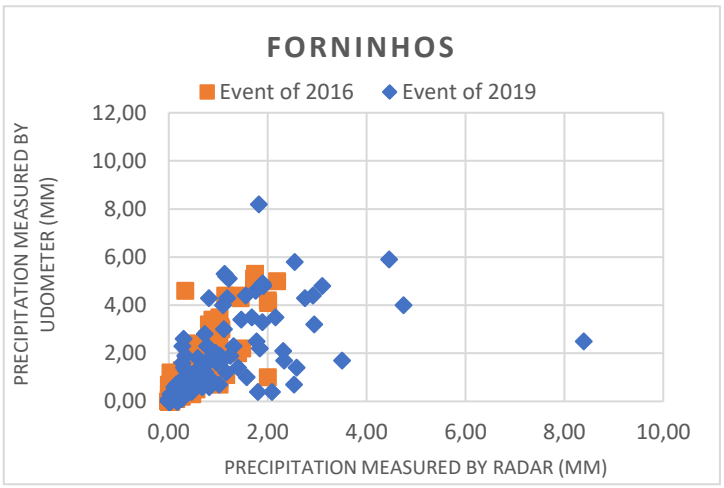

Figure D13- Relationship between precipitation data measured by Forninhos and the weather radar of Arouca.

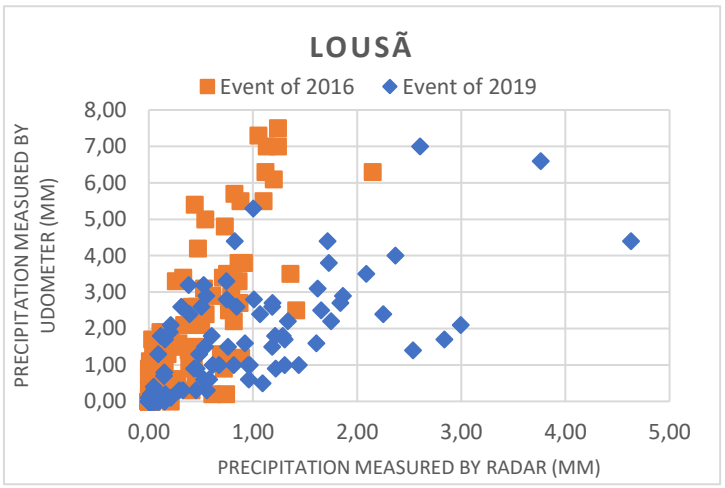

Figure D14- Relationship between precipitation data measured by Lousã and the weather radar of Arouca.

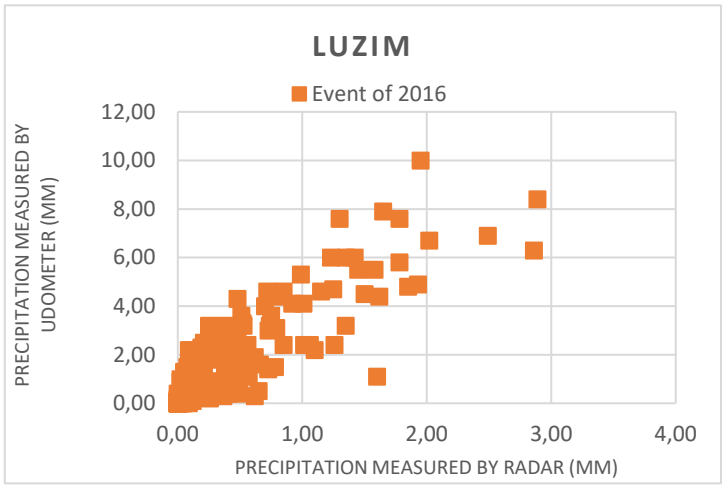

Figure D15- Relationship between precipitation data measured by Luzim and the weather radar of Arouca.

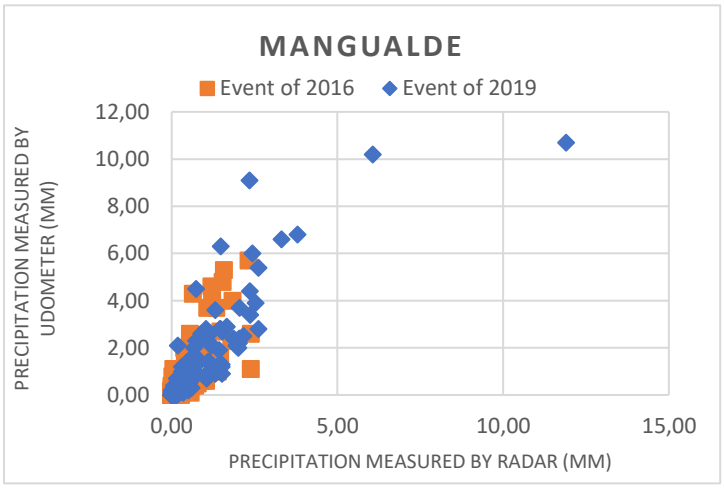

Figure D16- Relationship between precipitation data measured by Mangualde and the weather radar of Arouca.

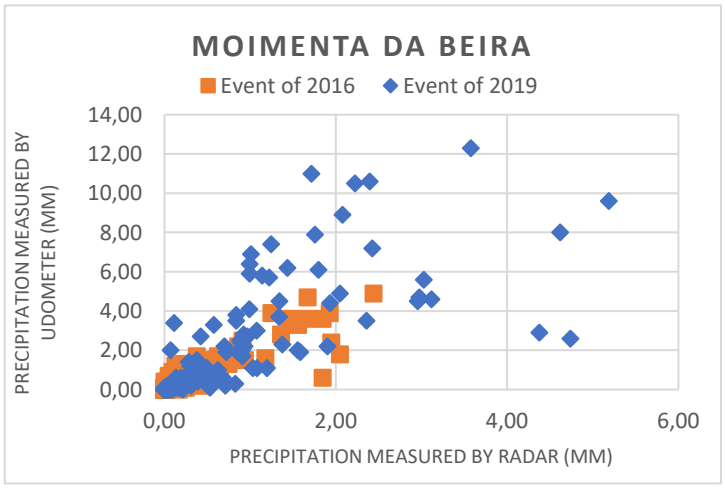

Figure D17- Relationship between precipitation data measured by Moimenta da Beira and the weather radar of Arouca.

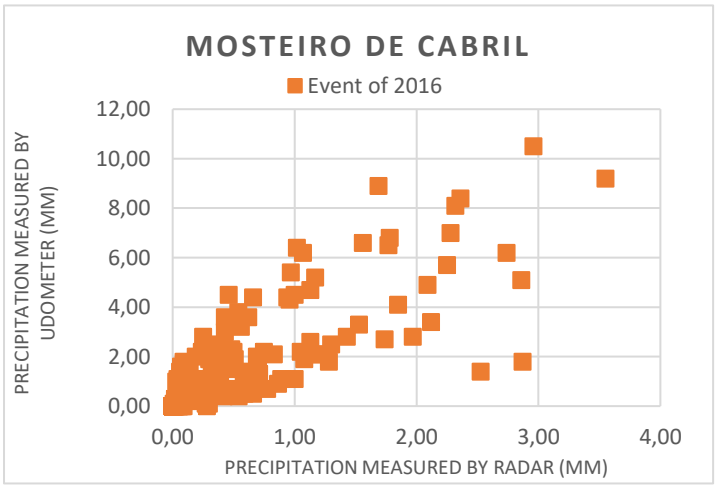

Figure D18- Relationship between precipitation data measured by Mosteiro Cabril and the weather radar of Arouca.

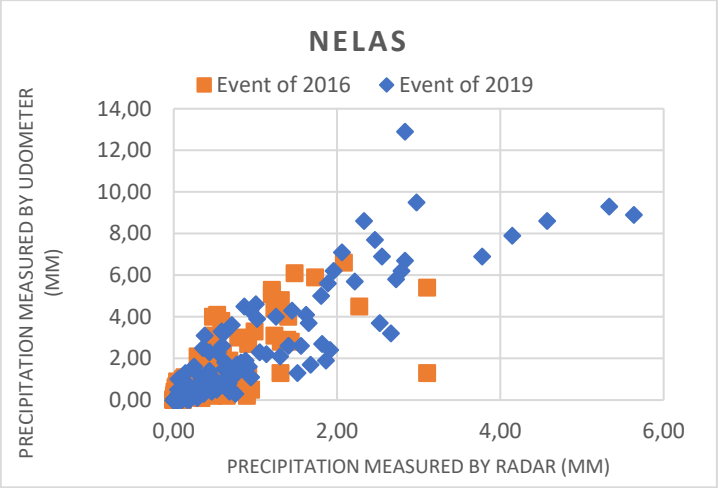

Figure D19- Relationship between precipitation data measured by Nelas and the weather radar of Arouca.

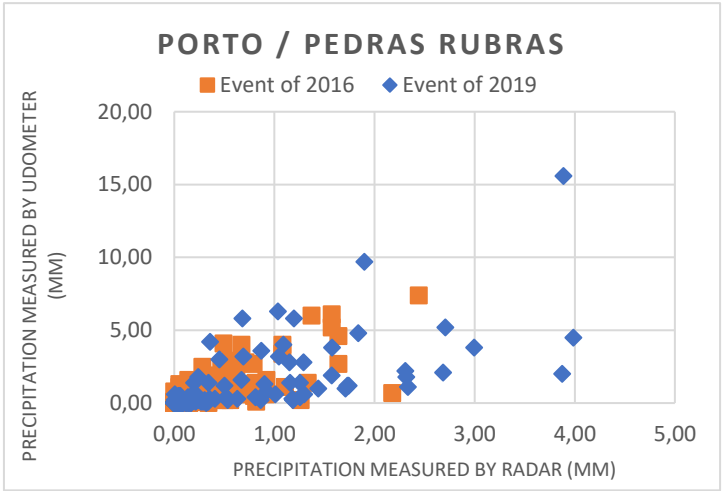

Figure D20- Relationship between precipitation data measured by Porto (Pedras Rubras) and the weather radar of Arouca.

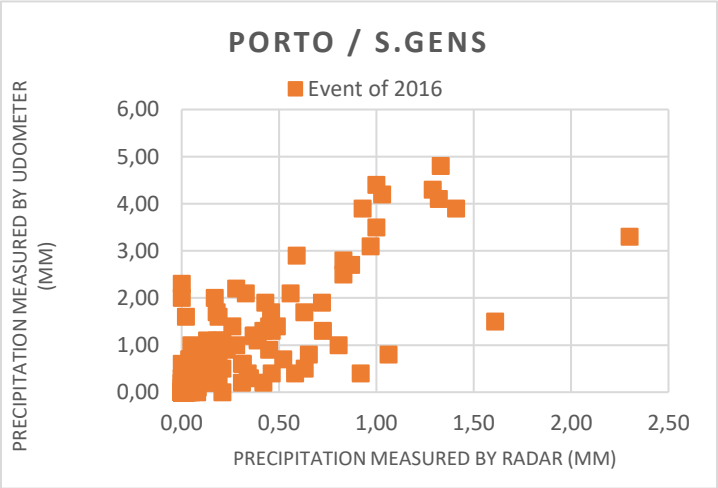

Figure D21- Relationship between precipitation data measured by Porto (S. Gens) and the weather radar of Arouca.

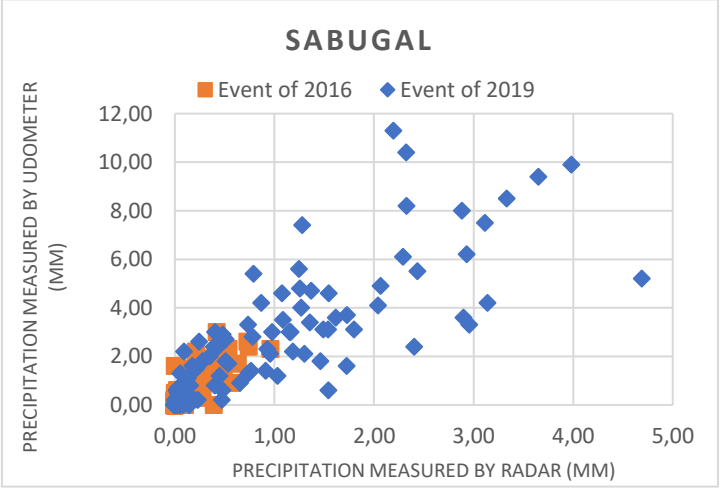

Figure D22- Relationship between precipitation data measured by Sabugal and the weather radar of Arouca.

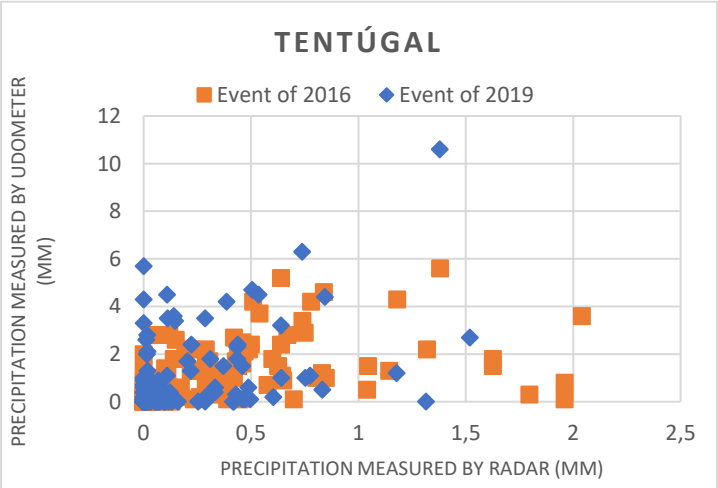

Figure D23- Relationship between precipitation data measured by Tentúgal and the weather radar of Arouca.

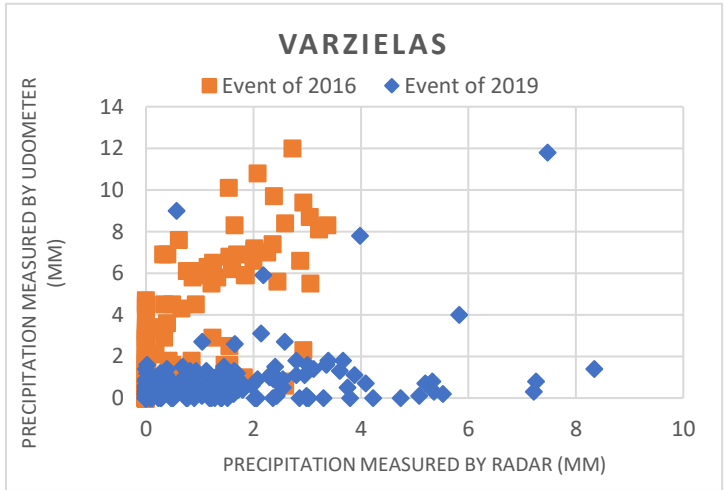

Figure D24- Relationship between precipitation data measured by Varzielas and the weather radar of Arouca.

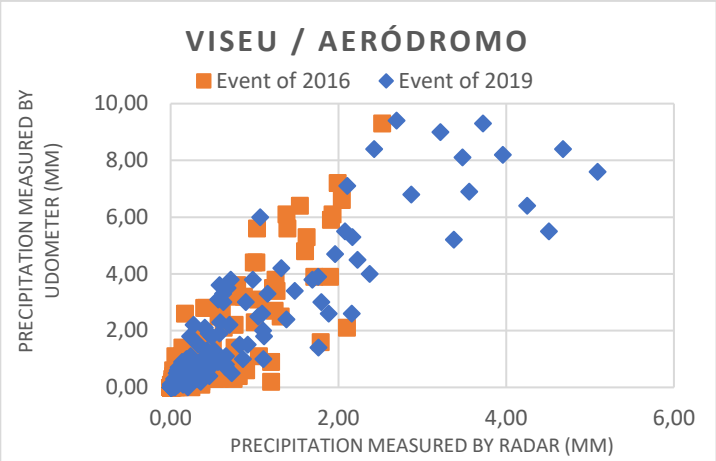

Figure D25- Relationship between precipitation data measured by Varzielas and the weather radar of Arouca.